

**MICROBIAL COLONIZATION OF MINERALS IN MARINE SEDIMENTS – METHOD DEVELOPMENT
AND ECOLOGICAL SIGNIFICANCE**

Thesis by

Benjamin Kimball Harrison

In Partial Fulfillment of the Requirements

for the Degree of

Doctor of Philosophy

California Institute of Technology

Pasadena, California

2011

(Defended May 5, 2011)

2011

Benjamin Kimball Harrison

All Rights Reserved

Chapter 1 reprinted

Applied Environmental Microbiology, "Variations in Archaeal and Bacterial Diversity Associated with the Sulfate-Methane Transition Zone in Continental Margin Sediments (Santa Barbara Basin, California)," 75 (2009): 1487-1499.

Chapter 2 reprinted

Geomicrobiology Journal, "Method for assessing Mineral Composition-Dependent patterns in Microbial diversity using Magnetic and Density Separation," accepted 2011, in press.

ACKNOWLEDGMENTS

To my wife Megan and her constant companionship within (and without) the difficult (and wonderful) aspects of scientific inquiry.

To my parents, David and Cynthia, whose interest in my studies has always fueled my ongoing curiosity.

To my advisor, Victoria Orphan, for the opportunity and support in researching a topic of endless promise, and sharing in the process of learning how best to pursue it.

To past and present members of the Orphan Lab group at Caltech who have consistently made the world of marine microbial ecology a larger and substantially more manageable place.

ABSTRACT

Interactions between microorganisms and minerals significantly impact microbial diversity and geochemical cycles in diverse settings. However, methodological difficulty has inhibited past study of microbe–mineral interactions in fine-grained subsurface environments. Conventional sampling poorly resolves microbial diversity at the fine scale necessary to perceive overall community differences between mineral substrates that are thoroughly mixed. In particular, the importance of microbial attachment to minerals in unconsolidated marine sediments remains poorly constrained despite extensive geobiological research in these settings. This study presents an approach for characterizing microbial colonization patterns using mineral separation techniques. Differences in density and magnetic susceptibility are used to enrich target minerals from bulk environmental samples, selecting for those minerals which may have importance as substrates for metabolic activity.

The application of this methodology to methane seep sediments of the Eel River Basin (ERB) on the California margin demonstrates that variations in microbial diversity between minerals are comparable to community differences across broad spatial scales and a range of porewater geochemistry. ERB colonization patterns determined by separation are shown to be reproducible and reflect *in situ* differences in the microbial community. Affinity of putative sulfide-oxidizing bacteria (primarily identified as *Gammaproteobacteria*) for mineral partitions enriched in authigenic sulfides suggests microbial attachment may reflect a metabolic role in sulfur cycling under reducing conditions. Mineral attachment is also shown to select between key archaeal phylotypes involved in the anaerobic oxidation of methane (AOM), providing

insight into physiological differences between these uncultured groups. Preliminary results demonstrate that mineral attachment may be a significant factor in the microbial diversity of the marine subsurface, and that such community differences will be ecologically relevant.

TABLE OF CONTENTS

Acknowledgments..... iii

Abstract v

Table of Contents vii

List of Figures and Tables ix

Introduction 1

Chapter 1. Variations in archaeal and bacterial diversity associated with the sulfate-methane transition zone in continental margin sediments (Santa Barbara Basin, CA)..... 7

Abstract..... 7

Introduction 8

Materials and Methods..... 11

Results..... 16

Discussion..... 29

Acknowledgments..... 35

References..... 35

Chapter 2. Method for assessing mineral composition-dependent patterns in microbial diversity using magnetic and density separation 41

Abstract..... 41

Introduction 42

Sampling and Methods 44

Results and Discussion 54

Conclusions 69

Acknowledgements..... 70

References..... 71

Chapter 3. Microbe-mineral interactions of Eel River Basin methane seeps—implications for sulfur cycling and anaerobic oxidation of methane 75

Abstract..... 75

Introduction 76

vii

<i>Methods</i>	77
<i>Results</i>	85
<i>Discussion</i>	98
<i>Conclusions</i>	109
<i>Acknowledgements</i>	110
<i>References</i>	110
Appendix I. Error analysis in Terminal Restriction Fragment Length Polymorphism	115
<i>Summary</i>	115
<i>Introduction</i>	116
<i>Methods</i>	117
<i>Results and Analysis</i>	118
<i>Pitfalls</i>	123
<i>References</i>	124
Appendix II. Supplemental methods—Variations in archaeal and bacterial diversity associated with the sulfate-methane transition zone in continental margin sediments (Santa Barbara Basin, CA)	125
<i>References</i>	125
<i>Supplemental Figures</i>	127
Appendix III. Supplemental figures—Eel River Basin community analyses by terminal restriction fragment length polymorphism	133

LIST OF FIGURES AND TABLES

Table 1-1. Microbial diversity of Santa Barbara Basin sediment.....	12
Figure 1-1. Porewater geochemical profiles of the Santa Barbara Basin sediment column.....	17
Table 1-2. Distribution of major phylogenetic groups.....	18
Figure 1-2. Bacterial 16S rRNA neighbor-joining distance tree for representative Santa Barbara Basin sequences.....	19-20
Figure 1-3. Archaeal 16S rRNA neighbor-joining distance tree for representative Santa Barbara Basin sequences.....	22
Figure 1-4. Neighbor-joining distance tree for dissimilatory sulfite reductase.....	25
Figure 1-5. Correspondence analysis of marine sedimentary bacterial communities.....	27
Figure 1-6. UniFrac cladograms for 16S rRNA gene Archaeal and Bacterial community composition.....	28
Figure 2-1. Ideal extraction ranges for selected minerals using magnetic and density separations.....	46
Figure 2-2. Results of mineral separation on a Lau Basin hydrothermal chimney and subsequent clone library analyses.....	55
Figure 2-3. Terminal Restriction Fragment Length Polymorphism electropherograms exhibiting methodological reproducibility.....	56
Figure 2-4. Assessment of cross-contamination of archaeal cells between magnetic fractions during separation.....	57
Table 2-1. Elemental abundances of Eel River Basin mineral partitions by SEM-EDS.....	59
Figure 2-5. Principal Component Analysis of elemental abundance measurements from SEM-EDS analyses.....	60
Figure 2-6. Photomicrographs of Fluorescence in situ hybridization and SEM imaging of Eel River Basin sediments.....	61
Table 2-2. Relative abundance of microbial phylotypes within Eel River Basin mineral partitions.....	63

Figure 2-7. Partial Terminal Restriction Fragment Length Polymorphism electropherograms of archaea associated with magnetic and density partitions.....	64
Figure 2-8. Hierarchical cluster analysis of archaeal community differences between density separates.....	67
Figure 3-1. X-Ray Diffractometry spectra of Eel River Basin mineral separates.....	86
Figure 3-2. Environmental distance between bulk sediment analyses and mineral separates.....	87
Table 3-1. Comparison of mineral separates of select Eel River Basin Sediment horizons by TRFLP.....	88
Figure 3-3. Distribution of key microbial phylotypes across an Eel River Basin methane seep.....	89
Figure 3-4. Fluorescence <i>in situ</i> hybridization images of mineral separates.....	91
Table 3-2. Significant indicator taxa for Eel River Basin density partitions.....	92
Figure 3-5. TRFLP electropherograms exhibiting 16S rRNA gene signal of key delta and gammaproteobacterial phylotypes.....	93
Figure 3-6. 2-way cluster analysis of 16S rRNA gene bacterial diversity of density partitions.....	95
Table 3-3. Summary of laboratory microcosms.....	97
Figure 3-7. Relative abundance of ANME 2 subgroups.....	100
Figure 3-8. Correlation of SEEP-SRB1a abundance with trends in ANME archaeal diversity.....	102
Figure 3-9. Relative abundances of oxidative and reductive sulfur-cyclers.....	105
Figure I-1. Precision of 5th degree polynomial size model.....	119
Figure I-2. Absolute value of difference between 5th degree polynomial size model and known fragment lengths.....	119
Figure I-3. Absolute value of difference between 3rd and 4th degree polynomial size models and known fragment lengths.....	120
Figure I-4. Fragment length vs. peak width for 29 representative analyses of a 600 bp size standard.....	121

Figure I-5. Peak shapes of types A, B and C defined by peak width.....	121
Figure I-6. Reproducibility of relative height and area.....	122
Figure II-S1. Bacterial and Archaeal rarefaction curves for Santa Barbara Basin clone libraries.....	127
Figure II-S2. Neighbor-joining distance tree of the methyl coenzyme M reductase gene.....	128
Figure II-S3. Correspondence analysis of marine sedimentary bacterial communities.....	130
Figure II-S4. UniFrac clustering of environmental clone libraries.....	130
Table II-S1. Bacterial diversity of marine sediments.....	131
Table II-S2. Correspondence analysis results.....	132
Table III-1. Summary of Eel River Basin environmental samples.....	134
Table III-2. Relative abundance of ERB T-RFs by HaeIII.....	135-142
Table III-3. Relative abundance of ERB T-RFs by RsaI.....	143-145
Table III-4. Relative abundance of archaeal ERB T-RFs by RsaI.....	146-147
Table III-5. Relative abundance of microcosm bacterial T-RFs by HaeIII.....	148-151
Table III-6. Relative abundance of microcosm archaeal T-RFs by HaeIII.....	152-153

Introduction

An estimated 55–85% of the Earth's prokaryotic biomass resides in the marine subsurface (Whitman et al., 1998), with the majority of this fraction concentrated in unconsolidated sediments—a measurement derived from a no more than 3-decades-old tradition of counting fluorescently-labeled cells recovered from the deep ocean (Parkes et al., 1994). Geomicrobiology of deep subsurface marine sediments has only recently become a focus of specific research expeditions, beginning with Ocean Drilling Program Leg 201 to the Peru Margin in 2002. Studies of microbial abundance and activity in sediments have often been associated with samples of opportunity from continental margins or oases of biological diversity on the seafloor (e.g., hydrothermal vent communities discovered in 1977 (Lonsdale, 1977), and cold seep fauna identified in the Gulf of Mexico in 1983 (Paull et al, 1984)). Recent characterization of open-ocean, oligotrophic deep sea sediments of the South Pacific Gyre observed microbial abundance of 10^3 cells/cm³ (D'Hondt et al., 2009), three orders of magnitude beneath minimum counts used in the Whitman et al. estimate. Nevertheless, marine sediments continue to accommodate a significant portion of microorganisms in the environment and represent a significant but poorly-quantified factor in global biogeochemical cycles (D'Hondt et al., 2002, 2004).

At the first order, spatial orientation of microbial activity in the marine subsurface is determined by successive depletion of terminal electron acceptors with depth below the sediment-water interface coupled to oxidation of organic matter (Froelich et al., 1979). The dominant metabolism is that which is most energetically favorable—reducing oxygen, nitrate, iron/manganese, and sulfate in discrete portions of the sediment column. However, resolution of these redox zones is limited by factors including organic matter-driven microniches (e.g.,

Jorgensen, 1977) and kinetic limitations on metal reduction (e.g., Schippers and Jorgensen, 2002; Riedinger et al., 2010). The initial chapter of this study (B.K. Harrison, H. Zhang, W. Berelson, and V.J. Orphan: *Variations in Archaeal and Bacterial Diversity Associated with the Sulfate-Methane Transition Zone in Continental Margin Sediments (Santa Barbara Basin, California)*) examines the resolution of redox zones in marine sediments in microbial diversity signatures. In the context of a case study of the Santa Barbara Basin sediment column, the manuscript constrains the utility of 16S rRNA gene surveys linking community structure to dominant metabolism. A microbial community signature specific to the sulfate-methane transition zone provides insight into the distribution and ecology of key taxa in marginal environments. Statistical analysis identifies characteristic features of the microbial community in the SMTZ and other redox horizons broadly applicable across past studies of the marine subsurface. Nevertheless, microbial communities of discrete redox zones exhibit considerable overlap, in which microscale ecological niches—including those attributable to differences in sediment lithology—likely play an important role.

In the terrestrial subsurface microbial attachment to mineral surfaces has been shown to drive significant variations in diversity (Mauck and Roberts, 2007; Boyd et al., 2007), and cell density and morphology is similarly differentiated by mineral composition of substrates introduced to the ocean floor (Edwards et al., 2003). Characterization of microbe-mineral interactions within marine sediments has been methodologically difficult. Substantial time and expense are necessary for *in situ* microcosm deployment, and fine-grained clays preclude sampling of the microbial community at the resolution of mineralogical heterogeneity. The majority of subsurface microorganisms are attached to particles (Alfreider et al., 1997), but cells have been microscopically observed a fixed distance from mineral surfaces, bound by

extracellular polymers (Ransom et al, 1999). Comparable proximity of different mineral substrates in well-mixed fine-grained sedimentary environments could inhibit composition-dependent changes in diversity (i.e., all minerals are equally proximal and metabolically relevant to a cell in the marine subsurface). Development of mineral separation methodology detailed in the second chapter (B.K. Harrison and V.J. Orphan: *Method for Assessing Mineral Composition-Dependent Patterns in Microbial Diversity Using Magnetic and Density Separation*) provides a means of characterizing the microbial community associated with specific mineral phases in marine sediments. Targeted minerals are enriched from bulk environmental samples by suspension in high-density liquids or by high-gradient magnetic separation. Downstream analyses of the 16S rRNA gene and epifluorescence microscopy coupled to fluorescence *in situ* hybridization confirm persistent physical association of cells with particles and variations in microbial diversity between mineral partitions. This approach is shown to reproducibly measure *in situ* microbial colonization patterns and is uniquely suited to investigation of marine sediments.

The ecological significance of mineral attachment in Eel River Basin (CA) marine methane seeps is evaluated in Chapter 3 (B.K. Harrison and V.J. Orphan: *Microbe-Mineral Interactions of Eel River Basin Methane Seeps—Implications for Sulfur Cycling and Anaerobic Oxidation of Methane*). Methane seeps are rich environments for microbial life primarily supported by the anaerobic oxidation of methane (AOM). AOM is a globally distributed process mediated by syntrophic consortia of sulfate-reducing bacteria and methane-oxidizing archaea (for review, see Knittel and Boetius, 2009). Over 90% of the methane produced in the marine subsurface is thought to be consumed by AOM (Reeburgh, 2007). Sulfate reduction coupled to AOM in these environments may deplete sulfate within the upper 20 cm of the sediment

column, and leads to extensive formation of authigenic sulfides. Hydrogen sulfide fuels a substantial oxidative community at the sediment–water interface including symbiont-bearing chemosynthetic macrofauna. The application of mineral separation methodology to Eel River Basin sediments in this final chapter demonstrates distinct patterns of microbial colonization by key, indigenous microbial taxa linked to AOM, sulfate reduction, and sulfide oxidation. Putative S-oxidizing phylotypes are shown to preferentially attach to authigenic sulfides at sediment depths dominated by sulfate reduction. Diverse archaeal phylotypes linked to AOM partition between mineral separates, providing insight into ecophysiological differences between these uncultured microorganisms. Environmental patterns of microbe-mineral attachment are further tested by laboratory microcosm experiments and cell growth on sterilized sulfur minerals. Overall variation in microbial diversity observed between mineral partitions is comparable to that observed across broad spatial scales in the methane seep environment.

The study of sedimentary microbe-mineral interactions from the Eel River Basin represents a first estimation of the role of mineral colonization, suggesting that preferential mineral attachment is widespread and significant in the prokaryotic diversity of the marine subsurface. Additionally, the implied metabolic relationship between microbes and minerals for which preferential attachment is demonstrated provides a unique opportunity to constrain potential physiology of uncultured microorganisms in the environment. The method presented in this study is broadly applicable to subsurface environments exhibiting mineralogical heterogeneity, and particularly suited to the study of previously intractable fine-grained environments.

References

- Alfreider, A., M. Krossbacher, and R. Psenner. 1997. Groundwater samples do not reflect bacterial densities and activity in subsurface systems. *Water Res* 31:832–840.
- Boyd, E. S., D. E. Cummings, and G. G. Geesey. 2007. Mineralogy influences structure and diversity of bacterial communities associated with geological substrata in a pristine aquifer. *Microb Ecol* 54:170–182.
- D'Hondt, S., B. B. Jorgensen, D. J. Miller, A. Batzke, R. Blake, B. A. Cragg, H. Cypionka, G. R. Dickens, T. Ferdelman, K. U. Hinrichs, N. G. Holm, R. Mitterer, A. Spivack, G. Z. Wang, B. Bekins, B. Engelen, K. Ford, G. Gettemy, S. D. Rutherford, H. Sass, C. G. Skilbeck, I. W. Aiello, G. Guerin, C. H. House, F. Inagaki, P. Meister, T. Naehr, S. Niitsuma, R. J. Parkes, A. Schippers, D. C. Smith, A. Teske, J. Wiegel, C. N. Padilla, and J. L. S. Acosta. 2004. Distributions of microbial activities in deep seafloor sediments. *Science* 306:2216–2221.
- D'Hondt, S., S. Rutherford, and A. J. Spivack. 2002. Metabolic activity of subsurface life in deep-sea sediments. *Science* 295:2067–2070.
- D'Hondt, S., A. J. Spivack, R. Pockalny, T. G. Ferdelman, J. P. Fischer, J. Kallmeyer, L. J. Abrams, D. C. Smith, D. Graham, F. Hasiuk, H. Schrum, and A. M. Stancin. 2009. Seafloor sedimentary life in the South Pacific Gyre. *Proc Natl Acad Sci USA* 106:11651–11656.
- Edwards, K. J., T. M. McCollom, H. Konishi, and P. R. Buseck. 2003. Seafloor bioalteration of sulfide minerals: Results from in situ incubation studies. *Geochim Cosmochim Acta* 67:2843–2856.
- Jorgensen, B. B. 1977. Bacterial Sulfate Reduction within Reduced Microniches of Oxidized Marine Sediments. *Mar Biol* 41:7–17.
- Knittel, K., and A. Boetius. 2009. Anaerobic Oxidation of Methane: Progress with an Unknown Process. *Annu Rev Microbiol* 63:311–334.
- Lonsdale, P. 1977. Clustering of Suspension-Feeding Macrobenthos Near Abyssal Hydrothermal Vents at Oceanic Spreading Centers. *Deep-Sea Res* 24:857–863.
- Mauck, B. S., and J. A. Roberts. 2007. Mineralogic control on abundance and diversity of surface-adherent microbial communities. *Geomicrobiol J* 24:167–177.
- Parkes, R. J., B. A. Cragg, S. J. Bale, J. M. Getliff, K. Goodman, P. A. Rochelle, J. C. Fry, A. J. Weightman, and S. M. Harvey. 1994. Deep Bacterial Biosphere in Pacific-Ocean Sediments. *Nature* 371:410–413.
- Paull, C. K., B. Hecker, R. Commeau, R. P. Freemanlynde, C. Neumann, W. P. Corso, S. Golubic, J. E. Hook, E. Sikes, and J. Curray. 1984. Biological Communities at the Florida Escarpment Resemble Hydrothermal Vent Taxa. *Science* 226:965–967.

- Ransom, B., R. H. Bennett, R. Baerwald, V. H. Hulbert, and P. J. Burkett. 1999. In situ conditions and interactions between microbes and minerals in fine-grained marine sediments: A TEM microfabric perspective. *Am Mineral* 84:183–192.
- Reeburgh, W. S. 2007. Oceanic methane biogeochemistry. *Chem Rev* 107:486–513.
- Riedinger, N., B. Brunner, M. J. Formolo, E. Solomon, S. Kasten, M. Strasser, and T. G. Ferdelman. 2010. Oxidative sulfur cycling in the deep biosphere of the Nankai Trough, Japan. *Geology* 38:851–854.
- Schippers, A., and B. B. Jorgensen. 2002. Biogeochemistry of pyrite and iron sulfide oxidation in marine sediments. *Geochim Cosmochim Acta* 66:85–92.
- Whitman, W. B., D. C. Coleman, and W. J. Wiebe. 1998. Prokaryotes: The unseen majority. *Proc Natl Acad Sci USA* 95:6578–6583.

Chapter 1

Variations in archaeal and bacterial diversity associated with the sulfate-methane transition zone in continental margin sediments (Santa Barbara Basin, CA)

Abstract

The sulfate-methane transition zone (SMTZ) is a widespread feature of continental margins, representing a diffusion-controlled interface where there is enhanced microbial activity. SMTZ microbial activity is commonly associated with the anaerobic oxidation of methane (AOM), which is carried out by syntrophic associations between sulfate-reducing bacteria and methane-oxidizing archaea. While our understanding of the microorganisms catalyzing AOM has advanced, the diversity and ecological role of the greater microbial assemblage associated with the SMTZ have not been well characterized. In this study, the microbial diversity above, within, and beneath the Santa Barbara Basin SMTZ was described. ANME-1-related archaeal phylotypes appear to be the primary methane oxidizers in the Santa Barbara Basin SMTZ, which was independently supported by exclusive recovery of related methyl coenzyme M reductase genes (*mcrA*). Sulfate-reducing *Deltaproteobacteria* phylotypes affiliated with the *Desulfobacterales* and *Desulfosarcina-Desulfococcus* clades were also enriched in the SMTZ, as confirmed by analysis of dissimilatory sulfite reductase (*dsr*) gene diversity.

Statistical methods demonstrated that there was a close relationship between the microbial assemblages recovered from the two horizons associated with the geochemically defined SMTZ, which could be distinguished from microbial diversity recovered from the sulfate-

replete overlying horizons and methane-rich sediment beneath the transition zone. Comparison of the Santa Barbara Basin SMTZ microbial assemblage to microbial assemblages of methane seeps and other organic matter-rich sedimentary environments suggests that bacterial groups not typically associated with AOM, such as *Planctomycetes* and candidate division JS1, are additionally enriched within the SMTZ and may represent a common bacterial signature of many SMTZ environments worldwide.

Introduction

The sulfate-methane transition zone (SMTZ) is defined as the horizon within the sediment column in which sulfate and methane coexist (Berelson et al., 2005, Treude et al., 2005). In diffusion-controlled marine systems, the SMTZ represents a deep redox interface exhibiting increased microbial activity (e.g., Parkes et al., 2005). Typically, sulfate is depleted with depth, and this interface divides a zone in which sulfate reduction is the dominant form of microbial respiration and a zone in which methanogenesis is the dominant form of microbial respiration. Within the SMTZ, most sulfate depletion is presumed to be directly coupled to the anaerobic oxidation of methane (AOM) (Devol and Ahmed, 1981; Reeburgh, 1980), and there are balanced rates of methane oxidation and sulfate reduction (Borowski et al., 1996; Iversen and Jorgensen, 1985; Nauhaus et al., 2002; Niewohner et al., 2008), as predicted by the stoichiometry of the reaction. In some sites, however, sulfate reduction cannot be balanced by AOM, which provides only a fraction of the total carbon and energy for sulfate reduction (Berelson et al., 2005; Dhillon et al., 2003; Joye et al., 2004; Thomsen et al., 2001; Treude et al., 2005). Discrepancies between sulfate flux and methane flux have been observed in a number of

sites off the California and Mexico coasts and may be a global phenomenon along continental margins (Berelson et al., 2005).

Geochemical modeling suggests that excess CO₂ flux may be balanced if sulfate reduction is coupled not only to AOM, but also to the enhanced breakdown of organic carbon (Berelson et al., 2005). The SMTZ sediment horizon may therefore represent a zone of enhanced overall microbial activity and remineralization coupled to rejuvenated organoclastic sulfate reduction. This raises questions of why presumably recalcitrant organic matter should pass through more shallow horizons directly above the SMTZ only to be coupled to sulfate reduction independent of AOM within the transition zone and whether microorganisms residing in the interface play a significant role in organic matter activation. A more detailed investigation of the full microbial assemblage specific to the SMTZ is needed to understand the role of the interface in early diagenesis. Distinct groups of uncultured sulfate-reducing *Deltaproteobacteria* and methane-oxidizing archaea (ANMEs) have been linked to the process of AOM in diverse marine environments and have been described primarily for advective near-seafloor sites where there is methane release, including methane seeps and mud volcanoes (Hinrichs et al., 1999; Knittel et al., 2003; Niemann et al., 2006; Orphan et al., 2001; Teske et al., 2002). Microbial assemblages from deeper, diffusion-limited environments along continental margins have been investigated to a lesser extent. Within these subseafloor habitats, ANMEs are present in some methane and hydrate-impacted sediments (Lanoil et al., 2001; Marchesi et al., 2001; Parkes et al., 2007; Reed et al., 2002; Thomsen et al., 2001), however their detection in other SMTZ-related sites has been inconsistent and has invoked speculation that additional archaeal groups distinct from the methanogen-related ANME groups may also be capable of AOM (Biddle et al., 2006; Inagaki et al., 2006; Sorensen and Teske, 2006). The co-associated bacterial assemblage surrounding the

SMTZ in these deeper diffusion controlled systems has been described in even fewer studies (Inagaki et al., 2006; Parkes et al., 2005; Parkes et al., 2007; Reed et al., 2002).

Here, the bacterial and archaeal diversity in the sediment horizons above, within, and below the diffusion-controlled SMTZ in the Santa Barbara Basin (SBB) was characterized using a combination of 16S rRNA genes and functional genes coding for methyl coenzyme M reductase (*mcrA*) and dissimilatory sulfite reductase (*dsrA*) to document changes in microbial assemblage diversity and structure associated with this globally important redox interface. The organic matter-rich sediments of the SBB are well suited for this type of investigation, having a well-defined sulfate-methane transition within gravity-core depth of the sediment-water interface and are a reasonable analogue for diverse diffusion controlled continental margin environments. This setting has also served as an important resource for paleoclimatological studies (e.g., Behl and Kennett, 1996), for which more extensive knowledge of subsurface diagenetic processes may be informative. The application of statistical comparisons of the microbial diversity recovered from SBB sediments above, within, and below the SMTZ with data from other available studies of bacterial and archaeal diversity in SMTZ, hydrate-bearing, methane seeps and organic matter-rich marine sediments was used to broadly define microbial groups which may be characteristic of SMTZs and to distinguish candidate groups potentially responsible for accelerated remineralization of organic matter within these horizons.

Materials and Methods

Site description and sampling

In June 2005, an expedition on the R/V *New Horizon* collected a series of sediment cores within the SBB (34°13.61'N, 119°59.42'W). At this location, the water depth was 587 m, and the bottom water oxygen content at the time of sampling was determined to be 0.2 μm (Berelson et al., 2005). Sediment was collected by either gravity coring or multicoring for pore water, isotope, mineralogical, and microbiological analyses. One gravity core (GC2) with geochemical properties representative of the majority of cores analyzed was selected for more detailed molecular analysis of the microbial community. Gravity core GC2 (length, 186 cm) was fully processed within 3 h of arrival on deck. Subsamples (~ 5 g) were taken from the center portion of the core using a cutoff 5 ml sterile syringe and immediately flash frozen in liquid nitrogen for nucleic acid extraction. Five sediment horizons were targeted in the study; the samples included one sample from the nominal sulfate reduction zone (50 cm), one sample from immediately above the SMTZ (103 cm), two samples from within the SMTZ (125 cm and 139 cm), and one sample from below the SMTZ (163 cm).

Pore water chemistry (sulfate and dissolved inorganic carbon)

The pore water sulfate and dissolved inorganic carbon contents were determined as previously described (Berelson et al., 2005). Multicores with an intact sediment-water interface were processed, and these cores served to link gravity cores to the sediment-water interface. Total CO₂ (TCO₂: [H₂CO₃]+[HCO₃⁻]+[CO₃²⁻]) was analyzed with a Coulemetrics coulometer as previously described (Berelson et al., 2005) and pore water sulfate was analyzed using the turbidimetric method (Tabatabai, 1974).

Nucleic acid extraction and purification

Total DNA was extracted from sediment samples (0.5 g) using a Powersoil DNA extraction kit (Mo Bio Laboratories, Carlsbad, CA). The Mo Bio protocol was modified by initially heating the sample at 65°C twice for 5 min, followed by bead beating using a Fastprep machine (Bio101-Thermo Electron Corp., Gormley, Ontario, Canada) set at a speed of 5.0 for 45 s. The extracts from two independent extractions were combined and cleaned by cesium chloride density gradient centrifugation as previously described (Orphan et al., 2001). The washed and purified DNA was recovered in Tris-EDTA buffer using a Microcon membrane device (YM-100 or Amicon Ultra-4; Millipore, Billerica, MA). Bacterial and archaeal 16S rRNA gene clone libraries from sediment horizons corresponding to depths above (50 cm and 103 cm), within (125 cm and 139 cm), and below (163 cm) the SMTZ were constructed. Parallel with the rRNA gene analysis, metabolic gene clone libraries for the fragment encoding the alpha and beta subunits of dissimilatory sulfite reductase (*dsrAB*; Wagner et al., 2005), and for the fragment encoding the alpha subunit of methyl coenzyme M reductase (*mcrA*) were constructed (Table 1).

TABLE 1. Microbial diversity of SBB sediment

Domain	Library	Richness	Total abundance	Shannon-Wiener diversity index	Evenness	Simpson's diversity index (1 - D)	PCR result ^a		
							16S rRNA	mcr	dsr
Bacteria	50-cm	18	168	2.586	0.895	0.906	+		
	103-cm	26	69	2.886	0.886	0.917	+		+
	125-cm	32	92	2.986	0.862	0.926	+		+
	139-cm	20	88	2.440	0.814	0.877	+		+
	163-cm	18	86	2.462	0.852	0.887	+		+
Archaea	50-cm	18	92	2.427	0.840	0.883	+		
	103-cm	24	96	2.194	0.690	0.763	+	-	
	125-cm	15	90	2.266	0.837	0.862	+		+
	139-cm	14	69	1.907	0.723	0.761	+		+
	163-cm	13	96	1.826	0.712	0.779	+		+

^a +, environmental clone library was assembled from the targeted gene; -, amplification by PCR was unsuccessful.

Archaeal and bacterial 16S rRNA gene, mcrA, and dsrAB library construction

PCR mixtures (25 µl) were prepared as follows: 1 µl Hotmaster PCR buffer with 1.5 mM MgCl₂, 0.2 mM of deoxynucleoside triphosphates, 0.1 µg of each primer, and 0.25 µl of Hotmaster *Taq* polymerase (Eppendorf AG, Hamburg, Germany). Archaeal 16S rRNA genes were

PCR amplified using archaeon-specific primers AR-8F (5'-TCCGGTTGATCCTGCC-3') and AR-958R (5'-YCCGGCGTT GAMTCCAATT-3'), and bacterial libraries were constructed using bacterium specific forward primer BAC-27F (5'-AGAGTTTGATCCTGGCTGAG-3') and universal reverse primer U-1492R (5'-GGTTACCTTGTTACGACTT-3', Delong, 1992; Lane, 1991). PCR amplifications were performed in a Eppendorf Mastercycler using an initial denaturing step of 95°C for 2 min, followed by 30 cycles (archaea) or 27 cycles (bacteria) of 94°C for 1 min, 54°C for 1 min, and 72°C for 1 min and then an elongation step of 72°C for 6 min. PCR mixtures started with 0.1, 1, and 2 µl template were pooled to minimize PCR artifacts associated with differences in template abundance (Polz and Cavanaugh, 1998).

A 480 bp fragment of *mcrA* was amplified with primers *MCR-F* (5'-GGTGG TGTMGGATTCACACAR-3') and *MCR-R* (5'-TTCATTGCRTAGTTWGR TAG-3') (Luton et al., 2002) using an initial denaturing step of 95°C for 3 min, followed by 40 (163 cm and 125 cm samples) or 45 cycles (139 cm sample) of 94°C for 1 min, 50°C for 1 min, and 72°C for 1 min and then a final elongation step of 72°C for 6 min. *mcrA* amplification was attempted for depths of 103 cm and below. The 103 cm horizon did not yield an *mcrA* amplicon. A 1.9 kb fragment of *dsrAB* was amplified using a mixture of primers, DSR1F mix and DSR4R mix (Wagner et al., 2005). To minimize significant nonspecific product formation observed using standard PCR, a touchdown PCR procedure was performed with the annealing temperature decreasing (1°C every two cycles) from 61 to 54°C for the first 15 cycles, which was followed by 22 cycles of 94°C for 1 min, 54°C for 1 min, and 72°C for 3 min and then a final elongation step of 72°C for 6 min. This touchdown procedure significantly reduced the products with multiple sizes observed with standard PCR and generated a robust 1.9 kb PCR product.

Sequence and phylogenetic analysis

PCR products of the correct size were cloned using either the pCR4-TOPO (Invitrogen, Carlsbad, CA) or pGEM-T Easy (Promega, Madison, WI) system according to the manufacturer's instructions. The amplified inserts were further analyzed by using restriction fragment length polymorphism (RFLP) with either *HaeIII* (for 16S rRNA genes and *dsrAB*) or *RsaI* (for *mcrA*) (New England Biolabs, Ipswich, MA) to identify unique RFLP patterns for sequencing. One or two unique clones from each RFLP pattern were selected. Unique clones from each library were bidirectionally sequenced using a CEQ 8800 capillary sequencer according to the DTCS protocol (Beckman Coulter, Fullerton, CA). For most samples, vector-targeted primers T7 and M13R were used. Inserts more than 1-kb-long (i.e., bacterial 16S rRNA gene and *dsrAB* libraries) were additionally sequenced using 16S rRNA targeted primer 515F (5'-GTGCCAGCMGCCGCGGTAA-3') and internal *dsrAB*-targeted primers 1FI (5'-CAGGAYGARCTBCAYCG-3') and 1R1 (5'-CCCTGGGTRTGNAYRAT-3') (Bahr et al., 2005, Dhillon et al., 2003). For phylogenetic analysis, only the *dsrA* subunit was used, resulting in a bidirectional sequence combining a vectortargeted primer with an internal *dsr* primer. Sequence assembly was performed using Sequencher 4.5 software (Gene Codes, Ann Arbor, MI). The closest relatives of the retrieved sequences in the GenBank database were identified using BLASTN (Altschul et al., 1997). Potential chimeric sequences were identified using CHIMERA_CHECK (Cole et al., 2005) and Bellerophon (Huber et al., 2004). For the 16S rRNA gene, sequence data were compiled by using the ARB software package (Ludwig et al., 2004) and were initially aligned using the ARB Fast Aligner utility. The resulting alignments were manually verified using known secondary structure regions. For phylogenetic analysis, the alignments were exported to PAUP*4.0 (Swofford et al., 1998). Bacterial 16S rRNA gene phylogenies were constructed using MEGA 4 (Tamura et al., 2007). Tree reconstruction was performed with the distance matrix and maximum parsimony algorithms.

For 16S rRNA genes, trees based on 519 and 1,251 unambiguously aligned positions were constructed for archaeal and bacterial 16S rRNA genes, respectively. *mcrA* and *dsrA* trees were based on 147 and 164 translated amino acid characters.

Statistical methods

Correspondence analysis (CA; Hill, 1974) was applied to SBB 16S rRNA clone libraries and libraries for similar marine sedimentary environments obtained from the literature (see Table S1 in the supplemental material) in order to discern patterns of variation among major phylogenetic groups for different geochemical environments. Clone libraries were characterized by previously described geochemistry data or by sediment description and were normalized to describe variation between 10 dominant groups (see Table S1 in the supplemental material). Data sets that contained fewer than 30 environmental clones or in which ~ 50% of the phlotypes fell outside these divisions were excluded (see Table S1 in the supplemental material). Correspondence analysis was implemented using DECORANA software (Hill and Gauch, 1980) and provides a visual representation of the relationship between samples (i.e., each library) and species (unique phylogenetic groups) along ordination axes calculated to maximize correlation between samples and species scores (Hill and Gauch, 1980). Neighbor-joining phylogenetic trees constructed for representative SBB 16S rRNA sequences and additional sequences from related environments were used in UniFrac analysis (Lozupone and Knight, 2005). UniFrac derives an environmental distance matrix from the portion of a phylogenetic tree that may be uniquely ascribed to a specific environment (clone library). We used both unweighted (Lozupone and Knight, 2005) and weighted (Lozupone et al., 2007) UniFrac to describe the similarity between clone libraries derived from common environmental conditions, as assigned above. Weighted UniFrac uses clonal abundance of specific sequences to

adjust the environmental distance calculated with the unweighted algorithm based on each environment's unique portion of the phylogenetic tree.

Nucleotide sequence accession numbers

The nucleotide sequences of the rRNA gene clones have been deposited in the GenBank database under accession no. EU181461 to EU181514 and FJ455875 to FJ455963, the nucleotide sequences of the *mcrA* clones have been deposited in the GenBank database under accession no. FJ456011 to FJ456019, and the *dsrA* sequences have been deposited in the GenBank database under accession no. FJ455964 to FJ456010.

Results

Geochemical analyses

Pore water profiles acquired from SBB gravity cores indicate that the SMTZ was approximately 140 cm beneath the sediment-water interface. The observed TCO₂ concentration gradient was linear ($R^2 = 0.91$) from 30 cm below the sediment-water interface down to about 120 cm to 155 cm, where a change in slope corresponding to the SMTZ was documented (Fig. 1). The sulfate concentration gradient was also linear through this portion of the core, and there was a change in the slope at the SMTZ. Models of these concentration gradients suggest that reactions involving sulfate and CO₂ occur within the SMTZ but cannot be explained by AOM exclusively (Berelson et al., 2005; W. M. Berelson and F. Sansone, unpublished data). Based on linear gradients and as determined by the methodology described by Berelson et al. (2005), the diffusive flux of methane to the sulfate-methane interface (0.5 ± 0.05 mmol/m²day) is less than the change in the TCO₂ flux occurring at the horizon (0.7 ± 0.1 mmol/m²day), thus, methane

oxidation is probably not the only source of TCO₂ added to this horizon, and we hypothesize that there may be an additional, localized source of TCO₂ generated by sulfate oxidation of organic carbon specifically at the SMTZ.

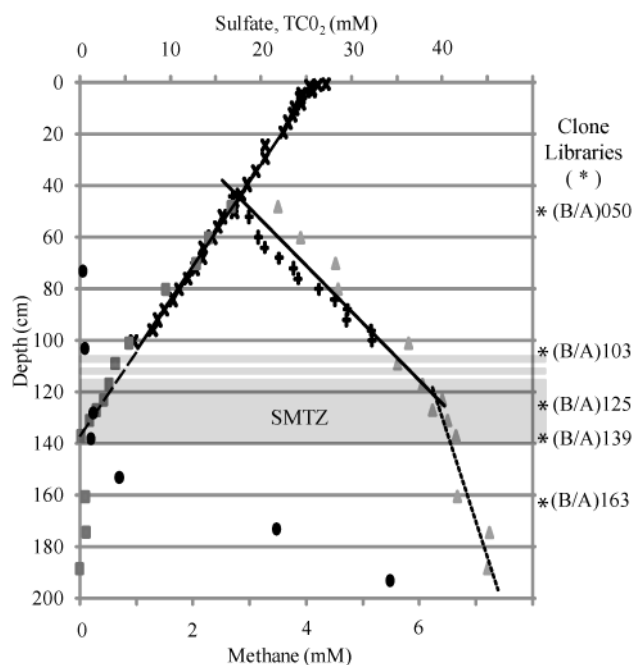


Fig. 1. Trendlines indicate approximate TCO₂ and sulfate profiles in Santa Barbara Basin Sediment. The change in slope of the TCO₂ gradient at ~ 125 cm suggests CO₂ production at depth. Methane measurements were taken from gravity core (GC) 5 (●), sulfate measurements from multicores (MC) 5 and 13 (X) and GC2 (■), and TCO₂ measurements from MC13 (+) and GC2 (▲).

Patterns of species richness in SBB

Microbial diversity was assessed by RFLP screening of 503 bacterial and 395 archaeal clones from the five discrete depth horizons from core GC-2 (see Fig. S1 in the supplemental material). Shannon-Wiener and Simpson's diversity indices indicate that there is decreasing archaeal diversity with increasing depth in SBB sediment, while the recovered bacterial 16S rRNA diversity appears to increase from the uppermost 50 cm to the 125 cm horizon in the upper part of the SMTZ and then declines at depths below 139 cm (Table 1). In all but the 50 cm depth horizon, the bacterial species richness was greater than the archaeal species richness.

Changes in diversity indices with depth were not consistent between archaeal and bacterial clone libraries. However, for each domain the 125 cm upper SMTZ horizon appeared to represent a local maximum for both diversity indices.

TABLE 2. Distribution of major phylogenetic groups

Domain	Division	Subdivision or subgroup	Abundance (%) in clone libraries ^a					Avg
			50-cm	103-cm	125-cm	139-cm	163-cm	
Bacteria	Proteobacteria	Alphaproteobacteria	1.8	1.4	3.3	0.0	0.0	1.4
		Betaproteobacteria	8.9	0.0	0.0	0.0	0.0	3.0
		Gammaproteobacteria	4.2	2.9	0.0	0.0	0.0	1.8
		Deltaproteobacteria	0.0	5.8	47.8	39.8	14.0	18.9
		DSS	0.0	4.3	19.6	8.0	14.0	
		Eel-1	0.0	1.4	28.3	31.2	0.0	
	Planctomycetes		26.8	20.3	7.6	29.5	7.0	19.5
	GNS		13.7	5.8	8.7	2.3	39.5	14.1
	Firmicutes		2.4	4.3	1.1	0.0	0.0	1.6
	Acidobacteria		0.0	1.4	0.0	3.4	0.0	0.8
	Actinobacteria		0.0	2.9	3.3	2.3	0.0	1.4
	JS1		1.2	5.8	10.9	5.7	4.7	5.0
	OP1		11.3	5.8	0.0	0.0	17.4	7.6
	OP8		17.3	27.5	4.3	5.7	1.2	11.5
	OP11		0.0	1.4	3.3	0.0	0.0	0.8
	Other		12.5	14.5	9.8	11.4	16.3	12.7
	Archaea	Crenarchaeota	MBGB	23.0	70.8	29.8	59.3	37.6
MCG			17.2	4.2	2.4	3.4	7.5	7.3
MHVG ^b			2.3	0.0	0.0	0.0	0.0	0.5
Other			1.1	0.0	0.0	5.1	0.0	0.7
Euryarchaeota		Thermoplasmatales (MBGD)	57.5	25.0	60.7	11.9	10.8	34.4
		ANME-1	0.0	0.0	7.1	20.3	24.7	10.4
	Other	0.0	0.0	0.0	0.0	19.4	0.4	

^a For Bacteria, the numbers of clones in the 50-cm, 103-cm, 125-cm, 139-cm, and 163-cm clone libraries were 168, 69, 92, 88, and 86, respectively, and for the Archaea the numbers of clones in these libraries were 87, 72, 84, 59, and 93, respectively.

^b MHVG, marine hydrothermal vent group.

Microbial diversity overlying the SMTZ

The major groups recovered from the 50 cm and 103 cm horizons above the SMTZ were the *Planctomycetes*, green nonsulfur bacteria (GNS) (*Chloroflexi*), and candidate division OP8 (Fig. 2). *Planctomycetes* was the dominant bacterial phylum above the transition zone (Table 2). The majority of *Planctomycetes* sequences fall into the uncultured WPS-1 clade (Elshahed et al., 2007), which is common in environments with significant concentrations of organic matter, including marine continental margins (Fig. 2C) (Elshahed et al., 2007). Candidate division OP8 clones constitute ~ 22% of the 50 and 103 cm bacterial libraries, and the percentage then declines with depth. This group is a minor component of marine sediments, but it has been detected in similar methane-impacted environments, such as the Guaymas Basin (Teske et al., 2002), the Gulf of Mexico (Lloyd et al., 2006), and the Peru and Cascadia Margins (Inagaki et al.,

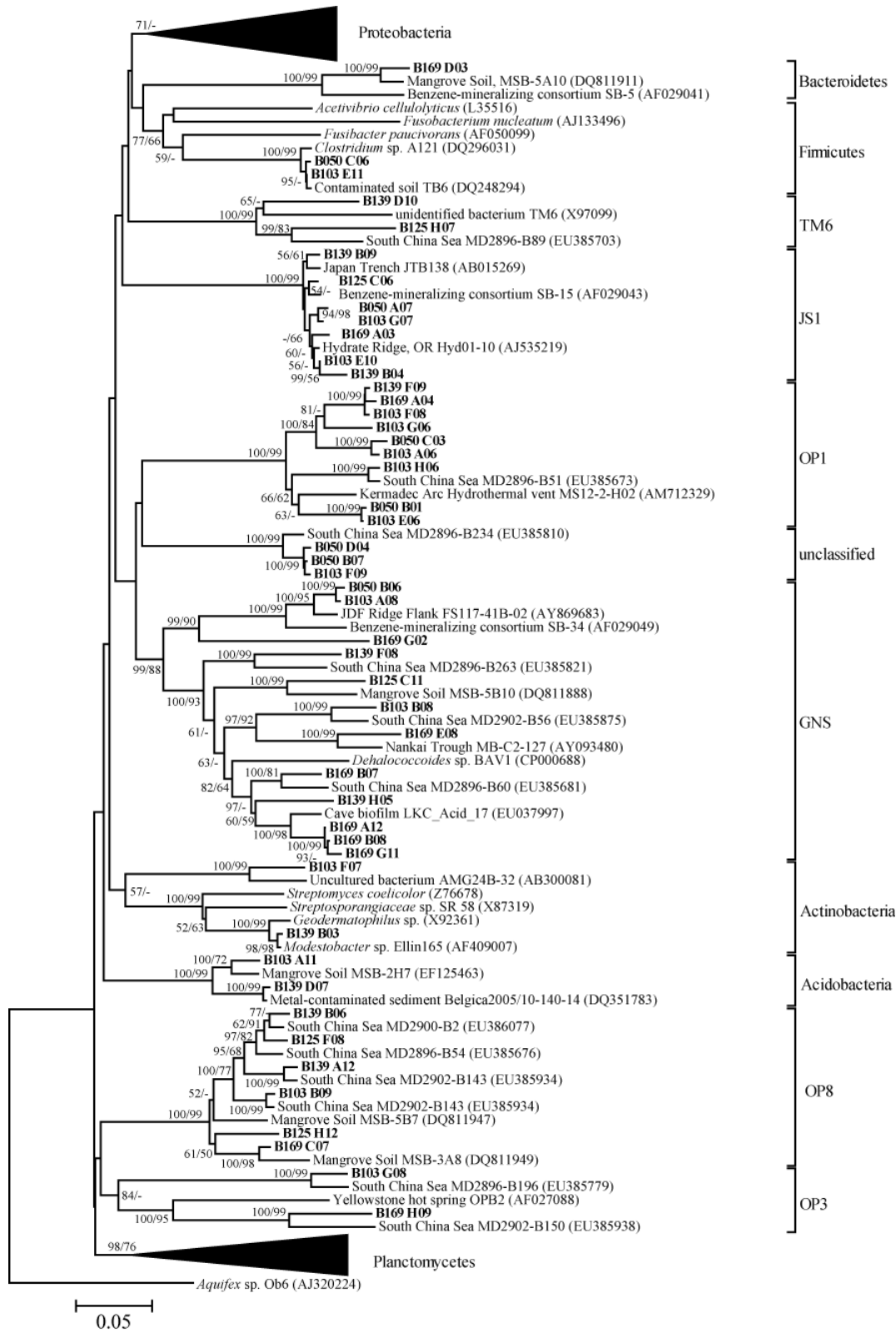


Fig. 2. Bacterial 16S rRNA Neighbor-Joining distance tree for representative Santa Barbara Basin sequences (in bold) based on 1465 characters. Bootstrap values are listed by distance/parsimony based on 2000/800 replicates. Values <50 are not listed. GNS: Green non-sulfur bacteria.

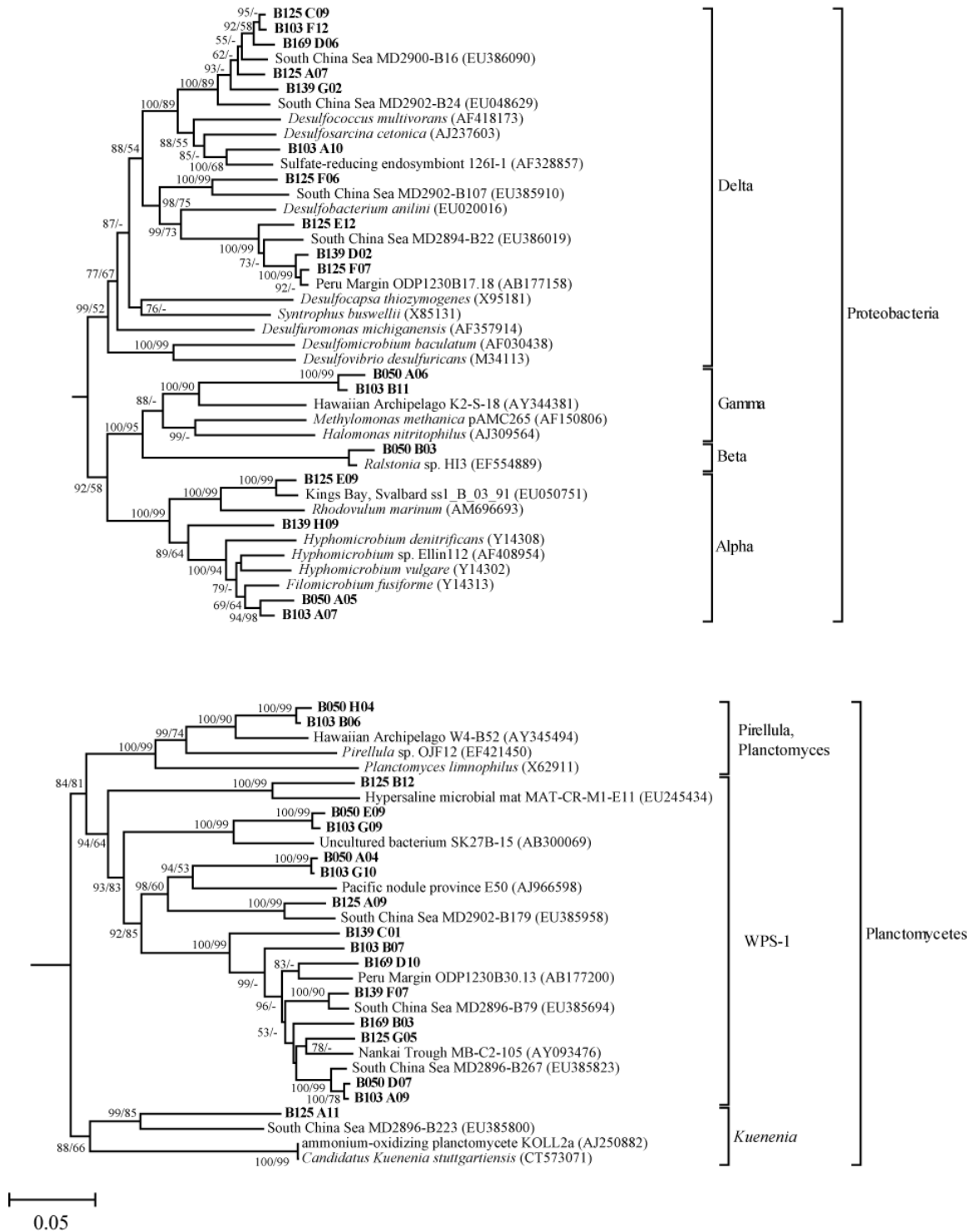


Fig. 2 (contd.). Expanded phylogeny of Bacterial 16S rRNA Neighbor-Joining distance tree for representative Santa Barbara Basin sequences (in bold) among b) proteobacteria and c) Planctomyces.

2006), as well as in iron- and sulfate-reducing zones of a hydrocarbon- contaminated aquifer (Dojka et al., 1998). *Gammaproteobacteria* and *Betaproteobacteria* sequences were recovered exclusively from sediments overlying the SMTZ (Table 2 and Fig. 2B). *Deltaproteobacteria* sequences were surprisingly absent from the 50 cm library and represented only 6% of the bacterial diversity recovered from the 103 cm sample. These low-abundance phylotypes were most closely related to putative sulfate reducing phylotypes recovered from the underlying SMTZ. The archaeal diversity at 50 cm was dominated (58%) by euryarchaeotal marine benthic group D (MBGD, Vetriani et al., 1999), related to the *Thermoplasmatales* (Fig. 3). The close relatives of the MBGD phylotypes included sequences recovered from other methane-impacted marine sediments (Hinrichs et al., 1999; Inagaki et al., 2006; Inagaki et al., 2003; Knittel et al., 2003), but they are not found exclusively in these habitats. Adjacent to and within the SMTZ, at 103 cm and 139 cm, *Crenarchaeota* marine benthic group B (MBGB) replaced MBGD as the dominant archaeal group, representing 71% and 61% of the clones, respectively.

Microbial diversity within the SMTZ

The most abundant bacterial phylotypes from the SMTZ were affiliated with the Eel-1 group within the *Deltaproteobacteria*, a cluster of putative sulfate-reducing bacteria first described from a methane seep in the Eel River Basin (Orphan et al., 2001) and distantly related to *Desulfobacterium anilini* (91% similarity). On average, the Eel-1 clade accounts for ~ 30% of both the 125 cm and 139 cm clone libraries (59% and 80% of the recovered *Deltaproteobacteria* phylotypes, respectively) (Table 2 and Fig. 3). The second most abundant clade of *Deltaproteobacteria* was related to the putative syntrophic *Desulfosarcina/Desulfococcus* clade (DSS) commonly recovered from seafloor methane seeps (Knittel et al., 2003, Orphan et al.,

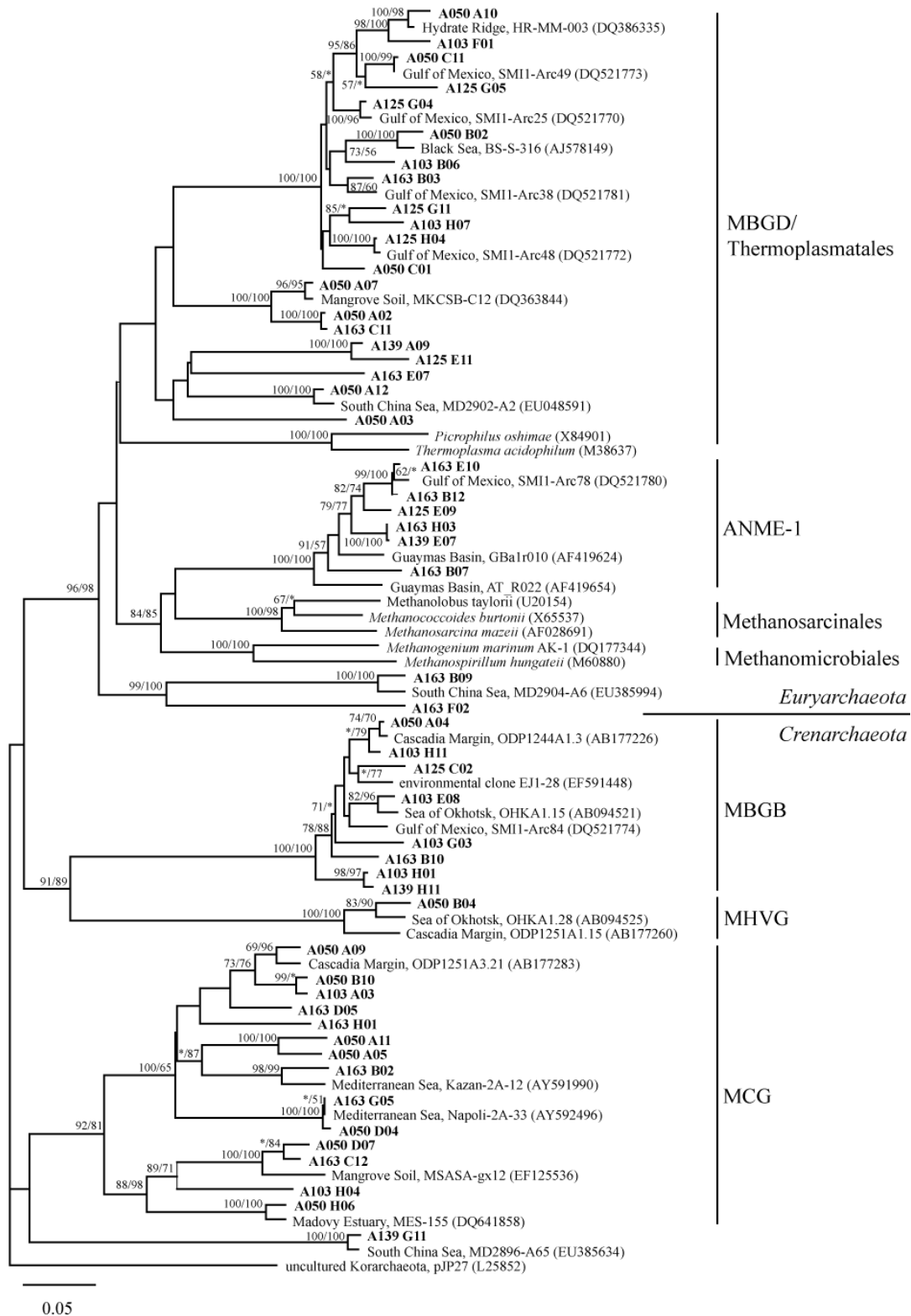


Fig. 3. Archaeal 16S rRNA Neighbor-Joining distance tree for representative Santa Barbara Basin sequences (in bold) based on 950 characters. Bootstrap values are listed by distance/parsimony based on 5000/200 replicates. Values <50 are not listed. MBGD: Marine Benthic Group D; MBGB: Marine Benthic Group B; MHVG: Marine Hydrothermal Vent Group; MCG: Miscellaneous Crenarchaeotal Group.

2001) (Table 2). In the SBB, DSS phylotypes were present within the SMTZ (~ 14% of the total), as well as the sediment above and below this zone. *Planctomycetes*-affiliated phylotypes related to the WPS-1 group were enriched in one of the SMTZ horizons; they represented 30% of the 139 cm bacterial library but only 8% of the 125 cm bacterial assemblage. Sequences belonging to candidate division JS1 represent only ~ 6% of the bacterial libraries. However, this group appears to be enriched within the SMTZ. Originally identified in Japan Sea sediments, members of candidate division JS1 have also been commonly recovered from methane hydrate-associated marine sediments, such as sediments from the Nankai Trough, Hydrate Ridge, and the Peru Margin (Inagaki et al., 2006; Knittel et al., 2003; Newberry et al., 2004). Additionally, sequences affiliated with the *Actinobacteria* were recovered with low abundance, but only from the SMTZ and the immediately overlying horizon (Fig. 2). Inferences based on the environmental distribution and cultured relatives suggest that these organisms are heterotrophic and may be adapted to sulfur- and/or methane-rich environments (Boschker et al., 1998).

In methane-containing horizons within and below the SMTZ, sequences closely related to uncultured ANME-1 archaea were recovered. These phylotypes were not present in the two sulfate-reducing horizons above the SMTZ (50 and 103 cm), which is consistent with their role in AOM. ANME-1-affiliated phylotypes accounted for 14% of the archaeal diversity within the SMTZ (125 and 139 cm), and the percentage increased to 24% in the sulfate-depleted sediments below this zone (163 cm). The ANME-1-affiliated sequences from all three depths formed two clades (95% similarity) falling in the ANME-1a group, which includes sequences from the Eel River Basin and Gulf of Mexico methane seeps (Hallam et al., 2003, Lloyd et al., 2006; Fig. 3).

Microbial diversity in sediments underlying the SMTZ

Members of the *Chloroflexi*, also referred to as the GNS, were the dominant bacteria beneath the SMTZ (163 cm) and represented 40% of the recovered bacterial diversity, compared to 6 to 14% in the horizons above the transition zone. GNS-affiliated sequences were quite diverse (75% overall similarity). Sequences from the 50 cm and 103 cm horizons group with the T78 clade, which is closely related to the dominant phylotype reported for Mediterranean sapropels (Coolen et al., 2002). Other sequences that were recovered from all depths but 50 cm and are dominant within and below the SMTZ group broadly with cultured strains of *Dehalococcoides*. Sequences associated with candidate division OP1 exhibited a distribution similar to that of the GNS group; the greatest abundance was recovered from the 163 cm library (17%), and these sequences were restricted primarily to sediments outside the SMTZ (50 cm, 103 cm, and 163 cm; Table 2).

Diversity of dissimilatory sulfite reductase and methyl coenzyme M reductase across the SMTZ

In order to further characterize the diversity of sulfate-reducing microorganisms associated with the SMTZ, dissimilatory sulfite reductase (*dsr*) genes were analyzed for the four lower horizons of the SBB core. Phylogenetic analysis of the most abundant *dsr* sequences confirmed the presence of sulfate-reducing *Deltaproteobacteria* (Fig. 4), with several sequences—exclusive to the SMTZ—clustering with *Desulfobacterium anilini* (group IV, Kaneko et al., 2007; and cluster D, Leloup et al., 2007). The sequences most commonly recovered from the 103 cm and 125 cm *dsr* libraries fall in a clade composed of uncultured *Deltaproteobacteria* and cluster with sequences from Black Sea and South China Sea sediments (DSS relatives, group I, Kaneko et al., 2007; and cluster B, Leloup et al., 2007). Additional *dsrA* diversity recovered from the SBB included deeply branching sequences related to *dsrA* genes reported from the

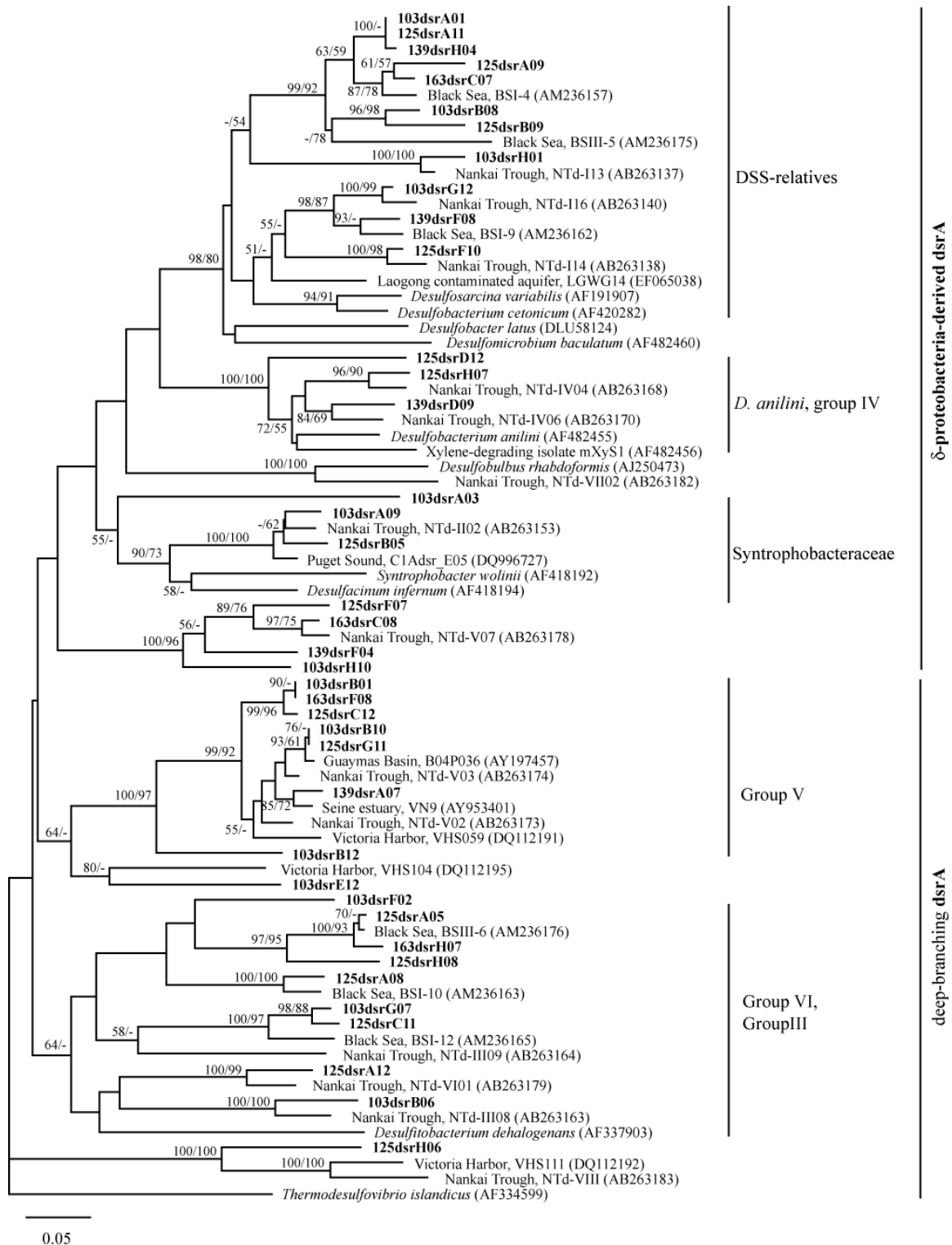


Fig. 4. Neighbor-joining distance tree based on 114 informative characters of translated partial dissimilatory sulfite reductase (dsrA) amino acid sequences from the Santa Barbara Basin. Bootstrap values are labeled by distance/parsimony based on 2000/100 replicates. Values <50 are not marked. Group names follow Kaneko et al., 2007.

Black Sea (clusters I, H, G, F; Leloup et al., 2007). The diversity and distribution of methanogens and methanotrophic archaea were examined using methyl coenzyme M reductase gene (*mcrA*) analysis. *mcrA* genes were successfully amplified from all sample depths below 125 cm but were not recovered from sediments above the SMTZ. *mcrA* phlotypes from the SBB exhibited limited diversity (92% similarity at the amino acid level), and all of them clustered within the previously described *mcrA* “group a”, which was assigned to the uncultured ANME-1 archaea (Hallam et al., 2003; Jorgensen et al., 2001; Lloyd et al., 2006; see Fig. S2 in the supplemental material).

Statistical comparison of diversity for methane-influenced marine sediments

As characterized by correspondence analysis (Hill, 1974), marine sediments harbor a diverse bacterial assemblage within which communities associated with different geochemical horizons and sediment depths (i.e., advective methane seeps and mud volcanoes, diffusion-controlled SMTZ, organic matter- and clay-rich sediments) overlap considerably (Fig. 5; see Fig. S3 in the supplemental material). Site-specific variations in physicochemical conditions, biogeographic influences, and a lack of standardized criteria for defining SMTZ horizons in the literature complicate the application of microbial diversity and abundance methods to statistically identify the SMTZ, the sulfate-replete horizon above the SMTZ, and the sulfate-depleted, methane-rich sediment below the SMTZ. Differences in the bacterial communities associated with these distinct geochemical horizons in the SBB are apparent; however, a statistically identifiable difference between the SMTZ and a lower methanogenic horizon was not observed, with both communities grouping within the 95% confidence interval defining the SMTZ-associated bacterial diversity (Fig. 5). Despite the coarse resolution afforded by correspondence analysis, trends in bacterial diversity between different geochemical and lithological sedimentary environments are apparent. For example, while there is substantial

overlap in the bacterial groups present in near-seafloor methane seeps and vents and diffusion-controlled deeper SMTZ horizons, the frequent enrichment of *Epsilonproteobacteria* in near-seafloor seeps along with the rare occurrence of this proteobacterial lineage at depth appears to be a distinguishing feature of these two methane-influenced habitats. Candidate division JS1 phylotypes are often associated with hydrate-bearing sediments (Webster et al., 2006), and may play a role in diffusion-based SMTZ horizons as well. Overall, the SMTZ-associated horizons cluster together as a subgroup in a broader range of marine sedimentary environments classified by high organic matter content (i.e., continental margin sediments) (Fig. 5; see Fig. S3 in the supplemental material).

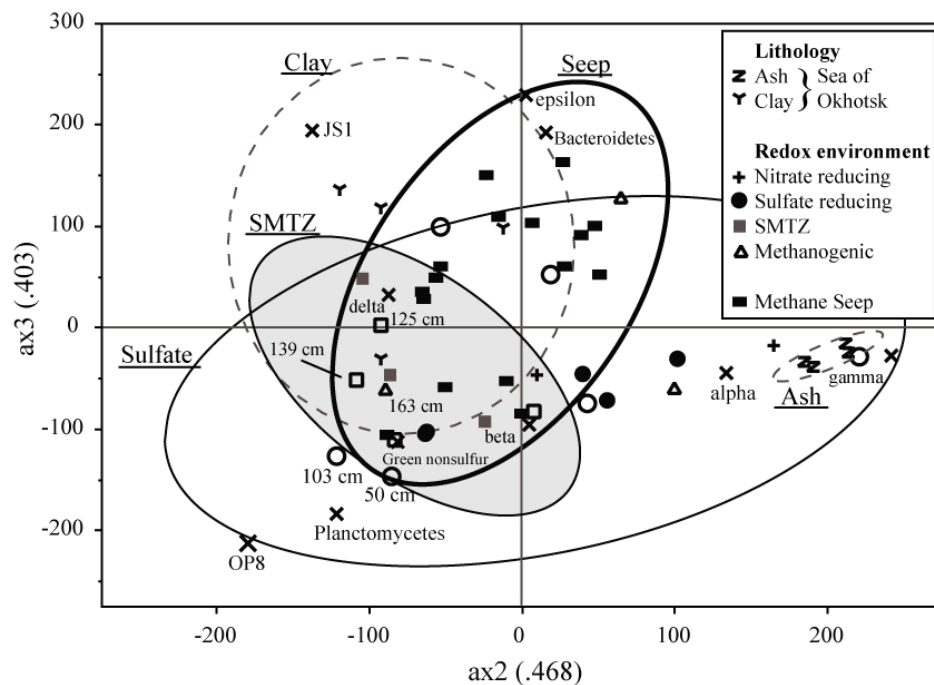


Fig. 5. Correspondence analysis (Hill, 1974) of marine sedimentary bacterial communities assigned to specific redox zones (Table S1). SMTZ-related communities overlap with near seafloor seep assemblages and other organic-rich sediments, similar in abundance of major phylogenetic groups and exhibiting enrichment particularly in the Deltaproteobacteria and, to a lesser extent, Planctomycetes. Detrended Correspondence Analysis (Hill and Gauch, 1980) and Principal Components Analysis exhibit similar distributions of sediment communities. Other significant axes of variation under the correspondence analysis exhibit similar environmental grouping (Figure S4). Open symbols indicate environments (>50 cmsf) and filled symbols reflect near seafloor habitats (0-30 cmsf). Redox zones and lithological classifications are as follows: ash (z), clay (y), SO₄ (●), NO₃ (+), CH₄ (▲), seafloor seep, vents and mud volcano (■), SMTZ (■). Alpha, Beta, Gamma, Delta and Epsilon correspond to their respective subdivisions among the proteobacteria (designated with X). 95% confidence ellipses are shown. The ellipse for SMTZ environments is shaded.

In our analysis, SMTZ horizons additionally exhibited enrichment of *Deltaproteobacteria*, consistent with dissimilatory sulfate reduction, and showed some enrichment of *Planctomycetes*-related phylotypes. Candidate division OP8 and *Betaproteobacterial* phylotypes also appear to be relatively abundant in some methane-impacted environments, but they were not enriched in the SBB SMTZ. The clustering of bacterial diversity within specific geochemical environments was similar when different axes of variation derived from correspondence analysis were used (see Fig. S3 and Table S2 in the supplemental material), as well as when detrended correspondence analysis and principal component analysis were used. Greater resolution of the variation in microbial assemblages associated with the transition through the SMTZ was achieved using the UniFrac metric (Lozupone and Knight, 2005). Applying UniFrac to the SBB sequences alone, we observed a close relationship between the SBB SMTZ horizons to the exclusion of sediments above and below, using the unweighted and weighted algorithms with our bacterial 16S rRNA data set (Fig. 6).

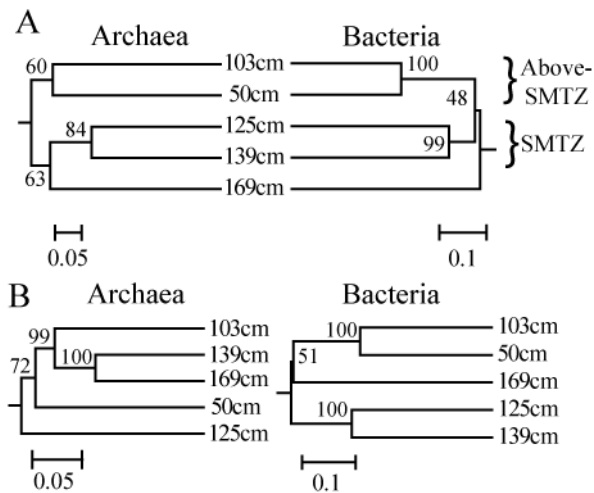


Fig. 6. UniFrac cladograms for 16S Archaeal and Bacterial community composition across the Sulfate-Methane Transition Zone (as assessed by environmental clone libraries). Jackknife values are based on 100 replicates. Values <40 are not listed. a) Unweighted UniFrac. b) Weighted UniFrac.

The relationship between SMTZ horizons persisted within the SBB *Deltaproteobacteria* (see Fig. S4 in the supplemental material). This observation suggests that the SMTZ horizons are broadly similar in terms of species richness and phylotype identity, predominantly within the *Deltaproteobacteria* but extending to other bacterial phyla as well. Compared to data for similar environments described previously (Heijs et al., 1998; Lloyd et al., 2006), SMTZ-related bacterial diversities from independent studies group together, again primarily due to close relationships within the *Deltaproteobacteria* (see Fig. S4 in the supplemental material). Similar clustering was observed for the archaea in the SBB; however, the clustering order was not maintained using the weighted algorithm, largely due to the abundance of MBGD sequences at 125 cm in contrast to the dominance of MBGB at 139 cm and the presence of ANME-1 in the 163-cm horizon (Fig. 6).

Discussion

Potential phylogenetic groups that may be associated with the unique physicochemical and ecological environment created by the intersection of methane and sulfate within the SBB SMTZ were characterized. A necessary component for increasing our understanding of the microbial ecology of this unique geochemical interface is a thorough characterization of microbial assemblages common to SMTZ horizons. Statistical analysis of common phylogenetic clades recovered from the SBB and previously published diversity surveys for similar environments highlight additional microbial groups not commonly associated with the anaerobic oxidation of methane which may be core components of the broader SMTZ microbial assemblage. While the physiology of phylotypes recovered in this study remains unresolved, the

distribution of the phylotypes in relation to the SMTZ provides some insight into their potential role in diffusion-controlled continental margin sediments.

Within the SBB, archaeal and bacterial libraries showed enhanced phylotype richness adjacent to and within the SMTZ, consistent with stimulation of phylogenetic and possibly metabolic diversity surrounding this redox transition zone (Table 1). Statistical analysis using the UniFrac metric demonstrated that there is a well-supported relationship between bacterial diversities within the upper and lower SMTZ horizons (Fig. 6). In general, the microbial community structure within the SBB SMTZ shares many similarities with the structures of other diffusion-controlled and advective marine organic matter-rich sedimentary systems, including phylotypes previously identified as mediators of AOM (ANME archaea and select *Deltaproteobacteria*) and other microorganisms in predominately uncultured clades, such as the *Planctomycetes*, GNS, and candidate divisions OP8 and JS1, whose ecological roles in this environment have not been defined. Compared to findings in studies of similar environments, a subset of SMTZ-related horizons from different geological settings cluster together within the bacterial domain using UniFrac, mainly due to close relationships within the *Deltaproteobacteria* and, to a lesser degree, *Planctomycetes* group WPS-1 (see Fig. S4 in the supplemental material).

Phyla characteristic of the SMTZ in the SBB

Within the SBB, members of the ANME-1a lineage appear to be the dominant methanotrophic archaeal group, based on analysis of 16S rRNA, recovered from both sediment horizons analyzed for the geochemically defined SMTZ. The presence of the ANME-1 group supports previous observations for advective methane seep environments indicating potential adaptation by this group to deeper sediments with reduced sulfate levels (Hinrichs et al., 1999; Knittel et al., 2005; Orphan et al., 2001). However, recent studies suggest that selective

pressures determining the distribution of the ANME groups are likely controlled by other ecological or physicochemical factors in addition to sulfate and methane concentrations (Kruger et al., 2008; Lloyd et al., 2006; Parkes et al., 2007). While data are limited, there appears to be no consistent trend for the ANME diversity recovered from diffusively controlled SMTZs. For example, organic matter-rich sediments of Skagerrak, Denmark, appeared to select for members of the ANME-2 and ANME-3 groups within and below the SMTZ (Parkes et al., 2007). The potential for distinct ANME groups to carry out AOM at disparate localities complicates the use of these groups for broadly characterizing SMTZ microbial diversity by statistical analyses.

Bacterial diversity, largely dominated by *Deltaproteobacteria*, was significantly correlated for the two SMTZ horizons, suggesting that there is selective colonization of the SMTZ by related bacterial phylotypes (Fig. 6; see Fig. S4 in the supplemental material).

Deltaproteobacteria sequences affiliated with sulfate-reducing bacteria were enriched within both SMTZ horizons relative to sediment horizons above and below this zone. Sulfate-reducing microorganisms that may be involved in sulfate-mediated AOM and/or organic carbon remineralization in the SMTZ included phylotypes previously reported for near-seafloor methane seeps, including members of the cosmopolitan DSS group and the *Desulfobacterium*-affiliated Eel-1 group (Orphan et al., 2001). The facultatively syntrophic DSS clade has been described for diverse marine sedimentary environments (Leloup et al., 2006; Musmann et al., 2005; Purdy et al., 2002; Ravensschlag et al., 1999), and members of this group were recovered from all horizons except the uppermost horizon in the SBB. Likewise, the distribution and enrichment of the *Desulfosarcina*-related *dsrA* sequence, closely related to sequences recovered from Black Sea sediments near the SMTZ (Leloup et al., 2007), further support the common occurrence of this SBB lineage in diverse marine sedimentary environments.

A comparison of methane-associated environments where members of the Eel-1 group have been recovered indicates co-occurrence and a possible relationship with members of the methanotrophic ANME-1 group (Hallam et al., 2004; Hinrichs et al., 1999; Lloyd et al., 2006; Orphan et al., 2001). The significant enrichment of this group within the SBB SMTZ relative to surrounding sediment horizons suggests that members of the Eel-1 clade may be linked to AOM and/or involved in sulfate-dependent organic carbon remineralization hypothesized to be enhanced within the transition zone. While the physiology of the uncultured Eel-1 clade has not been described, related *Desulfobacterales* isolates and Eel-1-containing enrichment cultures are capable of degrading aromatic hydrocarbons (Harms et al., 1999; Phelps et al., 1998), suggesting that members of the Eel-1 group may utilize complex sources of carbon associated with the SMTZ. As Eel-1 members have not been cultured, the associated *dsrAB* sequence is currently not known. However, the distributions of Eel-1 phylotypes and *Desulfobacterium*-related group IV *dsrA* suggest a possible link based on phylogenetic inference.

In addition to the *Deltaproteobacteria*-affiliated *dsrA* clades in the SBB, there were also a number of deeply branching *dsr* clades within and surrounding the SMTZ, implying that there may be additional, as-yet-unidentified microorganisms with the capacity for sulfate reduction that were not readily identified or recovered in the parallel 16S rRNA survey. Many of these *dsrA* phylotypes clustered with sequences recovered from similar environments, in particular sequences from the Nankai Trough (Kaneko et al., 2007) and Black Sea (Leloup et al., 2007). Some phylotypes, like the *Syntrophobacter*-affiliated clade, likely represent additional diversity within the *Deltaproteobacteria*, while other deeply branching clades were represented only by environmental sequences and may be associated with novel groups of sulfate reducing bacteria. While horizontal gene transfer may obscure the phylogenetic correlation between 16S rRNA and

dsr (Klein et al., 2001), the substantial diversity of uncultured 16S rRNA candidate divisions detected in the SBB and related methane-impacted sedimentary environments indicates that one or more of these uncultured lineages may be capable of dissimilatory sulfate reduction.

Defining a global community signature for the SMTZ by microbial phylogeny

Statistical evaluation of the microbial diversity recovered from the SBB revealed microbial groups common to the SMTZ whose clonal abundance changes across this geochemically defined horizon, including the *Planctomycetes*, candidate division JS1, *Actinobacteria*, Crenarchaeota MBGB, and *Thermoplasmatales*-related Euryarchaeota (Table 2). These groups contribute to a general SMTZ signature (Fig. 6) but are not necessarily associated with AOM. Correspondence analysis of a broad range of organic matter-rich and methane-impacted marine sedimentary environments in addition to the SBB revealed a possible relationship between *Deltaproteobacteria*, GNS, and *Planctomycetes* in SMTZ-related environments (Fig. 5; see Fig. S3 in the supplemental material).

In addition to the predicted enrichment of sulfate reducing *Deltaproteobacteria* within the SMTZ, the implied relationship between members of the *Planctomycetes*, GNS, and, in some settings, candidate division JS1 and *Betaproteobacteria* in the SMTZ is less clear. The *Planctomycetes*-affiliated WPS-1 clade was abundant in the lower 139 cm SMTZ horizon but was not confined exclusively to the redox interface in the SBB. The apparent affinity of this clade for organic matter-rich, anaerobic environments suggests that the WPS-1 clade may be an important group of heterotrophs within the SMTZ. The relative percentage of candidate division JS1 (previously identified as OP9 related, Webster et al., 2004) increased slightly within the SBB

SMTZ. The apparent relationship of the organisms in this clade with hydrate-bearing deep subseafloor habitats (Inagaki et al., 2006) and their ability to anaerobically metabolize organic carbon (Webster et al., 2004; 2006) suggest that this group may also contribute to enhanced carbon cycling within the SMTZ.

SMTZs frequently exhibit enrichment of one or more of the methanotrophic ANME groups; however, exceptions have been noted, opening the possibility that additional lineages (e.g., MBGB) may be involved in methane oxidation (Biddle et al. 2006; Sorensen and Teske, 2006). The distribution of archaeal diversity in our study supports the observation of MBGB enrichment in association with methane and active AOM assemblages (Inagaki et al., 2006). In contrast, the miscellaneous crenarchaeotal group (MCG) exhibited a negative relationship with the SBB SMTZ. Similar patterns of spatial segregation between the MCG and MBGB have been documented for other methane-influenced marine sediments (Inagaki et al., 2006; Sorensen and Teske, 2006), suggesting that unique adaptive traits and/or selective pressures may influence the distribution of the uncultured MBGB and MCG in these subseafloor habitats.

Geochemical modeling predicts that complex and integrated microbial processes involving anaerobic oxidation of methane and organic carbon mineralization are stimulated at the SMTZ. Through combined molecular analysis of microbial assemblages associated with SMTZ horizons around the globe, we are beginning to develop an understanding of the patterns of diversity associated with this important redox interface. The application of rigorous statistical tests to produce a unified overview of the common groups of microorganisms associated with the SMTZ within continental margin sediments is complicated by poor representation in the public databases, inconsistencies in defining and sampling the transition zone in published studies, and possible biogeographic differences. Nonetheless, characterization of key microbial

groups, such as the *Planctomycetes*, candidate division JS1, and the *Deltaproteobacteria* commonly inhabiting the SMTZ, in this and other studies is valuable and provides an essential framework for follow-up studies in which select lineages from the SMTZ can be studied in detail using quantitative measures.

Acknowledgments

We thank Shana Goffredi, Nicole Galli, Frank Sansone, Tapio Schneider and the shipboard party and crew of the *R/V New Horizon* for assistance with various aspects of this research. We also thank Abigail Green, David Fike, Patty Tavormina, Anne Dekas, Olivia Mason and for helpful comments and critical reading of this manuscript. This work was supported by a grant from the National Science Foundation (OCE-0433487) and a Gordon and Betty Moore Foundation young investigator award (to VJO).

References

- Altschul, S. F., T. L. Madden, A. A. Schaffer, J. Zhang, Z. Zhang, W. Miller, and D. J. Lipman. 1997. Gapped BLAST and PSI-BLAST: a new generation of protein database search programs. *Nucleic Acids Res.* 25:3389–3402.
- Bahr, M., B. C. Crump, V. Klepac-Ceraj, A. Teske, M. L. Sogin, and J. E. Hobbie. 2005. Molecular characterization of sulfate-reducing bacteria in a New England salt marsh. *Environ. Microbiol.* 7:1175–1185.
- Behl, R. J., and J. P. Kennett. 1996. Brief interstadial events in the Santa Barbara basin, NE Pacific, during the past 60 kyr. *Nature* 379:243–246.
- Berelson, W. M., M. Prokopenko, F. J. Sansone, A. W. Graham, J. McManus, and J. M. Bernhard. 2005. Anaerobic diagenesis of silica and carbon in continental margin sediments: Discrete zones of TCO₂ production. *Geochim. Cosmochim. Acta* 69:4611–4629.
- Biddle, J. F., J. S. Lipp, M. A. Lever, K. G. Lloyd, K. B. Sørensen, R. Anderson, H. F. Fredricks, M. Elvert, T. J. Kelly, and D. P. Schrag. 2006. Heterotrophic Archaea dominate sedimentary subsurface ecosystems off Peru. *Proc. Nat. Acad. Sci. U.S.A.* 103:3846–3851.
- Borowski, W. S., C. K. Paull, and W. Ussler. 1996. Marine pore-water sulfate profiles indicate in situ methane flux from underlying gas hydrate. *Geology* 24:655–658.
- Boschker, H. T. S., S. C. Nold, P. Wellsbury, D. Bos, W. de Graaf, R. Pel, R. J. Parkes, and T. E. Cappenberg. 1998. Direct linking of microbial populations to specific biogeochemical processes by ¹³C-labelling of biomarkers. *Nature* 392:801–805.
- Cole, J. R., B. Chai, R. J. Farris, Q. Wang, S. A. Kulam, D. M. McGarrell, G. M. Garrity, and J. M. Tiedje. 2005. The Ribosomal Database Project (RDP-II): sequences and tools for high-throughput rRNA analysis. *Nucleic Acids Res.* 33:D294–296.

- Coolen, M. J., H. Cypionka, A. M. Sass, H. Sass, and J. Overmann. 2002. Ongoing modification of Mediterranean Pleistocene sapropels mediated by prokaryotes. *Science* 296:2407–2410.
- DeLong, E. F. 1992. Archaea in coastal marine environments. *Proc. Nat. Acad. Sci. U.S.A.* 89:5685–5689.
- Devol, A. H., and S. I. Ahmed. 1981. Are high rates of sulphate reduction associated with anaerobic oxidation of methane? *Nature* 291:407–408.
- Dhillon, A., A. Teske, J. Dillon, D. A. Stahl, and M. L. Sogin. 2003. Molecular characterization of sulfate-reducing bacteria in the Guaymas Basin. *Appl. Environ. Microbiol.* 69:2765–2772.
- Dojka, M. A., P. Hugenholtz, S. K. Haack, and N. R. Pace. 1998. Microbial diversity in a hydrocarbon- and chlorinated-solvent-contaminated aquifer undergoing intrinsic bioremediation. *Appl. Environ. Microbiol.* 64:3869–3877.
- Elshahed, M. S., N. H. Youssef, Q. Luo, F. Z. Najjar, B. A. Roe, T. M. Sisk, S. I. Bühring, K. U. Hinrichs, and L. R. Krumholz. 2007. Phylogenetic and metabolic diversity of *Planctomyces* from anaerobic, sulfide- and sulfur-rich Zodletone Spring, Oklahoma. *Appl. Environ. Microbiol.* 73:4707–4716.
- Hallam, S. J., P. R. Girguis, C. M. Preston, P. M. Richardson, and E. F. DeLong. 2003. Identification of methyl coenzyme M reductase A (*mcrA*) genes associated with methane-oxidizing archaea. *Appl. Environ. Microbiol.* 69:5483–5491.
- Hallam, S. J., N. Putnam, C. M. Preston, J. C. Detter, D. Rokhsar, P. M. Richardson, and E. F. DeLong. 2004. Reverse Methanogenesis: Testing the Hypothesis with Environmental Genomics. *Science* 305:1457–1462.
- Harms, G., K. Zengler, R. Rabus, F. Aeckersberg, D. Minz, R. Rossello-Mora, and F. Widdel. 1999. Anaerobic oxidation of o-Xylene, m-Xylene, and homologous alkylbenzenes by new types of sulfate-reducing bacteria. *Appl. Environ. Microbiol.* 65:999–1004.
- Heijs, S. K., A. M. Laverman, L. J. Forney, P. R. Hardoim, and J. D. van Elsas. 2008. Comparison of deep-sea sediment microbial communities in the Eastern Mediterranean. *FEMS Microbiol. Ecol.* 64:362–377.
- Hill, M. O. 1974. Correspondence analysis: a neglected multivariate method. *Appl. Stat.* 23:340–354.
- Hill, M. O., and H. G. Gauch. 1980. Detrended correspondence analysis: An improved ordination technique. *Plant Ecology Appl. Environ. Microbiol.* 42:47–58.
- Hinrichs, K. U., J. M. Hayes, S. P. Sylva, P. G. Brewer, and E. F. DeLong. 1999. Methane-consuming archaeobacteria in marine sediments. *Nature* 398:802–805.
- Huber, T., G. Faulkner, and P. Hugenholtz. 2004. Bellerophon: a program to detect chimeric sequences in multiple sequence alignments. *Bioinformatics* 20:2317–2319.
- Inagaki, F., T. Nunoura, S. Nakagawa, A. Teske, M. Lever, A. Lauer, M. Suzuki, K. Takai, M. Delwiche, F. S. Colwell, K. H. Nealson, K. Horikoshi, S. D'Hondt, and B. B. Jorgensen. 2006. Biogeographical distribution and diversity of microbes in methane hydrate-bearing deep marine sediments on the Pacific Ocean Margin. *Proc. Nat. Acad. Sci. U.S.A.* 103:2815–2820.

- Inagaki, F., M. Suzuki, K. Takai, H. Oida, T. Sakamoto, K. Aoki, K. H. Nealson, and K. Horikoshi. 2003. Microbial communities associated with geological horizons in coastal subseafloor sediments from the sea of Okhotsk. *Appl. Environ. Microbiol.* 69:7224–7235.
- Iversen, N., and B. B. Jørgensen. 1985. Anaerobic methane oxidation rates at the sulfate-methane transition in marine sediments from Kattegat and Skagerrak (Denmark). *Limnol. Oceanogr.* 30:944–955.
- Jørgensen, B. B., A. Weber, and J. Zopfi. 2001. Sulfate reduction and anaerobic methane oxidation in Black Sea sediments. *Deep-Sea Res. Part I* 48: 2097–2120.
- Jiang, H. 2007. Microbial diversity in the deep marine sediments from the Qiongdongnan Basin in South China Sea. *Geomicrobiol. J.* 24:505–517.
- Jørgensen, B. B., A. Weber, and J. Zopfi. 2001. Sulfate reduction and anaerobic methane oxidation in Black Sea sediments. *Deep Sea Res. Part I* 48:2097–2120.
- Joye, S. B., A. Boetius, B. N. Orcutt, J. P. Montoya, H. N. Schulz, M. J. Erickson, and S. K. Lugo. 2004. The anaerobic oxidation of methane and sulfate reduction in sediments from Gulf of Mexico cold seeps. *Chem. Geol.* 205:219–238.
- Kaneko, R., T. Hayashi, M. Tanahashi, and T. Naganuma. 2007. Phylogenetic diversity and distribution of dissimilatory sulfite reductase genes from deep-sea sediment cores. *Mar. Biotechnol.* 9:429–436.
- Klein, M., M. Friedrich, A. J. Roger, P. Hugenholtz, S. Fishbain, H. Abicht, L. L. Blackall, D. A. Stahl, and M. Wagner. 2001. Multiple Lateral Transfers of Dissimilatory Sulfite Reductase Genes between Major Lineages of Sulfate-Reducing Prokaryotes. *J. Bacteriol.* 183:6028–6035.
- Knittel, K., A. Boetius, A. Lemke, H. Eilers, K. Lochte, O. Pfannkuche, P. Linke, and R. Amann. 2003. Activity, Distribution, and Diversity of Sulfate Reducers and Other Bacteria in Sediments above Gas Hydrate (Cascadia Margin, Oregon). *Geomicrobiol. J.* 20:269–294.
- Knittel, K., T. Losekann, A. Boetius, R. Kort, and R. Amann. 2005. Diversity and distribution of methanotrophic archaea at cold seeps. *Appl. Environ. Microbiol.* 71:467–479.
- Kruger, M., M. Blumenberg, S. Kasten, A. Wieland, L. Kanel, J. H. Klock, W. Michaelis, and R. Seifert. 2008. A novel, multi-layered methanotrophic microbial mat system growing on the sediment of the Black Sea. *Environ. Microbiol.* 10:1934–1947.
- Lane, D. J. 1991. 16S/23S rRNA sequencing, p. 115–175. *In* E. Stackebrandt and M. Goodfellow (ed.), *Nucleic Acid Techniques in Bacterial Systematics*. John Wiley and Sons, New York.
- Lanoil, B. D., R. Sassen, M. T. La Duc, S. T. Sweet, and K. H. Nealson. 2001. Bacteria and Archaea Physically Associated with Gulf of Mexico Gas Hydrates. *Appl. Environ. Microbiol.* 67:5143–5153.
- Leloup, J., A. Loy, N. J. Knab, C. Borowski, M. Wagner, and B. B. Jørgensen. 2007. Diversity and abundance of sulfate-reducing microorganisms in the sulfate and methane zones of a marine sediment, Black Sea. *Environ. Microbiol.* 9:131–142.
- Leloup, J., L. Quillet, T. Berthe, and F. Petit. 2006. Diversity of the *dsrAB* (dissimilatory sulfite reductase) gene sequences retrieved from two contrasting mudflats of the Seine estuary, France. *FEMS Microbiol. Ecol.* 55:230–238.
- Lloyd, K. G., L. Lapham, and A. Teske. 2006. An anaerobic methane-oxidizing community of ANME-1b archaea in hypersaline Gulf of Mexico sediments. *Appl. Environ. Microbiol.* 72:7218–7230.

- Lozupone, C., and R. Knight. 2005. UniFrac: a new phylogenetic method for comparing microbial communities. *Appl. Environ. Microbiol.* 71:8228–8235.
- Lozupone, C. A., M. Hamady, S. T. Kelley, and R. Knight. 2007. Quantitative and qualitative beta diversity measures lead to different insights into factors that structure microbial communities. *Appl. Environ. Microbiol.* 73:1576–1585.
- Ludwig, W., O. Strunk, R. Westram, L. Richter, H. Meier, Yadhukumar, A. Buchner, T. Lai, S. Steppi, G. Jobb, W. Forster, I. Brettske, S. Gerber, A. W. Ginhart, O. Gross, S. Grumann, S. Hermann, R. Jost, A. Konig, T. Liss, R. Lussmann, M. May, B. Nonhoff, B. Reichel, R. Strehlow, A. Stamatakis, N. Stuckmann, A. Vilbig, M. Lenke, T. Ludwig, A. Bode, and K. H. Schleifer. 2004. ARB: a software environment for sequence data. *Nucleic Acids Res.* 32:1363–1371.
- Luton, P. E., J. M. Wayne, R. J. Sharp, and P. W. Riley. 2002. The *mcrA* gene as an alternative to 16S rRNA in the phylogenetic analysis of methanogen populations in landfill. *Microbiology* 148:3521–3530.
- Marchesi, J. R., A. J. Weightman, B. A. Cragg, R. J. Parkes, and J. C. Fry. 2001. Methanogen and bacterial diversity and distribution in deep gas hydrate sediments from the Cascadia Margin as revealed by 16S rRNA molecular analysis. *FEMS Microbiol. Ecol.* 34:221–228.
- Mussmann, M., K. Ishii, R. Rabus, and R. Amann. 2005. Diversity and vertical distribution of cultured and uncultured *Deltaproteobacteria* in an intertidal mud flat of the Wadden Sea. *Environ. Microbiol.* 7:405–418.
- Nauhaus, K., A. Boetius, M. Kruger, and F. Widdel. 2002. In vitro demonstration of anaerobic oxidation of methane coupled to sulphate reduction in sediment from a marine gas hydrate area. *Environ. Microbiol.* 4:296–305.
- Newberry, C. J., G. Webster, B. A. Cragg, R. J. Parkes, A. J. Weightman, and J. C. Fry. 2004. Diversity of prokaryotes and methanogenesis in deep subsurface sediments from the Nankai Trough, Ocean Drilling Program Leg 190. *Environ. Microbiol.* 6:274–287.
- Niemann, H., T. Losekann, D. de Beer, M. Elvert, T. Nadalig, K. Knittel, R. Amann, E. J. Sauter, M. Schluter, and M. Klages. 2006. Novel microbial communities of the Haakon Mosby mud volcano and their role as a methane sink. *Nature* 443:854–858.
- Niewohner, C., C. Hensen, S. Kasten, M. Zabel, and H. D. Schulz. 1998. Deep Sulfate Reduction Completely Mediated by Anaerobic Methane Oxidation in Sediments of the Upwelling Area off Namibia-Reaktionen auf Variationen im Passat-Monsun-Windsystem und in der Advektion des Benguela-Kustenstroms. *Geochim. Cosmochim. Acta* 62:455–464.
- Orphan, V. J., K. U. Hinrichs, W. Ussler, 3rd, C. K. Paull, L. T. Taylor, S. P. Sylva, J. M. Hayes, and E. F. Delong. 2001. Comparative analysis of methane-oxidizing archaea and sulfate-reducing bacteria in anoxic marine sediments. *Appl. Environ. Microbiol.* 67:1922–1934.
- Parkes, R. J., B. A. Cragg, N. Banning, F. Brock, G. Webster, J. C. Fry, E. Hornibrook, R. D. Pancost, S. Kelly, N. Knab, B. B. Jorgensen, J. Rinna, and A. J. Weightman. 2007. Biogeochemistry and biodiversity of methane cycling in subsurface marine sediments (Skagerrak, Denmark). *Environ. Microbiol.* 9:1146–1161.
- Parkes, R. J., G. Webster, B. A. Cragg, A. J. Weightman, C. J. Newberry, T. G. Ferdelman, J. Kallmeyer, B. B. Jorgensen, I. W. Aiello, and J. C. Fry. 2005. Deep sub-seafloor prokaryotes stimulated at interfaces over geological time. *Nature* 436:390–394.

- Phelps, C. D., L. J. Kerkhof, and L. Y. Young. 1998. Molecular characterization of a sulfate-reducing consortium which mineralizes benzene. *FEMS Microbiol. Ecol.* 27:269–279.
- Polz, M. F., and C. M. Cavanaugh. 1998. Bias in template-to-product ratios in multitemplate PCR. *Appl. Environ. Microbiol.* 64:3724–3730.
- Purdy, K. J., T. M. Embley, and D. B. Nedwell. 2002. The distribution and activity of sulphate reducing bacteria in estuarine and coastal marine sediments. *Antonie van Leeuwenhoek* 81:181–187.
- Ravenschlag, K., K. Sahm, J. Pernthaler, and R. Amann. 1999. High bacterial diversity in permanently cold marine sediments. *Appl. Environ. Microbiol.* 65:3982–3989.
- Reeburgh, W. 1980. Anaerobic methane oxidation—rate depth distributions in Skan Bay sediments. *Earth Planet. Sci. Lett.* 47:345–352.
- Reed, D. W., Y. Fujita, M. E. Delwiche, D. B. Blackwelder, P. P. Sheridan, T. Uchida, and F. S. Colwell. 2002. Microbial communities from methane hydrate-bearing deep marine sediments in a forearc basin. *Appl. Environ. Microbiol.* 68:3759–3770.
- Sorensen, K. B., and A. Teske. 2006. Stratified communities of active Archaea in deep marine subsurface sediments. *Appl. Environ. Microbiol.* 72:4596–4603.
- Swofford, D. L. 1998. PAUP*. Phylogenetic Analysis Using Parsimony (* and Other Methods). Version 4. Sinauer Associates, Sunderland, Massachusetts.
- Tabatabai, M. A. 1974. Determination of sulfate in water samples. *Sulphur Inst. J.* 10:11–13.
- Tamura, K., J. Dudley, M. Nei, and S. Kumar. 2007. MEGA4: Molecular Evolutionary Genetics Analysis (MEGA) software version 4.0. *Mol. Biol. Evol.* 24:1596–1599.
- Teske, A., K. U. Hinrichs, V. Edgcomb, A. de Vera Gomez, D. Kysela, S. P. Sylva, M. L. Sogin, and H. W. Jannasch. 2002. Microbial diversity of hydrothermal sediments in the Guaymas Basin: evidence for anaerobic methanotrophic communities. *Appl. Environ. Microbiol.* 68:1994–2007.
- Thomsen, T. R., K. Finster, and N. B. Ramsing. 2001. Biogeochemical and molecular signatures of anaerobic methane oxidation in a marine sediment. *Appl. Environ. Microbiol.* 67:1646–1656.
- Treude, T., J. Niggemann, J. Kallmeyer, P. Wintersteller, C. J. Schubert, A. Boetius, and B. B. Jørgensen. 2005. Anaerobic oxidation of methane and sulfate reduction along the Chilean continental margin. *Geochim. Cosmochim. Acta* 69:2767–2779.
- Vetriani, C., H. W. Jannasch, B. J. MacGregor, D. A. Stahl, and A. L. Reysenbach. 1999. Population structure and phylogenetic characterization of marine benthic Archaea in deep-sea sediments. *Appl. Environ. Microbiol.* 65:4375–4384.
- Wagner, M., A. Loy, M. Klein, N. Lee, N. B. Ramsing, D. A. Stahl, and M. W. Friedrich. 2005. Functional marker genes for identification of sulfate-reducing prokaryotes. *Methods Enzymol.* 397:469–489.
- Webster, G., R. J. Parkes, B. A. Cragg, C. J. Newberry, A. J. Weightman, and J. C. Fry. 2006. Prokaryotic community composition and biogeochemical processes in deep subseafloor sediments from the Peru Margin. *FEMS Microbiol. Ecol.* 58:65–85.

- Webster, G., R. J. Parkes, J. C. Fry, and A. J. Weightman. 2004. Widespread occurrence of a novel division of bacteria identified by 16S rRNA gene sequences originally found in deep marine sediments. *Appl. Environ. Microbiol.* 70:5708–5713.
- Webster, G., L. C. Watt, J. Rinna, J. C. Fry, R. P. Evershed, R. J. Parkes, and A. J. Weightman. 2006. A comparison of stable-isotope probing of DNA and phospholipid fatty acids to study prokaryotic functional diversity in sulfate-reducing marine sediment enrichment slurries. *Environ. Microbiol.* 8:1575–1589.

Chapter 2

Method for assessing mineral composition-dependent patterns in microbial diversity using magnetic and density separation

Abstract

This study introduces a new method for characterizing mineral-associated microbial diversity in sedimentary environments, a habitat that has been intrinsically challenging to study in regard to microbe–mineral interactions. Mineral components were enriched from bulk environmental samples by magnetic susceptibility or density separation techniques and used in subsequent molecular and microscopic analyses. Testing and optimization of the method was performed on geochemically-distinct sediment horizons from Eel River Basin methane seeps and pyrite- and sphalerite-rich hydrothermal vent samples from the Lau Basin. Initial results show reproducible variations in microbial diversity between mineral fractions from marine sedimentary environments enriched in authigenic pyrite and/or transition metal-bearing clay minerals. Specifically, different archaeal clades associated with the anaerobic oxidation of methane and putative sulfate-reducing *Deltaproteobacteria* show preferential colonization patterns, suggesting potential ecophysiological differences between closely-related taxa. These results indicate that mineral colonization may influence the extent and distribution of microbial diversity throughout unconsolidated sediments of the marine subsurface. The combination of mineral separation and molecular analyses introduced here provide a new approach for revealing previously concealed patterns of mineral-associated microbial diversity across a wide range of environments, from hard rock habitats to fine-grained lithologies.

Introduction

Most microorganisms in subsurface environments are attached to solid particles (Alfreider et al., 1997). Initial contact between a living cell and a solid substrate may result from taxis (Childers et al., 2002) or passive transport (Morrow et al., 2005). These interactions are dependent upon properties of the cell wall as well as mineral structure and composition. Experimental studies have demonstrated that different attachment properties may be observed at the species level on diverse mineral substrates (e.g., Lower, 2005; Morrow et al., 2005; Bolster et al., 2006; Kim et al., 2009; Lutterodt et al., 2009; Andrews et al., 2010). The ecological and/or physiological causes of microbial association with specific mineral phases are varied. For example, mineral attachment may occur in response to environmental extremes (Decho, 2000) or be used as a predation defense (Matz et al., 2004; Wey et al., 2008). The abundance of active mineral-associated cells may be governed by nutrient availability and cell-cell interactions (Murray and Jumars, 2002). Microorganisms frequently exhibit increased abundance and growth on mineral substrates enriched in trace nutrients (Mauck and Roberts, 2007; Boyd et al., 2007; Roberts, 2004; Rogers and Bennett, 2004; Rogers et al., 1998) and may utilize mineral-bound electron acceptors or donors for the purpose of dissimilatory metabolism (Wirsen et al., 1998; Edwards et al., 2003; Lovley, 1991). Specific attachments between microorganisms and surfaces may result from mineral precipitation—either through initiating crystal nucleation (Fortin et al., 1997) or modifying chemical equilibria (Fortin et al., 1997; Tebo et al., 1997; Druschel et al., 2002; Southam and Saunders, 2005).

Mineral composition-dependent variation in microbial diversity may be detected by incubating a defined mineral substrate directly in the environment (e.g., Roberts, 2004; Edwards et al., 2003) or by sampling communities at coarse resolution from easily-segregated mineral

enclaves such as discrete zones of precipitation within hydrothermal chimneys (e.g., Kormas et al., 2006). These approaches are not easily applied to fine-grained environments such as marine and lacustrine muds. As a result, the impact of mineral composition on diversity in such environments has been difficult to characterize.

Recent efforts to study microbe-mineral associations in soil and sediment have prompted the development of new approaches for characterizing patterns of microbial colonization. For example, Wilson et al. (2008) used magnetic separation of minerals present within a soil followed by analysis of the dissociated mineral fractions to identify differences in the attached fungal communities. Magnetic susceptibility is an inherent property of all minerals derived from structural and chemical composition. This characteristic can be used to enrich for different mineral fractions within a heterogeneous mixture. Magnetic separation utilizes an applied magnetic field that extracts minerals having sufficient susceptibility from other components having a weaker response, typically with the use of an electromagnet (Rosenblum and Brownfield, 1999). Density separation may also discriminate mineral fractions of variable composition, including those having similar magnetic susceptibility (e.g., smectites, illites, kaolinite). Totten et al. (2002) found that clay minerals from a Gulf of Mexico sediment sample may be effectively partitioned with the use of high density liquids, for example. These electromagnetic and density-based separation methods have been commonly used to concentrate and differentiate minerals in geological and industry applications, but have not yet been broadly tested in geobiological studies.

We have developed an approach using separation of minerals by magnetic susceptibility and/or density, allowing the downstream molecular characterization of microbial diversity associated with discrete components of environmental samples. This method is suitable for

most environments exhibiting significant mineralogical diversity and ideal for the characterization of fine-grained marine sediments. We have tested this approach by characterizing the microbial diversity associated with discrete mineral phases of a hydrothermal black smoker chimney and separable partitions of a methane seep-influenced marginal marine sediment. Hydrothermal chimney sulfide minerals offer substrates differentiable by magnetic susceptibility which exhibit variable microbial colonization patterns (e.g., Kormas et al., 2006). Marine methane seeps offer highly active sedimentary environments in which microorganisms are spatially associated with, or induce the precipitation of, authigenic sulfides, carbonates, and clays (Tazaki and Fyfe, 1992). Terrigenous clay minerals supplied to the continental margin vary compositionally in the abundance of iron and other trace metals, which may be important for microbial metabolism within anoxic marine sediments (Vorhies and Gaines 2009). Based on previous observations that microorganisms in subsurface environments are predominantly attached to minerals and that preferential mineral colonization in diverse habitats can influence both the metabolism and growth of the associated microorganisms, as well as species composition, we predict that distinct colonization patterns between indigenous microorganisms and minerals are also prevalent in marine sediments, but have thus far been inaccessible due to a lack of appropriate methods. To explore these naturally-occurring associations in fine grained, heterogeneous sedimentary environments, we developed a cultivation-independent method that combines mineral enrichment methods with molecular techniques to identify specific minerals and microbial phylotypes that demonstrate composition-specific colonization patterns.

Sampling and Methods

Sampling

Sediment samples from the Northern Ridge of Eel River Basin (ERB) were collected at a depth of approximately 520 m using the HMDV *Alvin* in October of 2006. Sediment horizons from five push cores within and adjacent to methane seep communities (*Calyptogena* clams and sulfide-oxidizing microbial mats) were analyzed in this study, encompassing a range of porewater geochemical conditions. Push core 29 (PC29); described in Pernthaler et al (2008), was collected within an active methane seep, in a transition zone overlain by a sulfide-oxidizing microbial mat and chemosynthetic clams (40° 48.69' N, 124° 36.65'W). Push cores 23 and 17 were collected from the surrounding chemosynthetic clam beds. PC20 was collected approximately 5 m outside the mat and clam bed in an area lacking any visible seafloor expression of seepage. PC16 (Northern Ridge, ERB) was collected from a similar environment to PC20 at ~ 517 m water depth (40° 48.73' N, 124° 36.71' W). Characteristic geochemical profiles of these sediment core types have been previously described by Orphan et al. (2004). Subsamples were taken from sediments following pore water extraction of 3 cm-thick depth horizons. Samples were frozen shipboard at -80°C, transported on dry ice to the laboratory and stored at -80°C prior to processing. An additional sample was collected on a May 2005 expedition of the *R/V Melville* from an active black smoker hydrothermal chimney in the Kilo Moana vent field of the Lau Basin (20° 3.18'S, 176° 8.02'W, 2617m depth), transported to the lab on dry ice and stored at -80°C prior to processing.

Magnetic Separation

To partition environmental samples into discrete mineral components based on magnetic susceptibility, samples were first suspended in sterile 0.5M NaCl solution and then

passed through a magnetic trap to generate bimodal (paramagnetic vs. diamagnetic) separates, generating compositionally distinct mineral partitions. Separation ranges for targeted minerals were selected on the basis of literature values and experimental results (Fig. 1). Samples in this study were processed with a modified Frantz L-1 isodynamic magnetic separator (S.G. Frantz Co., Trenton, NJ).

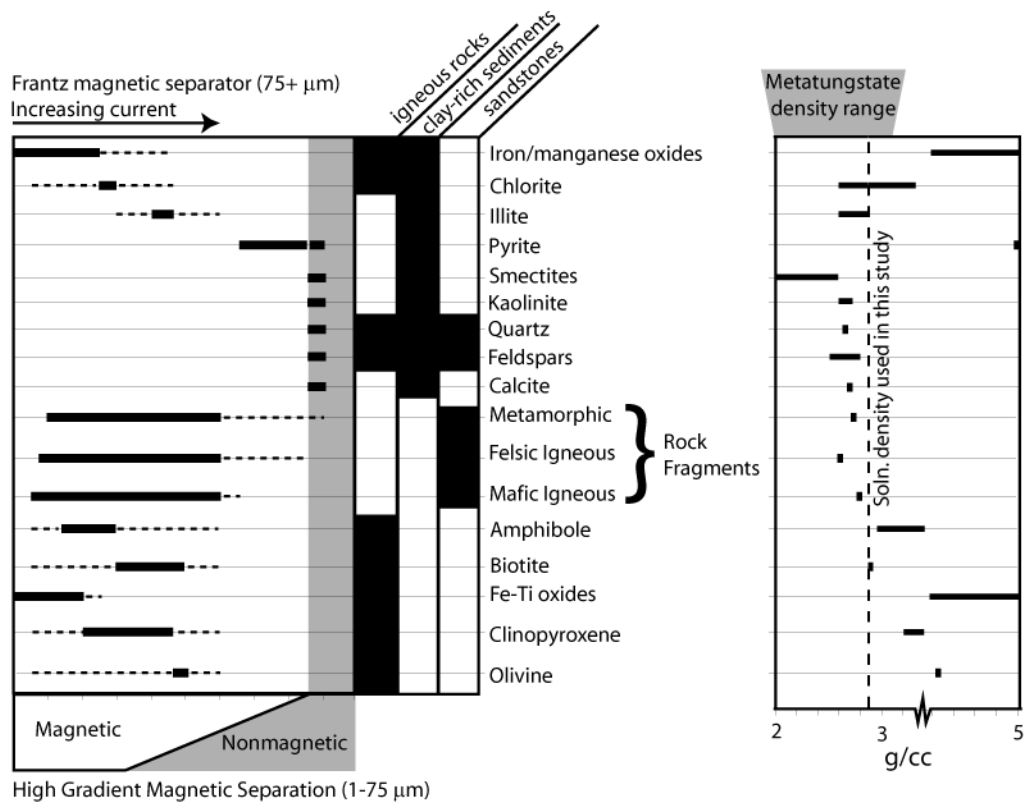


Fig. 1. Ideal extraction ranges for selected minerals using magnetic and density separations (solid lines). Dashed lines indicate full range of susceptibility. Shaded regions under particular lithological environments indicate typically encountered minerals. Mafic and felsic igneous and metamorphic rock fragment values refer to average composition. Values from Rosenblum and Brownfield (1999), Hunt (1995), and this study.

The Frantz separator is typically equipped with an open brass flow path for dry samples in which minerals are split according to magnetic susceptibility into parallel chutes. For fine-grained materials, such as those found in marine sediments and soils, mineral separation using the conventional Frantz separation protocol is difficult due to electrostatic interactions between

particles (Ghabru et al., 1988). Drying samples prior to separation is not well-suited for the preservation of attached cells. To improve compatibility with geobiological applications we designed an enclosed plastic flow path (after Lumpkin and Zaikowski, 1980) for use in the Frantz that may be used for magnetic separation of liquid slurries and is effective for large grain sizes ($> 75 \mu\text{m}$). Fine ($< 75 \mu\text{m}$) particles are not effectively separated in the modified Frantz flow path due to increasing relative force of drag in the liquid medium acting in opposition to magnetic force and the high rate of flow in a broad path. For fine slurries, High Gradient Magnetic Separation (HGMS) has been used in the purification of diamagnetic clays from liquid slurries by removing magnetic materials (e.g., Fe oxides; Schulze and Dixon, 1979) passed through a ferromagnetic trap within an applied magnetic field. Further studies have shown that Fe-bearing clay minerals may be concentrated in the magnetic fraction with this technique (Shulze and Dixon, 1979; Russell et al., 1984; Ghabru et al., 1988), using steel wire to bind paramagnetic particles. We have constructed HGMS flow paths using very fine steel wool for the $< 20 \mu\text{m}$ fraction and steel wires of 102, 200, and 280 μm diameter for the 20–75 μm fraction, inserted within Teflon tubing that had been pre-sterilized by UV-irradiation. Capture is optimal when the wire diameter is 2.31 times the diameter of the particle (Oberteuffer, 1974). The approach discussed in this study is therefore optimized for 50–100 μm but still effective for smaller grain sizes. More selective choice of wire size may improve separation quality.

Density separation

Density partitions of sediment samples were processed by suspension in sodium metatungstate (Krukowski, 1988) at 2.9g/cc, chosen to discriminate authigenic pyrite from other mineral components, centrifuged at 2,000g for 10 minutes at room temperature. “Dense” (negative buoyancy) minerals were concentrated in a pellet, while “light” (positive buoyancy) were concentrated in the supernatant. Repeat centrifugation steps were used to improve separation as needed. The supernatant was poured into a separate centrifuge tube and diluted to $< \sim 1.6$ g/cc medium density to recover the floating mineral partition in a separate pellet. The final supernatant, containing free cells and organic matter/biogenic debris, was discarded (this may, alternatively, be filtered for characterization of the free-living microbial community). Recovered minerals were rinsed twice in sterile media to remove trace amounts of metatungstate. Diluted metatungstate was passed through a 0.2 μm filter and UV-irradiated prior to drying and subsequent re-use. DNA was extracted from 1 g of pre-sterilized goethite that had been suspended in recycled metatungstate in order to test potential contamination. No amplicon for archaeal or bacterial 16S rRNA could be detected after 35 PCR cycles. Additionally, strong terminal fragments were not detected in samples separated using recycled metatungstate, suggesting sterilization protocols adequately prevent contamination of metatungstate solution in the studied environments.

Mineral composition analyses

Mineralogy subsamples were partitioned according to density and/or magnetic susceptibility, rinsed twice in 0.5M NaCl or nanopure H₂O, resuspended in 100% ethanol, and

dried for subsequent compositional analysis. A minimum of 0.5 g was recovered for X-Ray Diffractometry (XRD) and a minimum of 0.1 g for scanning electron microscopy (SEM). SEM images were acquired using a LEO 1550VP Field Emission SEM (Carl Zeiss SMT, Oberkochen, Germany) equipped with an INCA Energy 300 X-ray Energy Dispersive Spectrometer (EDS) system (Oxford Instruments, Abingdon, UK). XRD was performed on grain mounts of dried sample powders sieved to a < 53 μm size fraction, using a Philips PW1800 diffractometer (Philips Research Laboratories, Eindhoven, The Netherlands) according to standard XRD protocols.

DNA Extraction, PCR Amplification, and clone library construction

DNA was extracted from 0.1–1 g of each mineral partition using a MoBio soil DNA protocol modified for marine seep sediment samples according to Orphan et al. (2001) and, in the case of the hydrothermal chimney samples, a DNeasy tissue kit (Qiagen) was used. The 16S rRNA gene diversity of bacterial and archaeal DNA for the separated subsamples was assessed by PCR using the primers Ar8f, Bac27f, and U1492r (Lane et al., 1991; DeLong, 1992). PCR reaction mix was prepared in 25 μl reaction volumes as follows: 1X PCR buffer with 1.5 mM MgCl_2 ; 0.2 mM concentrations of deoxynucleoside triphosphates; 0.1 μg of each primer; 0.25 μl of Taq polymerase. Taq and buffer used were either Hotmaster Taq (Eppendorf AG, Hamburg, Germany) or Taq DNA Polymerase with ThermoPol Buffer (New England Biolabs, Ipswich, MA). Polymerase choice did not affect community signature in replicate analyses (data not shown). PCR utilized 30 or 32 cycles of 30 second, 94°C denaturing, 30 second, 54°C annealing, and 80 second, 72°C extension steps following an initial 2 minute, 95°C denaturing. Bacterial and archaeal environmental clone libraries using the PGEM T-Easy vector kit (Promega) were

assembled according to manufacturer's specifications for the pyrite-concentrated and bulk fractions of the Lau basin chimney sample. Bacterial and archaeal clone libraries were also generated for the 0–3 cm sediment horizon of PC29 composed of 87 and 92 clones, respectively. Clones were screened by RFLP using the HaeIII restriction enzyme (New England Biolabs, Ipswich, MA) and unique clones selected for partial sequencing for the identification of restriction sites. Full-length sequences derived from the Lau Basin hydrothermal chimney sample have been submitted to GenBank under accession numbers JF738090-JF738109.

T-RFLP

For terminal restriction fragment length polymorphism (T-RFLP) analysis, a 32-cycle PCR was carried out using fluorescently labeled Ar8f (WellRed dyes D2 or D4) and Bac27f (WellRed dye D3) primers and unlabeled reverse primers Ar958r (DeLong, 1992) and U1492r. For mineral samples producing a weak primary amplicon a second, 10-cycle PCR was performed on 1 µl of a 1:3 dilution of an initial unlabeled PCR product (amplified with U1492r) using reverse primers nested within the first amplicon (Ar958r and 519r (Lane et al., 1985); unlabeled Ar8f and Bac27f were used in the first amplification and labeled forward primers used in nested PCR). Fluorescently-labeled amplicons were digested at 37°C for ~ 2–10 hours using the HaeIII, RsaI, or Sau96I restriction enzymes (New England Biolabs, Ipswich, MA) and then frozen at -20°C. Restriction enzymes were selected based on prior analysis of cut sites in 16S rRNA gene sequences recovered from methane seep environments and the detection of key microbes involved in the dominant metabolism. Terminal fragments were measured by capillary electrophoresis using a Beckman CEQ 8800 system (Beckman Coulter, Fullerton, CA). The

phylogenetic affinities of terminal restriction fragments were identified using predicted restriction cut-sites of partial sequences recovered from the Eel River Basin and similar environments.

Statistical analyses

Relative abundances of specific operational taxonomic units (OTUs) defined by peak size (using a maximum bin size of 2 bp) were calculated by the area under electropherogram peaks. Fragments < 100 bp were excluded due to the presence of artifact peaks identified in non-templated PCR products. Comparison of separate fragment peak height and area using the *HaeIII* and *RsaI* restriction enzymes showed close agreement in the relative abundance of key phylotypes. The relative abundance of 9 significant archaeal *RsaI* OTUs in light mineral partitions was subtracted from their abundance in dense partitions to construct a difference matrix. The matrix was used in hierarchical cluster analysis by Euclidian distance and Ward's linkage method in PC-ORD version 5.10 (McCune and Mefford, 2006).

590 SEM-EDS measurements of individual sediment particles from magnetic and density separates of 4 sediment horizons were used in statistical analysis of the elemental composition of mineral separates. All samples were normalized to 100% total abundance of the elements Al, Ca, Fe, K, Mg, Na, P, S, and Si. 80 magnetic and 100 nonmagnetic measurements were subjected to principal component analysis (PCA) in PC-ORD to characterize elemental differences in magnetic separates. 100 measurements each of dense and light mineral partitions were randomly selected from the collected data (258 and 152 analyses, respectively) and used in PCA.

Monte Carlo tests (n=999) were conducted on both data sets with only the first three axes found to have significantly higher eigenvalues than derived from randomized data ($p < 0.05$).

Fluorescence in situ hybridization

Sediment samples for microscopic investigation were fixed shipboard in 2% paraformaldehyde overnight at 4°C, washed twice with 1X PBS followed by EtOH:PBS (1:1 volume) and resuspended in 100% EtOH prior to storage at -20°C (as described in Orphan et al., 2001). Mineral separation of these samples proceeded as described above, with the resulting fractions then re-suspended in EtOH and then captured on a 0.2 µm filter. Samples were stained with DAPI for cell counts/morphology or analyzed by fluorescence *in situ* hybridization (FISH) to determine phylogenetic association. FISH hybridization followed Pernthaler et al. (2001) using probes specific for ANME archaea (FITC-labeled Eel932; 60% formamide hybridization buffer; Boetius et al., 2000; Sigma Proligo, Sigma-Aldrich, St. Louis, MO), *Desulfobacteraceae* (FITC-labeled DSS658; 65% formamide; Sigma Proligo; Manz et al., 1998) which includes *Desulfosarcina* relatives associated with anaerobic methane oxidation (AOM) and *Epsilonproteobacteria* (Cy3-labeled EP404; 65% formamide; Sigma Proligo; Macalady et al., 2006). The EP404 sequence was modified from Macalady et al. (2006) to eliminate degeneracy in the 4th position from the 3' end, to match a target sequence 5'-TGGAGGATGACRCATTT-3'. This sequence was consistent with partial 16S rRNA gene sequences of Eel River Basin environmental clones. Catalyzed reporter deposition FISH (CARD-FISH) was applied to select samples to increase the fluorescent signal of archaeal ANME-2c cells associated with mineral surfaces. For these experiments, an HRP-labeled oligonucleotide probe ANME2c_760

(biomers.net, Ulm, Germany; Knittel et al. (2005)) was used in the hybridization (30 min at 46°C in a hybridization microwave, model BP111 Microwave Research & Applications Ltd., Laurel, MD) followed by 2x wash with 1X PBS and signal amplification using Alexa488 tyramide for 15 minutes at 46°C (Invitrogen Corp., Carlsbad, CA) following the protocol of Pernthaler and Pernthaler (2007). Prior to CARD-FISH hybridization, filtered samples were subjected to a series of cell wall permeabilization steps, including a 15 minute room temperature incubation in 0.01M HCl followed by a 1X PBS wash; a 5 minute incubation in 0.5% SDS solution in 1X PBS, and a 1 hour incubation in 10 mg/ml lysozyme in TE (Tris-EDTA, pH 8.0) at 37°C. After permeabilization, filters were treated with a three-step wash series consisting of 1X PBS, nanopure H₂O, and 80% EtOH, followed by drying at room temperature.

Hydrothermal chimney sample preparation

The well-lithified Lau basin chimney sample was ground using a mortar and pestle to a 100–170 µm size fraction and dried overnight at room temperature prior to magnetic separation. Using the Frantz magnetic separator (with an open bronze flow path) at an applied current of 0.5 amps, sphalerite was concentrated in the magnetically susceptible partition while pyrite was enriched in the nonmagnetic residue. DNA extracts were taken from an aliquot of the bulk sample and from the nonmagnetic, pyrite-enriched mineral fraction. Bacterial and archaeal 16S rRNA gene environmental clone libraries were constructed for each extract as described above.

Results and Discussion

Experimental controls

Preservation of mineral-associated community signatures

The Lau Basin hydrothermal chimney sample, largely composed of pyrite (FeS_2) and sphalerite (ZnS) crystals on the scale of 100 μm in diameter, was chosen as a proof-of-concept sample to determine whether magnetic separation was a viable method for microbial assemblage analysis given the close relationships between microorganisms and hydrothermal sulfides (Schrenk et al., 2003; Kormas et al., 2006) and previously observed changes in microbial diversity between mineralogically-distinct horizons (Kormas et al., 2006). Effective partitioning of the mineral components by magnetic separation was confirmed by SEM-EDS and XRD (Fig. 2), with sphalerite enriched in the magnetic partition (75:25 Zn:Fe by SEM-EDS on a grain mount, $n \sim 60$ individual particles) and pyrite enriched in the nonmagnetic fraction (32:68 Zn:Fe, $n \sim 60$).

High-molecular-weight DNA was successfully recovered from the pyrite and bulk mineral fractions despite the harsh preparation and separation procedure used with the hydrothermal chimney samples (e.g., powdering, drying, and sieving the samples prior to separation). 16S rRNA gene clone library analysis for archaea and bacteria revealed phylotypes that are common to hydrothermal vent environments as well as differences in the abundance of specific microbial lineages after mineral separation. Specifically, the pyrite fraction of the chimney showed increased abundance relative to the bulk sample of an archaeal phylotype most closely related

to the thermophilic sulfate-reducer *Archaeoglobus sp.* as well as *Gammaproteobacterial* phylotypes most closely related to sulfur-oxidizing strains (Fig. 2c).

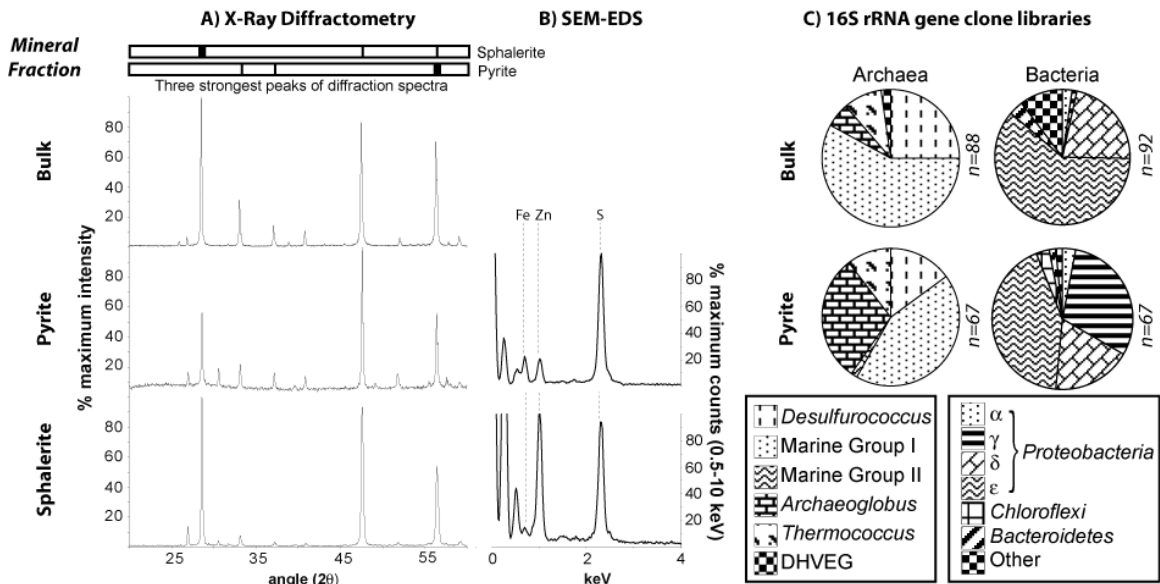


Fig. 2. Results of mineral separation on Lau Basin hydrothermal chimney and subsequent clone library analyses of associated archaeal and bacterial diversity. A) The top three reflections for pyrite and sphalerite by X-ray diffractometry are shown above profiles corresponding to mineral partitions. B) Scanning electron microscopy (SEM) analyses using energy dispersive spectroscopy (EDS) on grain mounts of the pyrite and sphalerite partitions are shown in the middle along with the peaks corresponding to elements of interest. C) Archaeal and bacterial 16S rRNA gene diversity recovered from the bulk and pyrite partitions. n indicates number of clones screened by RFLP. DHVEG: Deep Hydrothermal Vent Euryarchaeotal Group

Reproducibility of patterns of microbial diversity with specific mineral fractions

To assess reproducibility of colonization patterns detected by mineral separation, three successive subsamples of the 12–15 cm depth horizon within PC20 (adjacent to active seep, low flux methane habitat) were partitioned with sodium metatungstate at 2.9 g/cc and analyzed by T-RFLP. Differences in the major phylotypes (T-RF peaks) recovered between mineral partitions were consistent between the three environmental replicates, each showing an enrichment of ANME-2c phylotypes (tf246 by RsaI) to the relative exclusion of ANME-2ab (tf243) and ANME-1 (tf278) within the dense partition (Fig. 3). Minor T-RF peaks showed greater variation in abundance between subsamples, indicating some spatial variability between sediment aliquots

in the associated archaeal community. Peak abundance varied by as much as 7.2% between subsamples and individual peaks representing 4.9% of the detectable community could be absent from replicate subsamples.

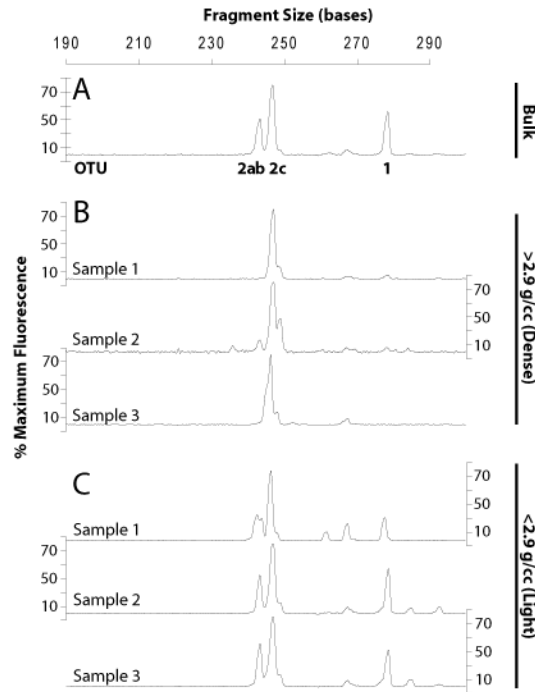


Fig. 3. Terminal restriction fragment length polymorphism electropherograms of a 12–15 cm horizon of an Eel River Basin push core. Samples 1–3 refer are biological replicates of 3 independent subsamples prior to density separation and DNA extraction. Electropherograms are shown for the archaeal diversity recovered from bulk sediment (A), “dense” (B) and “light” (C) fractions. Operational taxonomic units (OTUs) 2ab, 2c, and 1 correspond to ANME-2a and b, ANME-2c, and ANME-1 phylotypes, respectively.

Assessment of cross-contamination between mineral separates

To examine the potential for cross-contamination from minerals and/or associated microorganisms, aliquots from 2 mineral separates harboring a distinct microbial assemblage were homogenized and partitioned following our wet magnetic separation protocol for

environmental samples. Specifically, an aliquot of the magnetic fraction from the Lau basin hydrothermal chimney sample was mixed with a nonmagnetic fraction from Eel River Basin sediment and then re-separated and analyzed by T-RFLP. DNA extractions were performed on the pre-mix and post-mix separates and the communities compared by T-RFLP using the *RsaI* restriction enzyme to digest archaeal and bacterial 16S rRNA gene amplicons. Diagnostic T-RF peaks were present in each post-mixing fraction to indicate the primary sample from which the separate had been derived, however we also observed some overlap in the minor T-RF fragments after re-separation, suggesting incomplete separation (likely from the nonmagnetic fraction) or crossover of microbial cells (Fig. 4). Differences in relative abundance of > 6% in a given T-RF peak were consistently preserved, with greater peak abundance retained in the primary source partition.

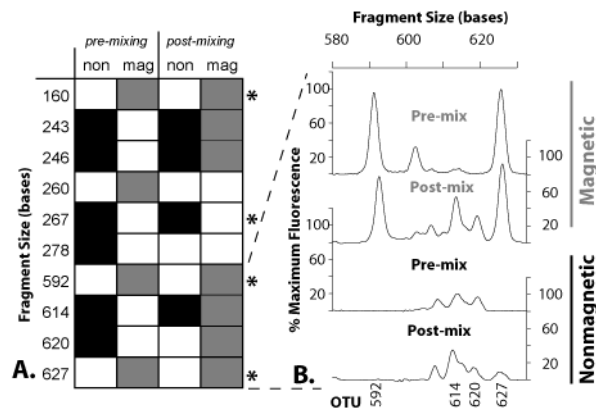


Fig. 4. Assessment of cross-contamination of archaeal cells between magnetic fractions during separation. The pre-mixture magnetic fraction was derived from a Lau basin hydrothermal chimney and the nonmagnetic fraction separated from an Eel River Basin sediment sample. The discrete separates were mixed together and then re-separated (post-mix). A) Filled squares indicate terminal fragments representing 5 percent or greater of the archaeal community. * indicates taxa that do not exhibit crossover. B) Partial TRFLP electrochromatograms for the pre and post-mixing mineral fractions.

Cross contamination between targeted mineral fractions may occur during sample processing due either to detachment and reattachment of cells or the impurity of mineral

separates. For example, magnetic particles may remain associated with the nonmagnetic partition during HGMS given insufficient sites for capture on the ferromagnetic trap, particles may be dislodged by flow strength, or aggregates of multiple mineral particles may exhibit different behavior than their components. Our experimental measure of typical cross-contamination exhibited greater migration of phylotypes from the nonmagnetic fraction to the magnetic, suggesting separate impurity is a greater concern than cell displacement. This problem may be reduced by re-processing mineral separates in order to better purify the target minerals from particles that may have been insufficiently discriminated during initial separation steps. The relative absence of cell displacement from the magnetic to nonmagnetic fractions further suggests that differing colonization patterns between mineral fractions are not likely to be generated through sample processing. However, cell detachment may depend on mineralogy and cell wall properties which are not constrained by this experiment and should be evaluated for each environment to be surveyed with this approach. The extent of cross contamination observed during the basic separation outlined in this study demonstrates that sample processing does not conceal existing patterns of microbial colonization for abundant phylogenetic groups. However, due to the potential for incomplete separation in heterogeneous environmental samples, this protocol should be viewed predominately as a mineral enrichment strategy, rather than a purification method.

Eel River Basin sediment mineralogy and microscopy

Eel River Basin samples were primarily composed of quartz, feldspar, biogenic debris, and authigenic pyrite along with a mixture of clay minerals including chlorite, illite, smectites, and kaolinite, consistent with Griggs and Hein (1980). Use of magnetic and density separation in series provides fine resolution of microbial association with a given mineral component. Both the "nonmagnetic, dense" and "magnetic, dense" partitions were enriched in pyrite above the bulk composition, while the "magnetic, light" partition enriched illite (iron-bearing phyllosilicates excluding chlorite) and the "nonmagnetic, light" fraction enriched quartz, feldspar, and metal-poor phyllosilicates. Mineral partitioning was confirmed by microscopy and SEM-EDS (Fig. 5; Table 1). Although the SEM-EDS analysis was biased towards large particles and is considered semi-quantitative, qualitative differences between mineral fractions were apparent, where both magnetic and dense partitions showed enrichment in iron and other trace metals found in pyrite, chlorite, and illite. Magnetic separation did not effectively partition sedimentary pyrite, likely due to a broad range of magnetic susceptibility (Hunt, 1995; Fig. 1).

TABLE 1. Elemental abundances of Eel River Basin mineral partitions by SEM-EDS

		<i>n</i>	Na	Mg	Al	Si	P	S	K	Ca	Fe
AD4256 PC20, PC29 (3 horizons)	<i>Dense</i>	259	3.3 (2.3–6.0)	5.3 (4.6–5.8)	15.8 (8.9–17.7)	51.0 (30.9–58.9)	0.7 (0.4–0.8)	9.5 (4.8–18.5)	0.7 (0.0–1.0)	4.3 (3.3–7.8)	9.3 (5.3–21.0)
	<i>Light</i>	152	3.8 (2.1–5.7)	5.6 (4.8–6.7)	19.6 (17.2–21.9)	65.9 (63.3–68.9)	0.0 (0.0–0.1)	0.8 (0.0–1.5)	1.4 (1.3–1.5)	0.4 (0.0–1.0)	2.4 (1.7–4.4)
AD4256 PC17 12–15cm	<i>Magnetic</i>	80	4.4	6	17.6	55.6	0	0.2	2.5	1.2	12.6
	<i>Nonmagnetic</i>	100	4.8	3.6	15.9	69.1	0	0.5	2.7	0.4	2.9

Mean elemental abundances of (*n*) SEM-EDS spectra. Values are atomic % normalized to 100. Shaded elements exhibit major differences between mineral partitions, with Fe/ S in authigenic sulfides partitioned in the dense fraction and Fe-bearing clay minerals partitioned into the magnetic and dense fractions. Values are semi-quantitative and should not be considered an accurate measure of bulk sediment composition. Values in parentheses represent the range of mean elemental abundances within three discrete sediment horizons measured in this analysis.

Sulfide mineral morphology in Eel River Basin sediments varied considerably with proximity to methane seeps and depth within the sediment column (Fig. 6 G–I), complicating our ability to consistently define mineral partitions. This mineralogical variability had a

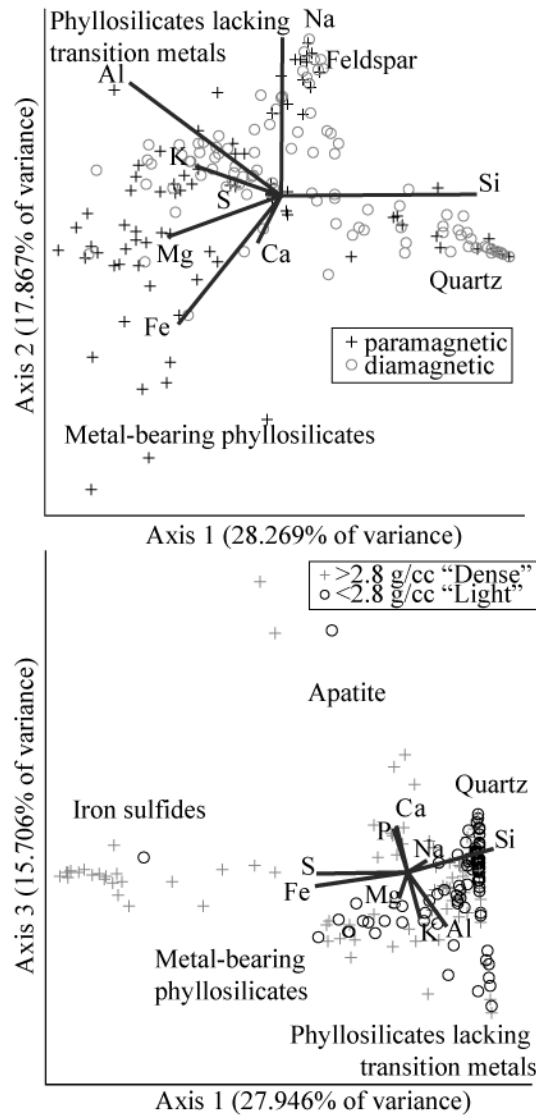


Fig. 5. Principal component analysis of elemental abundance measurements from SEM-EDS analyses of 4 discrete Eel River Basin sediment horizons. Minerals likely to be represented by plotted elemental measurements are named. Axis 3 for magnetic partitions (14.870% of variance) and axis 2 for density partitions (17.300% of variance) are not shown. Lines depict the eigenvectors for the corresponding elements.

potentially significant impact on the interpretation of microbial community differences, as attachment may be influenced by topography of the mineral surface (e.g., Luttge et al., 2005). Finely disseminated microcrystals on the scale of 1 μm or less (Fig. 6 G) occurred in surficial

sediments above the zone at which porewater sulfate is observed to decline, suggesting possible precipitation in the water column. Pyrite framboids (Fig. 6 H, I) were consistently encountered within the zone of sulfate reduction and represented a morphological range between well-ordered agglomerates of $\sim 1 \mu\text{m}$ anhedral microcrystals (Fig. 6 H) and $> 1 \mu\text{m}$ interpenetrate, euhedral crystals (Fig. 6 I). The poor crystal form of the anhedral framboids suggests growth within a restricted space, potentially constrained by organic matter (MacLean et al., 2008). These variations in morphology may influence the character of the “dense” mineral partition and, consequentially, the signature of the attached microbial community.

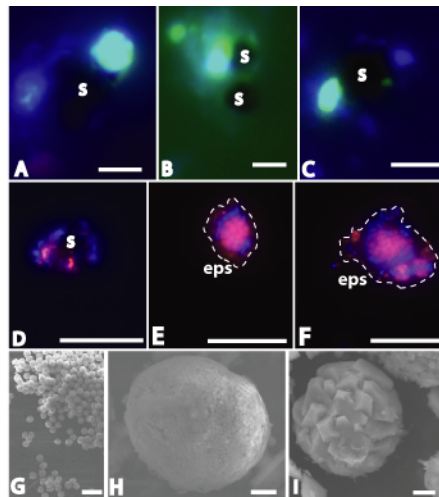


Fig. 6. A–C) Catalyzed reporter deposition fluorescence *in situ* hybridization (CARD-FISH) images of Eel River Basin sulfides (s) and associated cells. Green: ANME-2c_760 (specific to ANME-2c), blue: DAPI. D–F) Mono-labeled FISH images. D) Red: EP404 (epsilon-proteobacteria), blue: DAPI. E, F) Red: Eel932 (specific to ANME phylotypes), blue: DAPI. Dashed line indicates the extent of weak fluorescent signal suggesting a shell of extracellular polymers (eps) and minerals. G, H) Scanning electron microscope images of sulfide minerals from PC29, 0–3 cm. I) PC20, 12–15 cm. Scale bars A–C: 2 μm , D–F: 10 μm , G: 3 μm , H: 1 μm , I: 1 μm .

Microscopy of density separates using FISH and CARD-FISH revealed several common trends. Unattached cells were scarce, suggesting that microorganisms dissociated from mineral particles were discarded during processing with the < 1.6g/cc final supernatant. Hybridized and DAPI-stained cells were often observed in association with translucent particles interpreted as clay minerals, feldspar or quartz, or in proximity to opaque sulfide minerals concentrated in the dense mineral fraction (Fig. 6 A–D). Microbial consortia composed of methane-oxidizing archaea (ANME phylotypes) and sulfate-reducing bacterial partners associated with the anaerobic oxidation of methane (AOM; Orphan et al., 2001) were predominantly found in the “light” (< 2.9g/cc) partition associated with material interpreted as a mix of mineral particles and extracellular polymers (Fig. 6, E, F). Positively hybridized single archaeal cells associated with the ANME-2c were also observed associated with sulfide mineral surfaces independent of a *Deltaproteobacterial* partner (Fig. 6 A–C).

Several distinct clades of uncultured ANME archaea catalyze syntrophic sulfate-dependent anaerobic oxidation of methane, with the different groups frequently exhibiting variation in environmental distribution and abundance related to methane seep habitat (Orphan et al., 2001; Knittel 2005). The preliminary data from our mineral separation experiments additionally suggest that mineralogy may also contribute to the diversity and distribution of different ANME lineages, with different clades (ANME-2 vs. ANME-1) and subgroups (e.g., ANME-2c and ANME-2ab), showing preferential association with distinct mineral fractions within the same environment. For example, within the 12–15 cm depth horizon of PC16, collected from a low flux methane seep, the terminal fragment associated with ANME-2a and -2b (ANME-2ab) group was enriched in the magnetic partition and still more abundant in the “light, magnetic” separate, associated with the metal-bearing illites (Fig. 7; Table 2). Within the

magnetic (paramagnetic) partitions, the dense fraction was instead enriched in the ANME-2c subgroup, suggesting a possible association with pyrite. This trend was also observed in density separates of PC20, another core collected from a low methane flux site with similar geochemical properties (Fig. 7). In contrast to the observed preferential association of ANME-2 in the magnetic fraction, ANME-1 phylotypes were predominantly enriched in the light and nonmagnetic (diamagnetic) mineral partitions containing quartz, feldspar, and metal-free phyllosilicates. While variations in the different ANME groups associated with sediment depth and habitat have been previously reported from methane seeps (Knittel and Boetius, 2009), currently no consistent patterns exist in the distribution and physiology of these uncultured archaeal groups that help explain the mineral colonization patterns shown here. Nonetheless, these preliminary observations of selective mineral association by different ANME archaeal groups offer new research avenues to pursue in the future.

TABLE 2. Relative abundance of microbial phylotypes within Eel River Basin mineral partitions

	Archaea ¹			Bacteria ²						
	ANME 2c	ANME 2ab	ANME 1	ε-proteobacteria			AMO-syntrophic Desulfobacteraceae (DSS)			FISH counts ³ (aggregates/ particles) DSS
	T-RF 220	T-RF 317–319	T-RF 230	T-RF 457			T-RF 248			
				0–3 cm	3–6 cm	6–9 cm	0–3 cm	3–6 cm	6–9 cm	3–6 cm
Dense	78.0	10.7	0.0	68.9	61.0	53.9	0.0	0.0	0.0	2/106 (1.9%)
Light	26.1	38.1	12.3	64.5	29.5	43.5	1.7	4.8	4.4	10/86 (11.6%)
Magnetic	4.6	85.5	6.9	n.m.	n.m.	39.9	n.m.	n.m.	6.4	n.m.
Nonmagnetic	36.5	34.6	20.3	n.m.	n.m.	46.1	n.m.	n.m.	3.1	n.m.

Abundances are percent amplicon frequency (peak area/total area). ¹Archaeal abundances are derived from AD4252, PC16 12–15 cm (density) and AD4256, PC20 12–15 cm (magnetic). ²Bacterial abundances are derived from AD4256, PC29. ³FISH counts are reported as (hybridized aggregates/aggregate-size particles). The latter term may be considered to represent mineral or cell material on the scale of 5–20 mm.

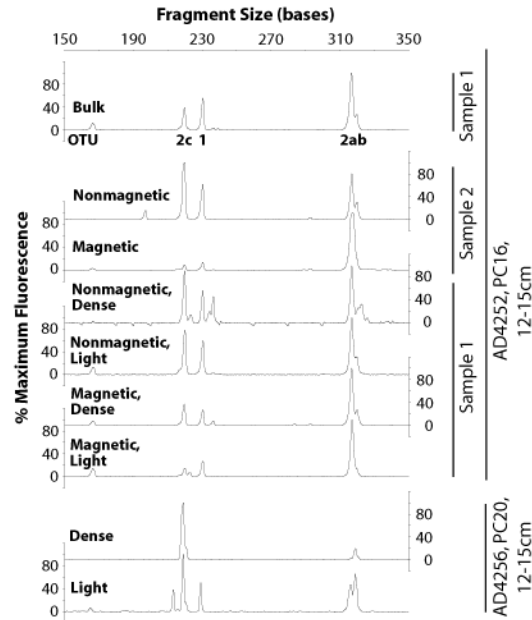


Fig. 7. Partial terminal restriction fragment length polymorphism (TRFLP) electropherograms of archaea associated with magnetic and density partitions of Eel River Basin sediment samples. OTUs 2c, 1, and 2ab correspond to ANME-2c (T-RF 220), ANME-1 (T-RF 230), and ANME-2a and b (T-RF 317–319) phylotypes, respectively. “Magnetic” and “nonmagnetic” refer to mineral partitions by high gradient magnetic separation while “dense” and “light” refer to density separates (at 2.9 g/cc). Sample numbers (1, 2) refer to discrete (pre-separation) subsamples of a given horizon.

Relationships between microbe-mineral association and geochemical setting

Sediment depth appeared to impact the bulk microbial assemblage and the character of preferential mineral association by specific groups, possibly linked with decreasing porewater sulfate and increased methane concentrations deeper in the sediment column (Orphan et al., 2004). Five successive depth horizons of PC29 (high-methane site) exhibited consistent partitioning of different ANME archaeal phylotypes when separated using sodium metatungstate (2.9 g/cc). In contrast to the ANME-mineral associations observed in sediments

characterized by lower AOM activity (low methane flux, PC20 and PC16), PC29 sediments from an active seep revealed a different pattern of ANME-mineral association, where all 5 sampled depth horizons showed an enrichment (~ 5–40%) in the ANME-2c group within the light (< 2.9) fraction containing quartz and metal-poor phyllosilicates (primarily smectites). Paired analysis of the dense mineral fraction (> 2.9 g/cc), containing authigenic pyrite and metal-bearing phyllosilicates, preferentially enriched for ANME-2ab phylotypes, representing ~ 15–20% more of the archaeal T-RFLP diversity). ANME-1 archaea were only detected at depth (6–9 cm and deeper) within PC29, consistent with previous work (Knittel and Boetius, 2009).

Throughout PC29, specific *Deltaproteobacterial* phylotypes associated with AOM-syntrophic members of the *Desulfobacteraceae* were present exclusively within the light fraction (2–5% detectable by *RsaI*). *Actinobacterial* phylotypes (T-RF 228 by *HaeIII*; difference of 5–8% between partitions) and *Epsilonproteobacterial* phylotypes (T-RF 456 by *RsaI*; 3–30% difference between partitions) were consistently more abundant within the dense fraction than in the light fraction (Table 2).

Hierarchical cluster analysis was performed on density separates of a set of depth horizons of adjacent microbial mat, clam bed, and “low activity, reference” cores to further test the observations of ANME mineral partitioning described above, as well as determine the consistency of mineral colonization patterns across a range of geochemical conditions (Fig. 8). Sediment horizons clustering with one another indicate similar changes in archaeal diversity between dense and light mineral partitions. Depth horizons exhibiting similar geochemical properties (e.g., near seabed sediments 0–9 cm underlying a sulfide-oxidizing microbial mat (PC 29) as well as a sulfidic horizon 15–18cm beneath a clam bed (PC23)) have similar microbial affinity for mineral fractions. However, differences in core type and sediment depth show

variable community responses to mineralogy. Exclusion of < 6% values from the difference matrix (conforming to the preservation of differences noted in the reproducibility experiment) had no significant impact on clustering patterns (data not shown) but excludes sample 2693. Its position in Fig. 8 should therefore be considered tentative.

Rapid detection of microbe-mineral interactions

Existing approaches for detecting microbe-mineral interactions in the environment often rely on introducing an artificial substrate for colonization (e.g., Edwards et al. 2003; Roberts, 2004) from which microbes are subsequently recovered and analyzed. *In situ* microcosms of this type may not fully represent environmental conditions or potential mineralogical diversity, and considerable time may be required for incubation. Furthermore, our initial results suggest that the degree of preferential colonization may vary on a fine scale, potentially driven by geochemical gradients (Fig. 8). Previous studies have observed that composition-dependent colonization may only be significant where limiting nutrients are supplied by the mineral substrate (Mauck and Roberts, 2007). On first investigation of a sedimentary environment, the limiting factors for microbial activity may not be readily apparent or may have a spatial scale outside the resolution of the microcosm or bulk analysis.

The mineral separation approach presented in this study provides a scalable method for rapid screening of preferential colonization patterns by T-RFLP or other DNA-based molecular survey method. In the case of T-RFLP, phylogenetic resolution may be improved either by selection of targeted primers for PCR or through broader selection of restriction enzymes used in product digestion. Sampling does not require foreknowledge of *in situ* geochemistry or

detailed lithology. Minimum sample size necessary for the technique is on the scale of 1 g for near-seafloor sediments when coupled to DNA extraction and subsequent T-RFLP or clone library analysis. This study and similar T-RFLP surveys in marginal marine sediments (e.g., Urakawa et al., 2000; Parkes et al., 2007; Mills et al., 2008; Edlund et al., 2008; Luna et al., 2009) demonstrate that T-RFLP is a robust method for screening community differences attributable to spatial distribution, redox differences, and mineral heterogeneity. Less than 1 g of material is required for FISH analysis. Samples may be processed in this manner without concealing pre-existing patterns of preferential attachment. Initial results using this approach may inform subsequent deployment of *in situ* microcosms or other detailed observations.

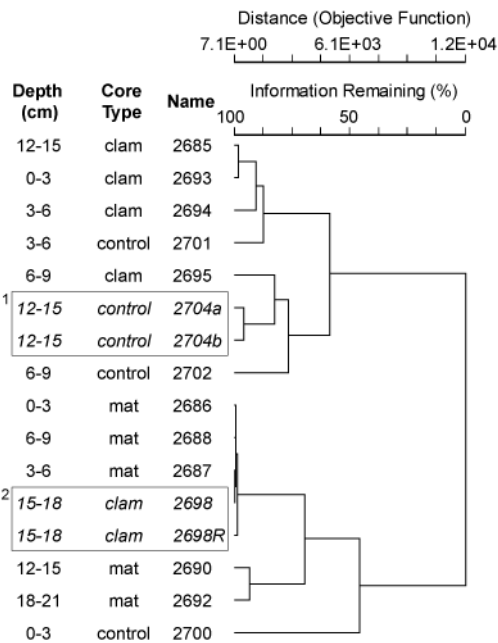


Fig. 8. Hierarchical cluster analysis of archaeal community differences between density separates of Eel River Basin sediments. 1) TRFLP generated by two discrete subsamples of sediment horizon 2704. 2) Replicates generated from a single set of DNA extracts from sediment horizon 2698. 2698R was subjected to a 32-cycle unlabeled PCR followed by a 25-cycle labeled reamplification step using a diluted product, while 2698 was generated by single, labeled 32-cycle PCR.

Mineral Colonization in Marine Sediments

Microbe–mineral interactions are an important factor in understanding activity in the terrestrial subsurface (Mauck and Roberts, 2007; Roberts et al., 2004). However, the role of mineral colonization on microbial activity in the marine subsurface remains unresolved. Direct attachment to a mineral surface may limit diffusion-limited nutrient uptake from pore space. Murray and Jumars (2002) suggest that this may explain the propensity of cells in the shallow marine subsurface to be held a specific distance from mineral surfaces by networks of extracellular polymers, a trait previously established by Transmission Electron Microscopy (Ransom et al., 1999). The reproducible preferential distribution of specific phylotypes between different mineral partitions in three replicate samples suggests that mineral association, whether or not by direct cell contact, influences the local microbial diversity in marine sediments (Fig. 3). The preliminary results of studying microbe-mineral interactions in marine sedimentary systems are broadly consistent with previous work in marine (Edwards et al., 2003; Santelli et al., 2009) and terrestrial (Boyd et al., 2007; Mauck and Roberts, 2007) systems demonstrating a relationship of mineral colonization to trace nutrient supply and dissimilatory metabolism. However, previous work in terrestrial systems suggests that other factors may play important roles in differential attachment to mineral surfaces between microbial taxa including cell hydrophobicity and electrostatic forces between cell wall and mineral surface (e.g., Morrow et al., 2005) as well as mineral surface microtopography and related processes of dissolution and precipitation (e.g., Luttge et al., 2005). A more thorough analysis of microbial colonization of marine sediments is necessary to adequately constrain the importance of all factors in generating patterns of cell attachment in this environment. The observation that colonization

patterns vary with geochemical setting suggests mineral attachment is related to microbial metabolism in the Eel River Basin seep environment.

The partitioning of archaeal phylotypes associated with the anaerobic oxidation of methane between mineral fractions suggests subtle ecophysiological differences likely exist between the closely-related subgroups of ANME archaea (e.g., ANME-2c and ANME-2ab), while variable attachment between ANME-2 and ANME-1 groups may reflect differences in cell morphology and life mode. The observations from different physico-chemical habitats in the methane seep environment (e.g., the deeper, low active sediments analyzed from PC16 and PC20 compared with the active PC29 with a higher methane flux) suggest that preferential mineral attachment is not constant for a given ANME lineage, but rather is influenced by a complex combination of both the geochemical environment (e.g., sulfate/sulfide) and *in situ* mineralogy.

Conclusions

Magnetic- and/or density-based mineral separation followed by molecular analysis is an effective culture-independent means of detecting differential mineral attachment of indigenous microorganisms in lithologically diverse environments. The application of this unique screening tool can be used to identify patterns between microbial diversity and mineral association in previously intractable environments such as marine sediments, and may facilitate the generation of new, testable hypotheses regarding the ecological and physiological relationships between specific sediment-dwelling microorganisms and clay and mineral constituents.

Hypothesis testing and verification of specific microbe-mineral patterns observed in T-RFLP or

16S rRNA clone library data can be validated through the use of complementary methods such as FISH and *in situ* microcosm incubation experiments using relevant mineral substrates. Here we demonstrated the reproducibility and effectiveness of this method for assessing variations in the archaeal and bacterial diversity associated with different mineral fractions from methane seep sediments, revealing previously unknown patterns of mineral association for distinct groups and subgroups of ANME archaea and *Epsilonproteobacteria* within specific sedimentary environments

Further research will be necessary to fully understand the role of mineral attachment in the microbial diversity of marine sediments in seep environments and elsewhere. However, the significant influence of mineral colonization in nutrient-rich sediments of the Eel River Basin suggests such patterns may be widespread. Broader study of the mineral affinity of uncultured marine subsurface microorganisms may yield insight into their ecophysiology. The approach detailed in this study provides unique context for future studies of microbial distribution and potential ecological physiology in the marine subsurface.

Acknowledgements

We thank the crew and shipboard parties and chief scientist B. Vrijenhoek of the R/V Melville (May, 2005) and R/V Atlantis (October, 2006) for support in sample collection. We also are grateful to S. Goffredi, A. Dekas, A. Green, J. Bailey, O. Mason, P. Tavormina, D. Fike, S. Connon, J. Steele, and two anonymous reviewers for helpful comments and editorial advice. This work was supported by a grant from the Gordon and Betty Moore Foundation (to VJO), a Schlanger Ocean Drilling Graduate Fellowship (to BKH), and funding from the NASA Astrobiology Institute (Grant award # 3903-CIT-NASA.A76A) as part of the Penn State Astrobiology Research Center (PSARC). Collection of samples from the Eel River Basin and Lau Basin was supported by funding from the National Science Foundation (MCB-0348492 to VJO) and (OCE-0241613 to B. Vrijenhoek).

References

- Alfreider A, Krossbacher M, Psenner R. 1997. Groundwater samples do not reflect bacterial densities and activity in subsurface systems. *Water Res* 31(4):832–840.
- Andrews JS, Rolfe SA, Huang WE, Scholes JD, Banwart SA. 2009. Biofilm formation in environmental bacteria is influenced by different macromolecules depending on genus and species. *Environ Microbiol* 12(9):2496–2507.
- Boetius A, Ravensschlag K, Schubert CJ, Rickert D, Widdel F, Gieseke A, Amann R, Jorgensen BB, Witte U, Pfannkuche O. 2000. A marine microbial consortium apparently mediating anaerobic oxidation of methane. *Nature* 407(6804):623–626.
- Bolster CH, Walker SL, Cook KL. 2006. Comparison of *Escherichia coli* and *Campylobacter jejuni* transport in saturated porous media. *J Environ Qual* 35(4):1018–1025.
- Boyd ES, Cummings DE, Geesey GG. 2007. Mineralogy influences structure and diversity of bacterial communities associated with geological substrata in a pristine aquifer. *Microb Ecol* 54(1):170–182.
- Childers SE, Ciuffo S, Lovley DR. 2002. *Geobacter metallireducens* accesses insoluble Fe(III) oxide by chemotaxis. *Nature* 416(6882):767–769.
- Decho AW. 2000. Microbial biofilms in intertidal systems: an overview. *Cont Shelf Res* 20(10-11):1257–1273.
- DeLong EF. 1992. Archaea in Coastal Marine Environments. *Proc Natl Acad Sci USA* 89(12):5685–5689.
- Druschel GK, Labrenz M, Thomsen-Ebert T, Fowle DA, Banfield JF. 2002. Geochemical Modeling of ZnS in biofilms: An example of ore depositional processes. *Economic Geol* 97(6):1319–1329.
- Edlund A, Hardeman F, Jansson JK, Sjöling S. 2008. Active bacterial community structure along vertical redox gradients in Baltic Sea sediment. *Environ Microbiol* 10(8):2051–2063.
- Edwards KJ, McCollom TM, Konishi H, Buseck PR. 2003. Seafloor bioalteration of sulfide minerals: Results from in situ incubation studies. *Geochim Cosmochim Acta* 67(15):2843–2856.
- Fortin D, Ferris FG, Beveridge TJ. 1997. Surface-mediated mineral development by bacteria. *Geomicrobiology: Interactions between Microbes and Minerals*. p 161–180.
- Ghabru SK, Starnaud RJ, Mermut AR. 1988. Use of High-Gradient Magnetic Separation in Detailed Clay Mineral Studies. *Can J Soil Sci* 68(3):645–655.
- Griggs GB, Hein JR. 1980. Sources, dispersal, and clay mineral-composition of fine-grained sediment off Central and Northern California. *J Geol* 88(5):541–566.
- Hunt CP, Moskowitz BM, Banerjee SK. 1995. Magnetic properties of rocks and minerals. *Rock Physics and Phase Relations: A Handbook of Physical Constants: American Geophysical Union*.

- Kim HN, Bradford SA, Walker SL. 2009. *Escherichia coli* O157:H7 Transport in Saturated Porous Media: Role of Solution Chemistry and Surface Macromolecules. *Environ Sci Technol* 43(12):4340–4347.
- Knittel K, Boetius A. 2009. Anaerobic Oxidation of Methane: Progress with an Unknown Process. *Annu Rev Microbiol* 63:311–334.
- Knittel K, Losekann T, Boetius A, Kort R, Amann R. 2005. Diversity and distribution of methanotrophic archaea at cold seeps. *Appl Environ Microbiol* 71(1):467–479.
- Kormas KA, Tivey MK, Von Damm K, Teske A. 2006. Bacterial and archaeal phylotypes associated with distinct mineralogical layers of a white smoker spire from a deep-sea hydrothermal vent site (9 degrees N, East Pacific Rise). *Environ Microbiol* 8(5):909–920.
- Krukowski ST. 1988. Sodium Metatungstate—A New Heavy-Mineral Separation Medium for the Extraction of Conodonts from Insoluble Residues. *J Paleontol* 62(2):314–316.
- Lane DJ. 1991. 16S/23S rRNA sequencing. In: Stackebrandt E, Goodfellow M, editors. *Nucleic acid techniques in bacterial systematics*. New York, NY: John Wiley and Sons. p 115–175.
- Lovley DR. 1991. Dissimilatory Fe(III) and Mn(IV) Reduction. *Microbiol Rev* 55(2):259–287.
- Lower SK. 2005. Directed natural forces of affinity between a bacterium and mineral. *Am J Sci* 305(6-8):752–765.
- Lumpkin GR, Zaikowski A. 1980. A Method for Performing Magnetic Mineral Separations in a Liquid-Medium. *Am Mineral* 65(3-4):390–392.
- Luna GM, Stumm K, Pusceddu A, Danovaro R. 2009. Archaeal Diversity in Deep-Sea Sediments Estimated by Means of Different Terminal-Restriction Fragment Length Polymorphisms (T-RFLP) Protocols. *Curr Microbiol* 59(3):356–361.
- Lutterodt G, Basnet M, Foppen JWA, Uhlenbrook S. 2009. The effect of surface characteristics on the transport of multiple *Escherichia coli* isolates in large scale columns of quartz sand. *Water Res* 43(3):595–604.
- Luttge A, Zhang L, Neelson KH. 2005. Mineral surfaces and their implications for microbial attachment: Results from Monte Carlo simulations and direct surface observations. *Am J Sci* 305(6-8):766–790.
- Macalady JL, Lyon EH, Koffman B, Albertson LK, Meyer K, Galdenzi S, Mariani S. 2006. Dominant microbial populations in limestone-corroding stream biofilms, Frasassi cave system, Italy. *Appl Environ Microbiol* 72(8):5596–609.
- MacLean LC, Tyliczszak T, Gilbert PU, Zhou D, Pray TJ, Onstott TC, Southam G. 2008. A high-resolution chemical and structural study of framboidal pyrite formed within a low-temperature bacterial biofilm. *Geobiology* 6(5):471–80.
- Manz W, Eisenbrecher M, Neu TR, Szewyk U. 1998. Abundance and spatial organization of Gram-negative sulfate-reducing bacteria in activated sludge investigated by in situ probing with specific 16S rRNA targeted oligonucleotides. *FEMS Microbiol Ecol* 25(1):43–61.

- Matz C, Bergfeld T, Rice SA, Kjelleberg S. 2004. Microcolonies, quorum sensing and cytotoxicity determine the survival of *Pseudomonas aeruginosa* biofilms exposed to protozoan grazing. *Environ Microbiol* 6(3):218–226.
- Mauck BS, Roberts JA. 2007. Mineralogic control on abundance and diversity of surface-adherent microbial communities. *Geomicrobiol J* 24(3-4):167–177.
- McCune, B., Mefford, M. J., 2006: PC-ORD: Multivariate Analysis of Ecological Data, Version 5.10, MjM Software, Gleneden Beach, OR.
- Mills HJ, Hunter E, Humphrys M, Kerkhof L, McGuinness L, Huettel M, Kostka JE. 2008. Characterization of nitrifying, denitrifying, and overall bacterial communities in permeable marine sediments of the northeastern Gulf of Mexico. *Appl Environ Microbiol* 74(14):4440–4453.
- Morrow JB, Stratton R, Yang HH, Smets BF, Grasso D. 2005. Macro- and manoscale observations of adhesive behavior for several E-coli strains (O157 : H7 and environmental isolates) on mineral surfaces. *Environ Sci Technol* 39(17):6395–6404.
- Murray JLS, Jumars PA. 2002. Clonal fitness of attached bacteria predicted by analog modeling. *Bioscience* 52(4):343–355.
- Oberteuffer JA. 1974. Magnetic Separation—Review of Principles, Devices, and Applications. *IEEE Trans Magn* 10(2):223–238.
- Orphan VJ, Hinrichs KU, Ussler W, 3rd, Paull CK, Taylor LT, Sylva SP, Hayes JM, Delong EF. 2001. Comparative analysis of methane-oxidizing archaea and sulfate-reducing bacteria in anoxic marine sediments. *Appl Environ Microbiol* 67(4):1922–34.
- Orphan VJ, Ussler W, Naehr TH, House CH, Hinrichs KU, Paull CK. 2004. Geological, geochemical, and microbiological heterogeneity of the seafloor around methane vents in the Eel River Basin, offshore California. *Chem Geol* 205(3–4):265–289.
- Parkes RJ, Cragg BA, Banning N, Brock F, Webster G, Fry JC, Hornibrook E, Pancost RD, Kelly S, Knab N and others. 2007. Biogeochemistry and biodiversity of methane cycling in subsurface marine sediments (Skagerrak, Denmark). *Environ Microbiol* 9(5):1146–1161.
- Pernthaler A, Pernthaler J. 2007. Fluorescence in situ hybridization for the identification of environmental microbes. *Methods Mol Biol* 353:153–64.
- Pernthaler J, Glöckner FO, Schönhuber W, Amann R. 2001. Fluorescence in situ hybridization with rRNA-targeted oligonucleotide probes. In: Paul J, editor. *Methods in Microbiology: Marine Microbiology*. London: Academic Press Ltd.
- Ransom B, Bennett RH, Baerwald R, Hulbert VH, Burkett PJ. 1999. In situ conditions and interactions between microbes and minerals in fine-grained marine sediments: A TEM microfabric perspective. *Am Mineral* 84(1–2):183–192.
- Roberts JA. 2004. Inhibition and enhancement of microbial surface colonization: the role of silicate composition. *Chem Geol* 212(3–4):313–327.

- Rogers JR, Bennett PC. 2004. Mineral stimulation of subsurface microorganisms: release of limiting nutrients from silicates. *Chem Geol* 203(1–2):91–108.
- Rogers JR, Bennett PC, Choi WJ. 1998. Feldspars as a source of nutrients for microorganisms. *Am Mineral* 83(11–12):1532–1540.
- Rosenblum S, Brownfield IK. 1999. Magnetic susceptibilities of minerals. U.S. Geological Survey, Open-File Report 99-529.
- Russell JD, Birnie A, Fraser AR. 1984. High-Gradient Magnetic Separation (Hgms) in Soil Clay Mineral Studies. *Clay Miner* 19(5):771–778.
- Santelli CM, Edgcomb VP, Bach W, Edwards KJ. 2009. The diversity and abundance of bacteria inhabiting seafloor lavas positively correlate with rock alteration. *Environ Microbiol* 11(1):86–98.
- Schrenk MO, Kelley DS, Delaney JR, Baross JA. 2003. Incidence and diversity of microorganisms within the walls of an active deep-sea sulfide chimney. *Appl Environ Microbiol* 69(6):3580–3592.
- Schulze DG, Dixon JB. 1979. High-Gradient Magnetic Separation of Iron-Oxides and Other Magnetic Minerals from Soil Clays. *Soil Sci Soc Am J* 43(4):793–799.
- Southam G, Saunders JA. 2005. The geomicrobiology of ore deposits. *Economic Geol* 100(6):1067–1084.
- Tazaki K, Fyfe WS. 1992. Microbial Green Marine Clay from Izu-Bonin (West Pacific) Deep-Sea Sediments. *Chem Geol* 102(1–4):105–118.
- Tebo BM, Ghiorse WC, vanWaasbergen LG, Siering PL, Caspi R. 1997. Bacterially mediated mineral formation: Insights into manganese(II) oxidation from molecular genetic and biochemical studies. *Geomicrobiology: Interactions between Microbes and Minerals*. p 225–266.
- Totten MW, Hanan MA, Knight D, Borges J. 2002. Characteristics of mixed-layer smectite/illite density separates during burial diagenesis. *Am Mineral* 87(11–12):1571–1579.
- Urakawa H, Yoshida T, Nishimura M, Ohwada K. 2000. Characterization of depth-related population variation in microbial communities of a coastal marine sediment using 16S rDNA-based approaches and quinone profiling. *Environ Microbiol* 2(5):542–554.
- Vorhies JS, Gaines RR. 2009. Microbial dissolution of clay minerals as a source of iron and silica in marine sediments. *Nat Geosci* 2(3):221–225.
- Wey JK, Scherwass A, Norf H, Arndt H, Weitere M. 2008. Effects of protozoan grazing within river biofilms under semi-natural conditions. *Aquat Microb Ecol* 52(3):283–296.
- Wilson MJ, Certini G, Campbell CD, Anderson IC, Hillier S. 2008. Does the preferential microbial colonisation of ferromagnesian minerals affect mineral weathering in soil? *Naturwissenschaften* 95(9):851–858.
- Wirsen CO, Brinkhoff T, Kuever J, Muyzer G, Molyneux S, Jannasch HW. 1998. Comparison of a new *Thiomicrospira* strain from the Mid-Atlantic Ridge with known hydrothermal vent isolates. *Appl Environ Microbiol* 64(10):4057–4059.

Chapter 3

Microbe-mineral interactions of Eel River Basin methane seeps—implications for sulfur cycling and anaerobic oxidation of methane

Abstract

In the subsurface biosphere, microbial colonization patterns corresponding to mineral composition are known to express significant variations in cell density and diversity between particles. Microbe–mineral interactions play important roles in metabolic reactions and the precipitation and dissolution of minerals, significantly impacting global biogeochemical cycles. Detailed study of the relationship of microbial diversity and mineralogy may therefore provide insight into the activity and environmental significance of microbial communities, including those which defy culture-based determinations of physiology and metabolism. In the past, analytical difficulty has hampered the study of microbe-mineral interactions in marine sediments. Application of new mineral separation methodology to the study of microbial colonization patterns in Eel River Basin methane seep sediments presents a first approximation of the importance of mineral attachment in driving microbial diversity. Additionally, microbe-mineral interactions present unique observations concerning sulfur cycling and the anaerobic oxidation of methane. Molecular analyses of archaeal and bacterial diversity by Terminal Restriction Fragment Length Polymorphism show that differences between mineral fractions of marine sediment are comparable to those observed across broad spatial and geochemical scales in the methane seep environment. Affinity of putative S-oxidizing *Gammaproteobacteria* with mineral fractions enriched in authigenic sulfides suggests persistent reoxidation of solid-state sulfides may persist at significant depth within redox zones characterized by sulfate reduction.

Phylogenetically disparate archaeal groups linked to the anaerobic oxidation of methane (ANMEs) are shown to preferentially colonize mineral substrates, presenting physiological differences between metabolically similar groups. Differences in mineral affinity between microbial taxa are further supported by laboratory microcosms. Future research into additional marine sedimentary environments may improve understanding of mineral attachment as a factor in microbial diversity and yield insight into the physiology of widespread uncultured microorganisms.

Introduction

Marine methane seeps are environments impacted by advection of methane-rich fluids through the sediment column towards the seafloor. Thermogenic production from deep reservoirs and hydrate dissolution are common sources of seep methane, and seeps are typically encountered in continental margin settings due to the abundance of sedimentary organic matter, changing hydrate stability from tectonic forcing, and supply of heat at active margins (Levin, 2005). The supply of methane fuels a diverse community primarily through the anaerobic oxidation of methane (AOM) coupled to sulfate reduction. Production of hydrogen sulfide as a byproduct of AOM in turn leads to abundant bacterial sulfide oxidation at and near the sediment-water interface, often manifest in microbial mats surrounding sites of active methane bubbling and beds of symbiont-bearing chemosynthetic clams.

Ongoing research has substantially increased our understanding of the microbial community in methane seep environments. Microbial consortia of "ANME" archaea and sulfate-reducing *Deltaproteobacteria* have been implicated in carrying out AOM (Boetius et al., 2000;

Orphan et al., 2001). Past studies have broadened the phylogenetic diversity of microorganisms known to occupy this metabolic role, both among ANME archaea (Orphan et al., 2002; Knittel et al., 2005; Losekann et al., 2007) and *Deltaproteobacteria* (Pernthaler et al., 2008). Seep communities have been surveyed in great detail by culture-independent methods targeting DNA and RNA (Lloyd et al., 2010), functional genes (Dhillon et al., 2003; Hallam et al., 2003; Dekas et al., 2009), and metagenomics (Hallam et al., 2003; Meyerdierks et al., 2005; Pernthaler et al., 2008). Despite considerable progress, the vast majority of microorganisms identified in methane seeps—and marine sediments in general—remain uncultured and physiologically unknown. The resolution of surveys of microbial diversity in seep environments has been limited by methodology, and knowledge is relatively scarce at a fine spatial scale.

Microbial attachment to solid particles has been shown to drive variations in community diversity related to metabolism and mineral composition in diverse subsurface environments (Rogers and Bennett, 2001; Roberts, 2004; Boyd et al., 2007; Mauck and Roberts 2007). Microbe–mineral interactions have not been described extensively in marine sediments due to analytical difficulty. Our previous work (Harrison and Orphan, in press) details the development of a method to detect patterns of microbial diversity between discrete mineral fractions in fine-grained sediment using density and/or magnetic separation. The investigation of methane seep microbial ecology by mineral separation offers a unique opportunity to study community architecture at a fine resolution and provide insight into the potential ecophysiology of key uncultured phylogenetic groups.

Methods

Sampling

Sediment samples from the Northern Ridge of Eel River Basin (ERB) were collected at a depth of approximately 520 m using the HMDV *Alvin* in October of 2006. Twenty-one discrete 3 cm-thick sediment horizons were sampled from eight push cores within and adjacent to methane seep communities (*Calyptogena* clams and sulfide-oxidizing microbial mats). The bubbling site, mats, clam beds, and low-flux periphery form a “bulls-eye” characteristic of methane seep expression on the seafloor (Barry et al., 1996). Fourteen samples were collected from a transect (40° 48.69' N, 124° 36.65' W) of three push cores taken at intervals stepped out from an active seep: PC29 from sediment overlain by a sulfide-oxidizing microbial mat (previously described in Perthaler et al., 2008; serial numbers 2686-2692 corresponding to individual horizons), push core 23 (PC23; serials 2693-2698) from an adjacent chemosynthetic clam bed, and PC20 (serials 2700-2704) from low-CH₄-flux sediment located approximately 5 m outside the mat and clam bed. Subsamples for mineral separation and DNA extraction were taken following pore water extraction and frozen at -80°C for transportation and storage. Hydrogen sulfide was measured in extracted pore waters using the Cline (1969) method. 2cc sediment aliquots were sealed in vials containing 5ml NaOH for subsequent methane measurement. Methane concentrations in vial headspace were assessed by gas chromatography with a flame ionization detector (Goffredi et al., 2008). Sulfate concentrations in pore water extracts were measured as previously described (Goffredi et al., 2008)

Microcosm assembly

Laboratory incubations were prepared in 40 cc serum bottles. Mud used as inoculum was gathered from 0–9 cm of an Eel River Basin mat core and stored shipboard under N_2 at 4°C. 5 cc aliquots of wet sediment were added to each bottle with or without 1 g of pre-sterilized synthetic pyrite. Pyrite was washed twice with 100% ethanol prior to rinse steps in 0.1 N HCl and deoxygenated water. Sediments were taken up in carbonate-buffered artificial seawater media with variable initial concentrations of sulfate (0–20 mM) and nitrate (0–10 μ M). 2 mM nitrate spikes were added at 3 months to select incubations. Vial headspace was replaced and overpressured with CH_4 . 200 μ l water samples were collected at regular intervals for sulfide measurement using the Cline (1969) method. A final incubation (cultS) was assembled using a dilute (< 0.1 g sediment) 100 μ l slurry of sediment stored under methane for two weeks in basal salt media (lacking sulfate and nitrate). This inoculum was added to autoclaved, filtered seawater amended with 0.5 g elemental sulfur and 2 mM thiosulfate. Vial headspace was overpressured with 1:1 $H_2:CO_2$. All microcosms were incubated in darkness at 11°C.

Mineral separation

Bimodal magnetic and density separates were derived from bulk environmental samples as previously described (Harrison and Orphan, in press). Paramagnetic (“magnetic”) and diamagnetic (“nonmagnetic”) mineral fractions were generated using a Frantz L-1 isodynamic magnetic separator (S.G. Frantz Co., Trenton, NJ) modified for High Gradient Magnetic Separation (HGMS) in a UV-sterilized Teflon flow path using very fine steel wool and steel wires of 102, 200, and 280 μ m diameter designed for sediment processing (Harrison and Orphan, in

press). Density partitions of sediment samples were processed by suspension in sodium metatungstate (Krukowski, 1988) at 2.8 g/cc, chosen to discriminate authigenic pyrite from other mineral components. “Dense” (negative buoyancy; e.g., iron sulfides) minerals were concentrated in a pellet, while “light” (positive buoyancy; e.g., quartz) minerals were concentrated in the supernatant.

Mineral composition analyses

Mineralogy subsamples were partitioned according to density and/or magnetic susceptibility, rinsed twice in 0.5 M NaCl or nanopure H₂O, re-suspended in 100% ethanol, and dried for subsequent compositional analysis. A minimum of 0.5 g was recovered for X-Ray Diffractometry (XRD) and a minimum of 0.1 g for scanning electron microscopy (SEM). SEM images were acquired using a LEO 1550VP Field Emission SEM (Carl Zeiss SMT, Oberkochen, Germany) equipped with an INCA Energy 300 X-ray Energy Dispersive Spectrometer (EDS) system (Oxford Instruments, Abingdon, UK). Samples were prepared for XRD as previously described (Harrison and Orphan, in press) and analyzed with a Terra XRD (Olympus Innov-X, Woburn, MA) with a Co source, according to standard protocols.

DNA extraction, PCR amplification, and clone library construction

DNA was extracted from 0.1-1 g of each mineral partition using a MoBio soil DNA protocol modified for methane seep sediment samples following Orphan et al. (2001). The 16S rRNA gene diversity of bacterial and archaeal DNA for the separated subsamples was assessed

by PCR using the primers Ar8f (archaea-specific), Bac27f (bacteria-specific), and U1492r (universal; Lane et al., 1991; DeLong, 1992). PCR reactions were prepared in 25 µl reaction volumes as follows: 1X ThermoPol PCR buffer (New England Biolabs, Ipswich, MA) with 1.5 mM MgCl₂; 0.2 mM concentrations of deoxynucleoside triphosphates; 0.1 µg of each primer; 0.25 µl of Taq DNA polymerase (New England Biolabs). Successive 1:10 template:H₂O dilutions were used to minimize PCR inhibition. Amplifications derived from the lowest successful dilution factor (typically 1:10 for dense/magnetic and 1:100 for bulk/light/nonmagnetic partitions) were used in statistical analysis. PCR utilized 30 cycles of 30-second 94°C denaturing, 30-second 54°C annealing, and 80-second 72°C extension steps, following an initial 2-minute 95°C denaturing. Bacterial and archaeal clone libraries were assembled for the 0–3 cm sediment horizon of PC29 using the PGEM T-Easy vector kit (Promega), composed of 87 and 92 clones, respectively. Clones were screened by RFLP using the HaeIII restriction enzyme (New England Biolabs) and unique clones selected for partial sequencing for the identification of restriction sites. For terminal restriction fragment length polymorphism (T-RFLP) analysis, a 30-cycle PCR was carried out using fluorescently labeled Ar8f (WellRed dyes D2 or D4) and Bac27f (WellRed dye D3) primers and unlabeled reverse primers Ar958r (archaea-specific; DeLong, 1992) and U1492r. For mineral samples producing a weak primary amplicon, a second, 10-cycle PCR was performed on 1 µl of a 1:3 dilution of an initial unlabeled PCR product (amplified with U1492r) using reverse primers nested within the first amplicon (Ar958r and 519r (Lane et al., 1985); unlabeled Ar8f and Bac27f were used in the first amplification and labeled forward primers used in nested PCR). Fluorescently-labeled amplicons were digested at 37°C for ~ 2–10 hours using the HaeIII, RsaI, or Sau96I restriction enzymes (New England Biolabs, Ipswich, MA) and then frozen at -20°C. Restriction enzymes were selected based on prior analysis of cut sites in 16S rRNA gene sequences recovered from methane seep environments and the detection of key microbes

involved in the dominant metabolism. Terminal fragments were measured by capillary electrophoresis using a Beckman CEQ 8800 system (Beckman Coulter, Fullerton, CA). The phylogenetic affinities of terminal restriction fragments were identified using predicted restriction cut-sites of partial sequences recovered from the Eel River Basin and similar environments (Orphan et al., 2001; Pernthaler et al., 2008; Beal et al., 2009).

Fluorescence in situ hybridization

2%-formaldehyde-fixed sediments were separated and prepared for fluorescence *in situ* hybridization (FISH) as previously described (Harrison and Orphan, in press) to determine phylogenetic association of cells and spatial relationships to mineral substrates. Hybridization followed Pernthaler et al. (2001) using probes specific for *Desulfobacteraceae* (FITC-labeled DSS658; 65% formamide; Sigma Proligo; Manz et al., 1998) which includes *Desulfosarcina* relatives associated with anaerobic methane oxidation (AOM), and probes for the *Gammaproteobacteria* (FITC-labeled Gam42; 35% formamide; Sigma Proligo; Manz et al., 1992).

Statistical analyses

T-RFs of disparate electropherograms were binned using Beckman CEQ 8800 system software. Maximum bin size was set to 2.5 bp and a y threshold (dye signal) of 200 set to exclude erroneous peaks derived from signal crossover by the DNA size standard. Remaining cross-dye peaks were manually excluded. Peaks exhibiting heights beneath 1% of the second highest sample peak were excluded to remove noise. Fragments shorter than 80 bp and longer than 560 bp were removed due to presence of artifacts and inconsistencies in electropherogram analysis length. Binned analyses of relative amplicon frequency (fluorescent signal) were converted to relative abundance based on relative peak area ($\text{Area}_{\text{BIN}}/\text{Area}_{\text{SampleTotal}}$).

OTUs represented in fewer than 2 samples were deleted from all data matrices used in statistical analysis in order to remove statistical outliers. 11 paired analyses of dense and light community diversity (using the HaeIII restriction enzyme) from density separates of Eel River Basin sediment horizons were chosen for statistical analysis in PC-ORD v. 5.10. 126 unique OTUs were identified in the 22 electropherograms. A pruned data set was analyzed in parallel with only the 28 OTUs represented in 15+ separates in order to control for potential bias related to extraction sample volume (i.e., low DNA yield from small sample volumes may selectively exclude low-abundance taxa). Sample volume bias was excluded by commonality of the full and pruned data matrices as well as intercomparison of magnetic and dense low-volume partitions (magnetic and dense dissimilarity is inconsistent with bias determined by sample volume). Total OTU abundance within samples was normalized to 1 following bin removal. 9 paired analyses of magnetic and nonmagnetic were analyzed as described above. 122 unique OTUs were identified in the initial matrix, of which 26 remained following removal of taxa not present in at least 12 of 18 electropherograms. The two matrices were analyzed in parallel following normalization of OTU abundance.

Statistical significance of community difference between dense (> 2.8 g/cc) and light (< 2.8 g/cc) mineral partitions was assessed by Blocked Multi-response Permutation Procedures (MRBP; Mielke and Berry, 1982) using Euclidian distance with groups defined by mineral fraction type and blocks defined by sediment horizon. Chance-corrected within-group agreement (A)—related to the statistical variance within the pre-defined groups—was 0.0637 for the full matrix and 0.0436 for the pruned analysis. Both values indicate greater similarity within groups than expected by chance (A=0) but indicate significant heterogeneity. Parallel analyses on the 126 OTU and 28 OTU density matrices were carried out with values weighted by taxon ubiquity ($b_{ij} =$

$x_{ij} * N_j / N$ where b_{ij} is the adjusted value, x_{ij} the original value, N_j is the number of samples in which the OTU is present, and N the total number of samples) in order to test potential bias in template quality or amplification strength differentiated between separate types. Indicator species analysis (Dufrene and Legendre, 1997) was used to identify key OTUs exhibiting variation between mineral separates and between core types. Indicator species were only identified where maximum taxon abundance in the dataset exceeded 5% in order to exclude potential error derived from separation methodology (Harrison and Orphan, in press). A 9999 permutation Monte Carlo test was used to determine the statistical significance of indicator values. 2-way cluster analyses were performed on density data matrices using Sorensen Distance and the Flexible Beta linkage method ($B = -0.25$). Clustering of TRFLP OTUs followed normalization of matrix values to OTU maxima ($b_{ij} = x_{ij} / x_{j(max)}$ in which the division is the maximum abundance of each taxon within the studied samples).

Select sediment horizons in which each of the bulk, dense, and light bacterial communities were analyzed (4 horizons by HaeIII and 8 by RsaI) were used to determine OTUs discarded in the final < 1.5 g/cc supernatant, corresponding to biogenic debris, organo-mineral aggregates and unattached cells. Bulk sediment-affiliated T-RFs were identified by indicator species analysis using a 4999 permutation Monte Carlo test. OTUs were considered significant indicators with a maximum p-value of 0.05 and minimum mean abundance of 1%.

Results

Sediment mineralogy and geochemistry

Eel River Basin sediments were primarily composed of quartz, feldspar, phyllosilicates (smectites, chlorite, and illite) and authigenic sulfides (Fig. 1). Sulfide mineral XRD spectra were consistent with pyrite (FeS_2 ; Fig. 1) and framboidal pyrite (Kohn et al., 1998; Ohfuji and Rickard, 2005) was commonly observed by SEM across all core types. Mineral separations reproducibly concentrated mineral phases in expected fractions. However, some dominant mineral components (e.g. quartz, expected to segregate in the “light” and “nonmagnetic” fractions) were detected in all partitions by XRD, indicating that separation protocols are useful for enrichment, but cannot “purify” minerals of interest. Harrison and Orphan (in press) further characterized ERB mineralogy and the efficacy of mineral separation by SEM. Dense partitions at 2.8 g/cc enriched pyrite and chlorite (Fe/Mg-bearing phyllosilicate) with proportional depletion in the light partition, while magnetic partitions enriched chlorite and illite (Fe/Mg-bearing phyllosilicates). Dense and magnetic partitions represented minor fractions of the bulk sediment (~ 0.02 – 0.1 g per 1.0 g wet sediment processed).

Porewater methane concentrations increased with proximity to seafloor expression of active seepage and with depth from the sediment-water interface, while sulfate exhibited the inverse trends. Depletion of sulfate beneath 6 cm in mat core PC29 indicated active dissimilatory sulfate reduction. Flat sulfate profiles above 6 m and from 0–15 cm in clam core PC23 and low-flux core PC20 were consistent with relatively low rates of sulfate reduction and/or porewater mixing through bioturbation. Orphan et al. (2004) presented a more extensive description of porewater geochemistry by habitat in Eel River Basin methane seeps.

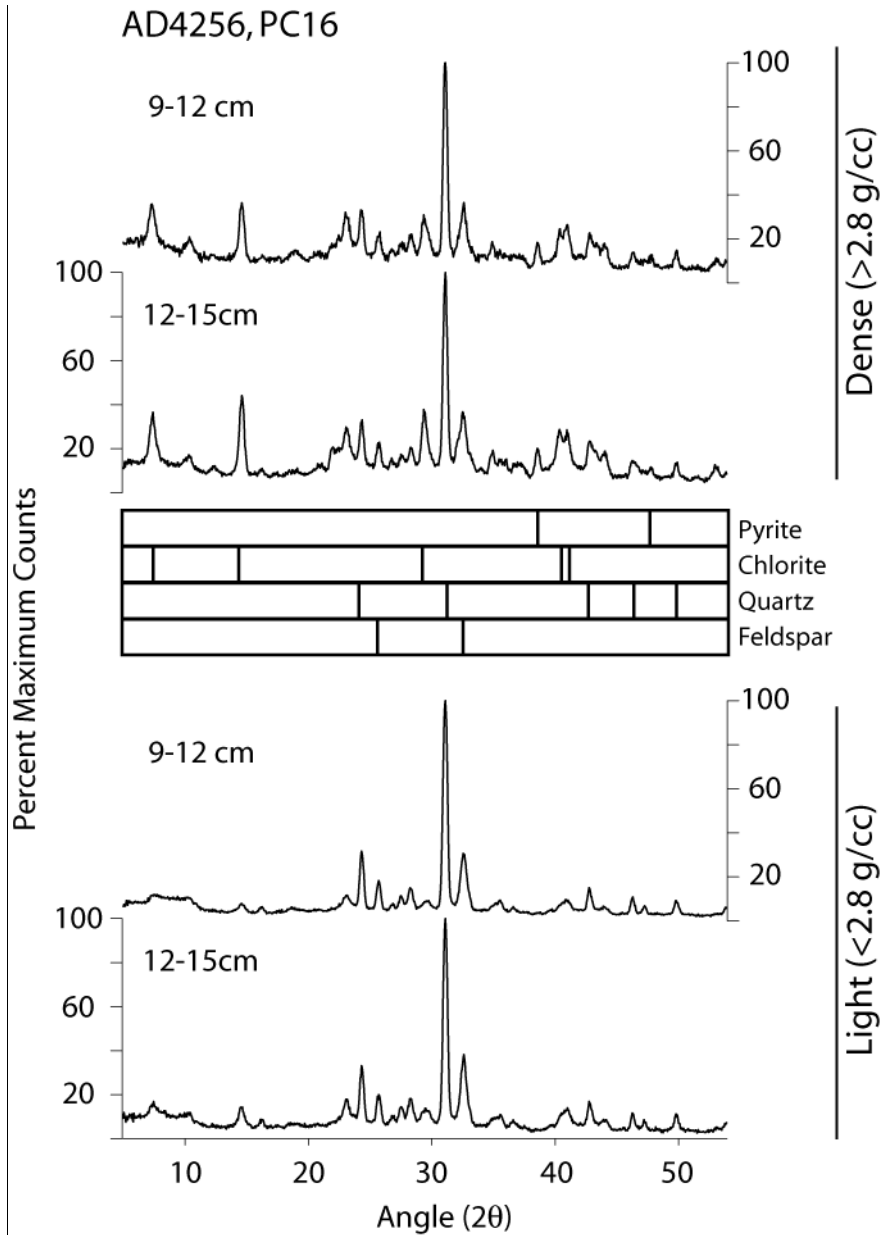


Fig. 1. X-ray diffractometry spectra of Eel River Basin mineral separates. Diagnostic peaks corresponding to key mineral phases are shown.

Microbiology of environmental samples

TRFLP analysis of Eel River Basin sediments showed statistically significant differences in diversity between mineral separates when compared to methodological error and processing error attributable to mineral separation protocols (Fig. 2; Harrison and Orphan, in press).

Phylogenetic distance was greater among bacterial OTUs than among archaea, although distance also exhibited dependence upon restriction enzyme selection. Comparison of paired analyses of dense/light and magnetic/nonmagnetic mineral fractions after median alignment by MRBP revealed bacterial community differences at greater than 98% confidence (Table 1). Dense and magnetic bacterial communities were less diverse than light and nonmagnetic signatures derived from the same sediment horizons.

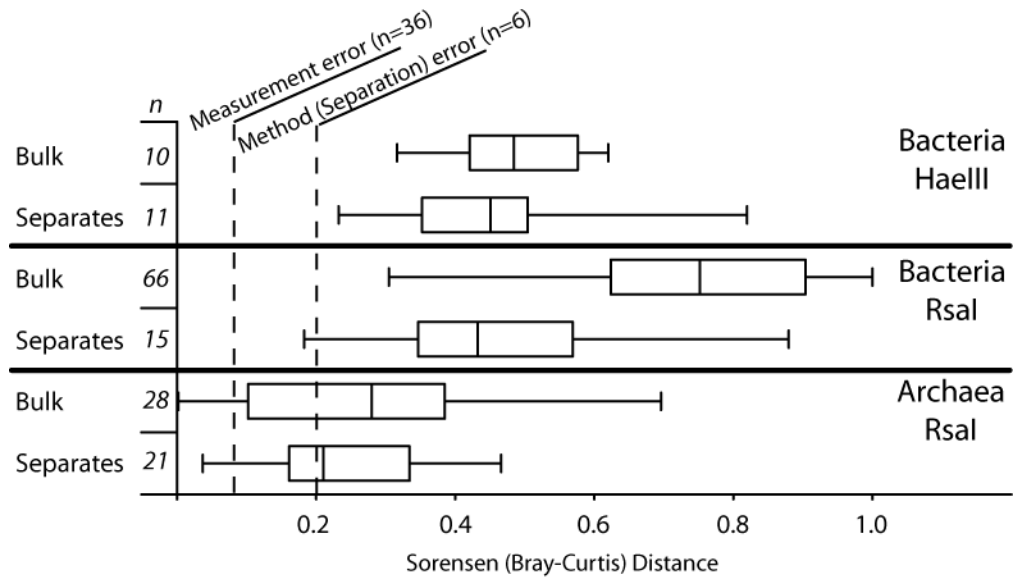


Fig. 2. Environmental (phylogenetic) distance between bulk sediment analyses and mineral separates of the Eel River Basin using terminal restriction fragment length polymorphism. Error measurements are mean+2 σ . "Measurement" error was determined by replicates of a DNA size standard across multiple instrument runs. "Method" error was determined by replicated density separation and archaeal community measurement of a pre-homogenized sediment sample.

TABLE 1. Comparison of mineral separates of select Eel River Basin sediment horizons by TRFLP

Fraction	126 OTUs			28 OTUs (15/22 samples threshold)			Abundance (%) of select phylotypes (HaeIII)			
	Species Richness	Shannon Diversity	MRBP (p-value)	Species Richness	Shannon Diversity	MRBP (p-value)	208 (δ)	225 (Chfx)	258 (γ)	508 (ϵ)
Dense (> 2.8 g/cc)	46.0	2.889	0.00140	20.7	2.290	0.01549	5.9±6.8	2.5±2.1	5.8±5.2	16.5±10.4
Light (< 2.8 g/cc)	61.8	2.961		25.1	2.488		10.9±7.3	5.8±6.3	0.9±0.7	17.1±7.8
Fraction	122 OTUs			26 OTUs (12/18 samples threshold)						
	Species Richness	Shannon Diversity	MRBP (p-value)	Species Richness	Shannon Diversity	MRBP (p-value)	206–208 (δ)	225 (Chfx)	257 (γ)	271 (δ)
Magnetic	55.4	2.703	0.00371	20.1	2.026	0.00377	27.6±16.7	3.0±2.6	3.0±2.6	10.0±8.6
Nonmagnetic	52.2	2.779		20.7	2.194		17.3±11.4	4.8±5.8	4.0±4.7	10.3±6.7

Chfx: Chloroflexi. δ , γ and ϵ refer to respective proteobacterial classes.

Across 57 representative samples, an average of 73% of archaeal phylotypes (detectable by RsaI) were identified as ANMEs, predominantly falling within the ANME 2ab (44.8%) and ANME 2c (21.3%). Although partial sequences recovered from PC29 fell within the ANME 2b subgroup, as is typical of Eel River Basin seeps, the selected restriction enzymes do not resolve phylogenetic differences between ANME 2a and 2b. No significant trends were observed in the distribution of non-ANME archaea across the studied horizons and separates. ANME 1 archaea (7.2%) were not detected in dense fractions (14 sediment horizons) and exhibited significantly reduced abundance in magnetic partitions by comparison to paired within-horizon nonmagnetic analyses (7 horizons). Mineral-adherent ANME 2c phylotypes were more commonly encountered at depths 12cm and below the sediment-water interface (Fig. 3). In mat core PC29, ANME 2c fragments exhibited light fraction “mineral affinity”—defined as increased abundance on a mineral or sediment fraction enriched in specific mineralogy—relative to ANME 2ab abundance, while the opposite relationship was observed in low-flux core PC20.

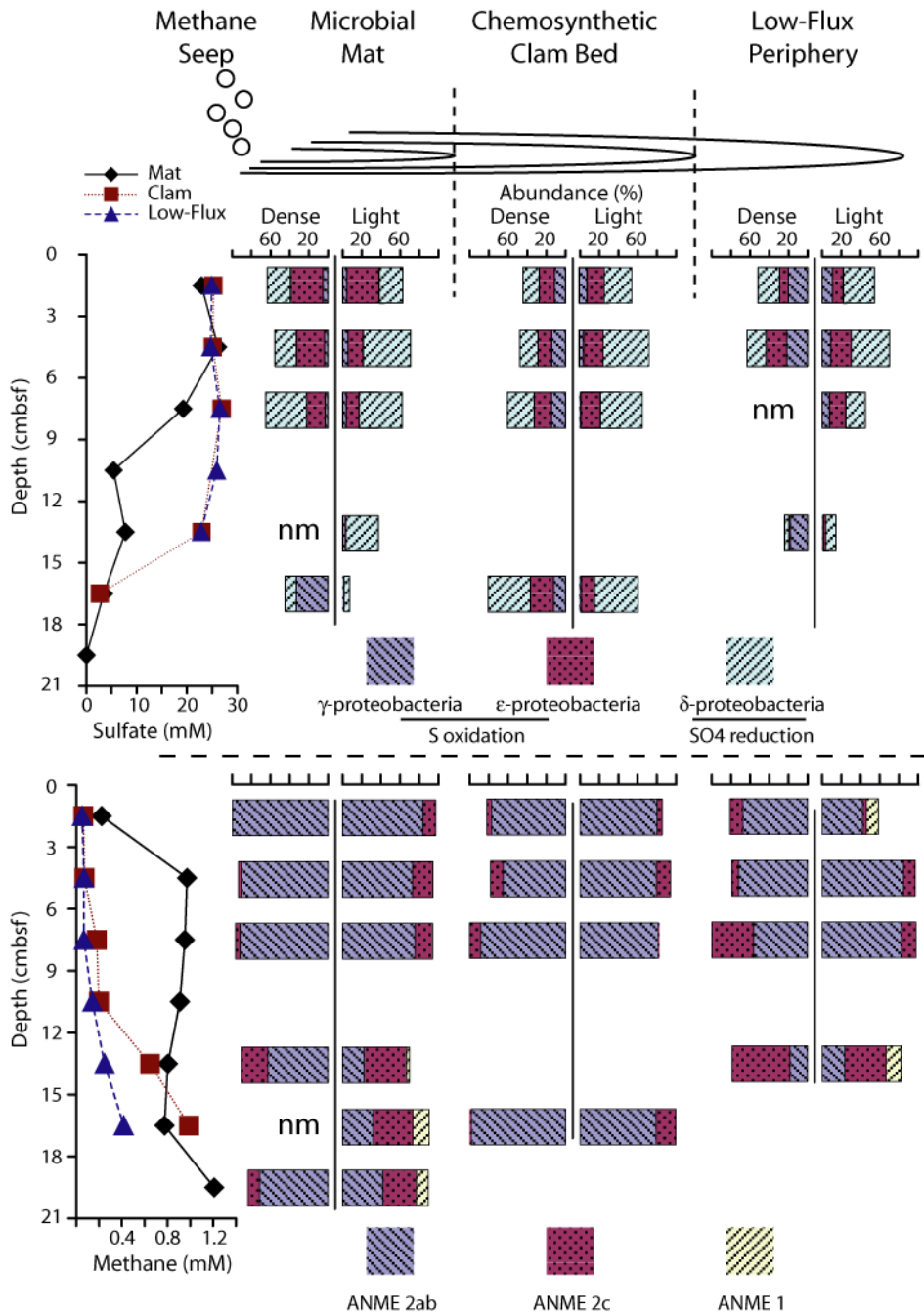


Fig. 3. Distribution of key microbial phylotypes across an Eel River Basin methane seep. Abundances are percent of detectable community determined by TRLFP using the HaeIII (Bacteria) and RsaI (Archaea) restriction enzymes. nm: not measured

From 156 T-RF bins identified in HaeIII bacterial analysis, 21 exhibited an average relative abundance of greater than 1% across the 26 selected samples, accounting for 80.6% of the total signal. 20 of these common bins were assigned a likely phylogenetic identity based on known cut sites within 1 bp of measured fragment length and the presence of comparably abundant peaks in known cut sites by the RsaI restriction enzyme. Within this group, *Deltaproteobacteria* (38.3% average relative abundance) were the dominant taxa, ranging from 6.6% to 56.8% of the T-RF signal restricted to common OTUs. *Deltaproteobacterial* diversity derived from partial sequences and T-RFs fell within the *Desulfobulbaceae* (DSB, ~ 27.7% average abundance) and *Desulfubacteraceae* (DSS, ~ 10.6%), consistent with previous investigations of the Eel River Basin (Orphan et al., 2001; Pernthaler et al., 2008; Beal et al., 2009). Poor resolution of peaks in the 207–208 bp range of HaeIII electropherograms and non-measurable fragment sizes by RsaI prevented accurate comparison of DSB and DSS relative abundances. At the class or phylum level, only *Deltaproteobacteria*, *Epsilonproteobacteria* (20.3%), *Gammaproteobacteria* (12.5%), *Chloroflexi* (formerly known as Green Nonsulfur Bacteria; 10.4%), and *Acidobacteria* (6.2%) exhibited greater than 5% average abundance across the studied horizons. The presence of AOM-syntrophic DSS phlotypes was confirmed by FISH in PC29 3–6 cm using FITC-labeled probe DSS658 in this and previous studies (Fig. 4; Pernthaler et al., 2008)

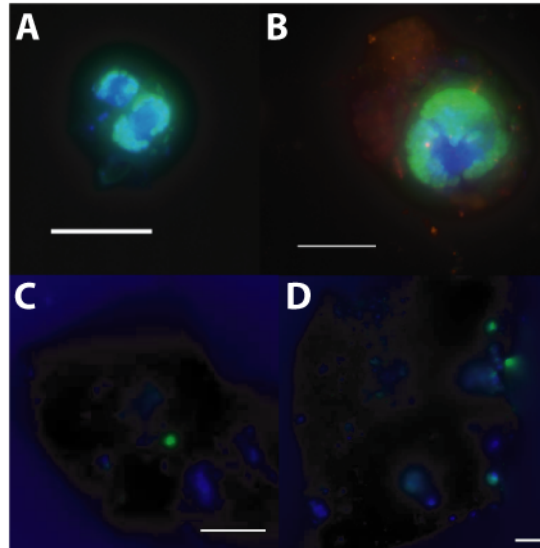


Fig. 4. Fluorescence *in situ* hybridization images of mineral separates of an Eel River Basin sediment horizon (A,B) and pyrite-amended microcosm (C,D). A, B) AOM aggregates associated with EPS and phyllosilicate minerals (unincorporated surrounding the aggregate). Green: FITC-labeled DSS658; blue: DAPI. C, D) Cells attached to pyrite grains post-incubation. Green: FITC-labeled Gam42; blue: DAPI. All scale bars are 10 μm .

Dominance of *Delta*, *Epsilon*, and *Gammaproteobacteria* and *Chloroflexi* was broadly consistent with environmental clone libraries derived from methane seep environments (summarized in Harrison et al., 2009). *Epsilonproteobacteria* belonging to the *S*-oxidizing genus *Sulfurovum* (Takai et al., 2004) were most abundant in surface sediments—particularly in microbial mat cores—but persisted at depths where sulfate was significantly depleted (< 20 mM) from seawater values (Fig. 3.; mat core PC29 6–9 cm, clam core PC23 15–18 cm). Indicator species analysis demonstrated segregation of OTUs by core type (Table 2), with *Deltaproteobacteria* in high-methane mat and clam cores. Low-flux cores, in contrast, showed enrichment in putative *Gammaproteobacteria* (Hae258) and *Chloroflexi* (Hae222, Hae2225).

TABLE 2. Significant (90% confidence) indicator taxa for Eel River Basin density partitions and habitat types

otu	Abundance		Frequency				Original Groupings				Monte Carlo (n=9999)		p-value	Max. Rel. Abundance (%)	Putative phylogeny
	Dense	Light	Dense	Light	Dense	Light	Dense	Light	Mean	S.Dev					
	Mat	Clam	Low	Mat	Clam	Low	Mat	Clam	Low	Mat	Clam	Low			
Dense (> 2.8 g/cc)	Hae258	87	13	82	91	82	79	11	54.6	8.86	0.0150	15.5	γ		
Light (< 2.8 g/cc)	Hae208	35	65	100	82	29	65	65	53.8	6.46	0.0654	19.7	δ		
	Hae222	28	72	100	64	18	72	72	54.6	9.61	0.0591	21.9	<i>Chloroflexi</i>		
	Hae225	30	70	100	91	27	70	70	58.5	7.16	0.0730	22.3	<i>Chloroflexi</i>		
	Hae270	37	63	100	73	27	63	63	51.2	6.17	0.0531	5.7	δ		
Mat	Hae208	48	33	19	100	73	100	48	24	19	39.0	5.45	0.0759	19.7	δ
Clam Bed	Hae203	30	48	22	100	100	71	30	48	16	39.3	4.78	0.0558	24.7	δ
Low-flux	Hae222	24	14	62	75	82	100	18	12	62	43.7	8.39	0.0268	21.9	<i>Chloroflexi</i>
	Hae225	13	27	60	88	100	100	11	27	60	44.3	6.07	0.0044	22.3	<i>Chloroflexi</i>
	Hae258	7	30	63	88	73	100	6	22	63	42.4	8.34	0.0209	15.5	γ

δ and γ refer to respective proteobacterial classes

Comparison of T-RFLP electropherograms showed affinity of key *Gammaproteobacterial* OTUs for the dense, > 2.8 g/cc mineral fraction and *Deltaproteobacteria* for the light, < 2.8 fraction, and was reproducible across disparate sediment horizons (Fig. 5). Elution of the *Gammaproteobacterial* HaeIII fragment ranged from 257–259 bp—resolved by analytical software as two discrete bins. Dense fraction abundance of the paired bin was $8.4 \pm 5.9\%$ compared to a light fraction abundance of $2.0 \pm 1.5\%$. Closest relatives of *gammaproteobacterial* sequences bearing consistent HaeIII cut sites predominantly fell within uncultured clades across too great a phylogenetic range to be assigned unambiguous genus-level identification. *Deltaproteobacterial* fragments across the 203–208 bp range (spanning 3 T-RF bins) similarly exhibited reproducible enrichment in the light mineral fraction ($22.2 \pm 11.9\%$ dense, $32.2 \pm 11.4\%$ light). Cut sites indicated ambiguous membership in the DSS or DSB clades and could not be fully resolved. However, dominant peaks in the 203–206 bp range were more consistent with DSB and relatives of *Desulforhopalus* (Isaksen and Teske, 1996). DSS phylotypes forming archaeal/bacterial cell aggregates linked to AOM (Orphan et al., 2001; Knittel et al., 2005; Fig. 4) were more abundant in the light fraction (8 aggregates out of 84 particles in the 5–50 micron size range) than the dense (2/106) as assessed by FISH.

Indicator species analysis confirmed dense partition mineral affinity of Hae258 and light fraction affinity of Hae208 at greater than 90% confidence (Table 2). OTUs identified as *Chloroflexi* (Hae222 and Hae225) and additional *Deltaproteobacteria* (Hae270) also partitioned favorably in the light fraction. In 9 of 11 studied horizons, the light fraction selected the putative *Chloroflexi*, but strong (> 5%) differences were found in only 4 samples (e.g. PC20, 12–15 cm). > 5% differences in relative abundance between mineral fractions were not detected for HaeIII270.

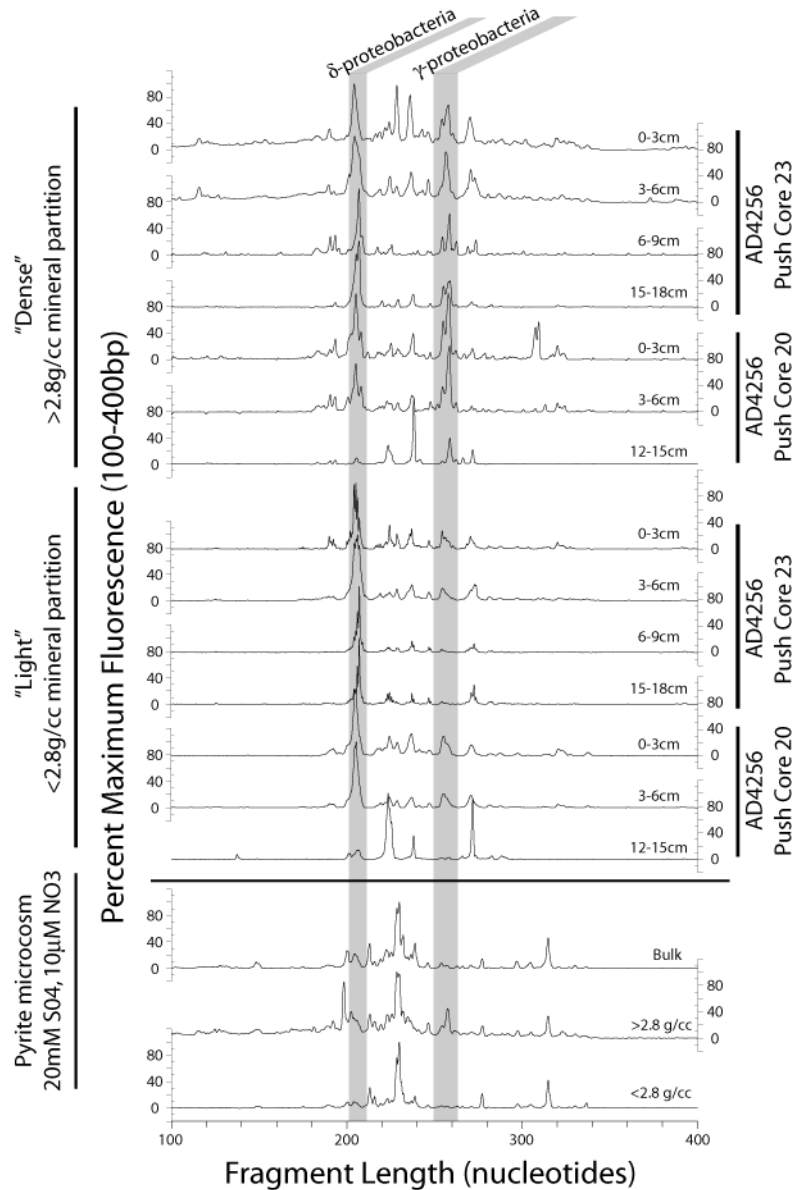


Fig. 5. TRFLP electropherograms exhibiting 16S rRNA gene signal of key delta and gammaproteobacterial phylotypes for select Eel River Basin sediment horizons

2-way cluster analysis of density separates (Fig. 6) revealed groups defined by individual sediment horizons (e.g., 2686), core (2702, 2704) and mineralogy (dense fractions of 2693, 2694). Clade membership did not vary significantly between the full, 126-OTU matrix and the

28-OTU restricted matrix limited to common phylotypes: groups established by pruning the cladogram at 62.5% information remaining are identical for 21/22 horizons, and nearest neighbors were consistent between the two matrices for all but 3 samples. The distribution and abundance of putative *S*-oxidizing *Epsilonproteobacteria* (Hae508) correlated with key sulfate-reducing *Deltaproteobacterial* taxa (Hae206, 208).

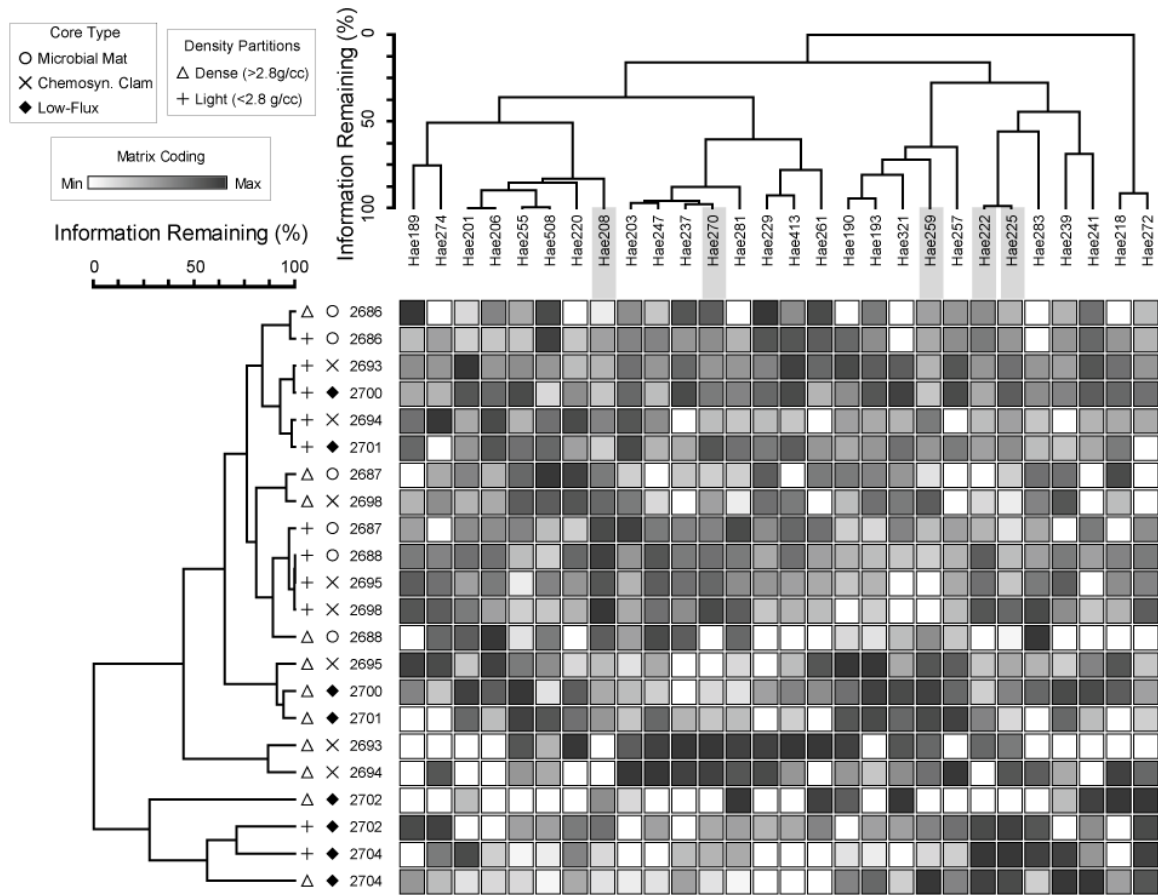


Fig. 6. 2-way cluster analysis of 16S rRNA gene bacterial diversity recovered from “dense” and “light” mineral separates from 11 Eel River Basin sediment horizons. Samples were analyzed by terminal restriction fragment length polymorphism (TRFLP) using the *HaeIII* restriction enzyme. Cluster analysis presented corresponds to the 28 fragments represented by no fewer than 15 of the 22 samples. Shading indicates statistically significant indicator taxa corresponding to mineral separate types.

Indicator species analysis demonstrated affinity of 4 minor OTUs for bulk sediments in comparison to density separates, suggesting preferential partitioning of unattached (non-mineral-adherent) cells. Hae241 (mean abundance 1.2% in bulk analyses, $p=0.0086$) was

tentatively affiliated with *Planctomycete* division WPS-1 phylotypes and *Deltaproteobacterial* clade Eel-1. Hae272 (3.2%, $p=0.0176$) was consistent with diverse *Deltaproteobacteria* and with Candidate Division OP8. Hae193 (2.0%, $p=0.0264$) was identified with uncultured *Alphaproteobacteria*. Cut site Hae234 (2.1%, $p=0.0488$) was consistent with the T78 clade of the *Chloroflexi*. Each T-RF was ubiquitous in bulk analysis across the 4 horizons surveyed. Affinity for the organic/unattached community requires further investigation given low abundance and the use of a discrete sediment aliquot for bulk analysis (i.e., comparison to dense and light fractions included minor spatial heterogeneity).

Microcosm incubations

Low porewater sulfide levels were detectable in only two of six microcosms in which pre-sterilized pyrite was included, and all pyrite microcosms exhibited suppression of key *Deltaproteobacterial* phylotypes (Hae208) compared to the inoculum (Table 3). Mineral affinity of Hae259 and Hae270 was broadly consistent with their partitioning in environmental samples, preferred in the dense and light fractions, respectively. *Gammaproteobacterial* cells were imaged in physical association with microcosm cult09 pyrite particles using FITC-labeled FISH probe Gam42 (Fig. 4), and cell counts confirmed affinity for the dense partition (20% hybridized of 541 counted cells) over the light (4% of 444). 62 distinct bacterial OTUs were identified among microcosm bulk samples and mineral separates using the HaeIII restriction enzyme. Dominant (> 10% relative abundance) OTUs from pyrite microcosms were tentatively identified as members of the *Actinobacteria*, *Acidobacteria*, *Bacteroidetes*, *Firmicutes*, and Candidate Division JS1. These T-RF identities were consistent with sequences recovered from the Eel River Basin, but dominant taxa were not comparable to known environmental samples.

Archaeal communities in non-pyrite microcosms (cult04, cult05) partitioned in a similar manner to high-methane environmental samples: ANME-1 exhibited affinity for light fraction; ANME-2ab/2c ratio was greater in the dense fraction. Across the 4 pyrite microcosms for which archaeal communities were analyzed, ANME-1 phylotypes consistently favored the dense partition over the light. Overall ANME abundance was reduced (average 67.3%) compared to the inoculum (82.4%) largely due to suppression of ANME-2 OTUs. Marine Benthic Group B (MBGB, HaeII293) and Miscellaneous Crenarchaeotal Group (Hae236) phylotypes accounted for 5.2 and 11.0% of the detectable community in pyrite microcosms, respectively. MBGB exhibited affinity for the dense fraction ($4.3 \pm 1.4\%$ greater than light fraction abundance, $n=4$).

Discussion

The magnitude of bacterial and archaeal community (phylogenetic) distances between mineral separates measured by TRFLP demonstrates mineral attachment is a significant component of microbial diversity in marine sediments (Fig. 2), suggesting that mineral composition exerts selective pressure on microorganisms. Previous studies of microbial colonization patterns in terrestrial environments have suggested that strong differences result from the unique presence of limiting nutrients within the mineral substrate (Mauck and Roberts, 2007). The dependence of microbial diversity on mineral colonization in marine sedimentary environments representing variable redox chemistry and organic matter availability remains unclear. Within Eel River Basin sediments, significant (above-error) differences are broadly distributed with depth below the sediment-water interface and proximity to methane seeps. Mineral affinity of specific microbial taxa persists for sulfate concentrations from seawater to depletion and in shallow sediment horizons where more energetically favorable electron

acceptors (O_2 , NO_3) likely are not fully consumed. The sample types considered in this study may therefore serve as a useful first-order approximation of the breadth of porewater geochemical conditions encountered on continental margins. However, the large proportion of authigenic minerals from early diagenesis observed in methane seeps may be atypical, and further application of this approach in diverse environments is needed to fully characterize the role of microbe-mineral interactions in the marine subsurface.

Archaeal mineral affinity and implications for AOM

Within both microbial mat core PC29 and low-flux core PC20, mineral-associated ANME 2c archaea were predominantly found in deeper sediment horizons 12+ cm beneath the seafloor. However, the mineral affinity exhibited by ANME 2c phylotypes differs between the two cores, showing light fraction association in high-methane horizons and dense fraction association in low-methane sediment (Fig. 7). This pattern indicates that mineral association may be influenced by geochemistry/redox/zonation and may also show ecophysiological differences between ANME 2ab and ANME 2c clades. Mineral attachment likely restricts the availability of methane in pore fluids (Murray and Jumars, 2002). Therefore, mineral attachment could represent an adaptation to lower methane concentrations among methanotrophs, but this factor would not be expected to differentiate between minerals unless significant differences in surface structure were encountered (e.g., pits, cleavage planes). High levels of porewater methane may instead reduce environmental pressure opposing mineral attachment.

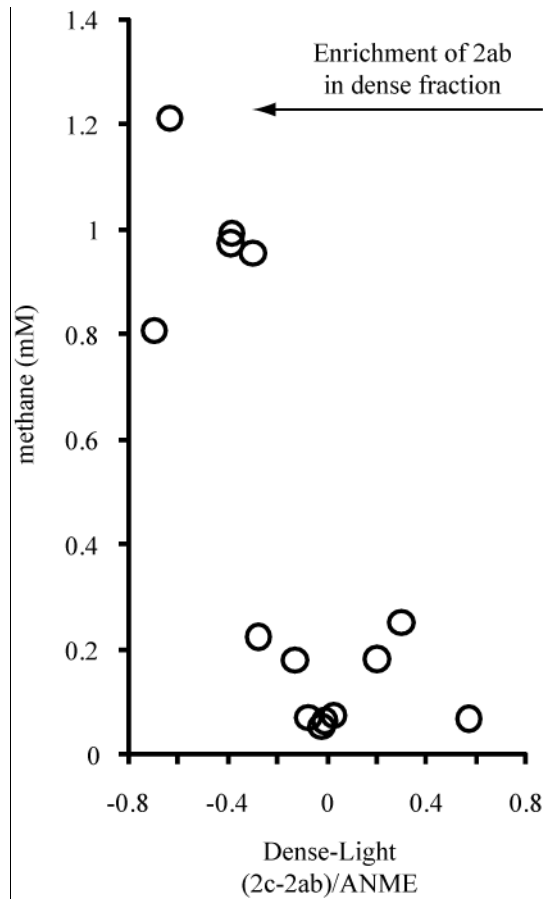


Fig. 7. Relative abundance of ANME-2 subgroups between mineral separates in Eel River Basin sediments determined by TRFLP. ANME is sum of abundances of all ANME phylotypes.

Alternatively, distribution of ANME phylotypes could be driven by association with *Deltaproteobacterial* syntrophic partners. T-RFs uniquely identified as *Deltaproteobacteria* by HaeIII are significantly less abundant at 12–15 cm in PC20 in comparison to other sulfate-replete horizons in this study. Given that *Deltaproteobacterial* abundance and/or diversity are not consistent between the two cores, co-partitioning of AOM syntrophs may represent a parsimonious interpretation of the differing mineral affinity of ANME groups.

Schreiber et al. (2010) identify SEEP-SRB-1a, a specific clade of the *Desulfobacteraceae*, as the dominant syntrophic partner of ANME 2 archaea. Analysis of SEEP-SRB-1a sequence data from the eastern North Pacific continental margin shows HaeIII cut sites of 209 and 211 and RsaI cut sites of 248 and 250. T-RF RsaI250 was not detected among 50 analyses used in Ar/Bac cross-reference, and HaeIII209 is not easily resolved from other common *Deltaproteobacteria* in the Eel River Basin methane seeps. Where RsaI248 is detected, our data are broadly consistent with a positive correlation between its abundance and the relative abundance of ANME phylotypes (all subgroups) compared to other archaeal taxa (Fig. 8). Similarly, a positive relationship was observed between the abundance of bacterial RsaI248 and Archaeal RsaI246/244 ratio (ANME 2c/ANME 2a). However, ANME phylotypes are the dominant archaeal taxa throughout the sampled horizons (minimum 58.5% detectable by RsaI) while bacterial RsaI248 is a maximum 6.5% of the detectable community across 50 analyses of bulk sediment and mineral partitions. *Deltaproteobacterial* diversity is persistently dominated by terminal fragments primarily associated with the *Desulfobulbaceae*. This supports the contention by that other *Deltaproteobacterial* clades may be significantly involved in AOM syntrophy (Losekann et al., 2007; Pernthaler et al., 2008). T-RFLP serves as an adequate measure of the relative abundance of the specific SEEP-SRB1a clade due to the extensive sequence information recovered from the Eel River Basin sediments in this and other studies. Great caution should be taken in extrapolating these T-RF cut sites to interpret *Deltaproteobacterial* abundance in other localities, given the broad diversity of the phylum in the environment.

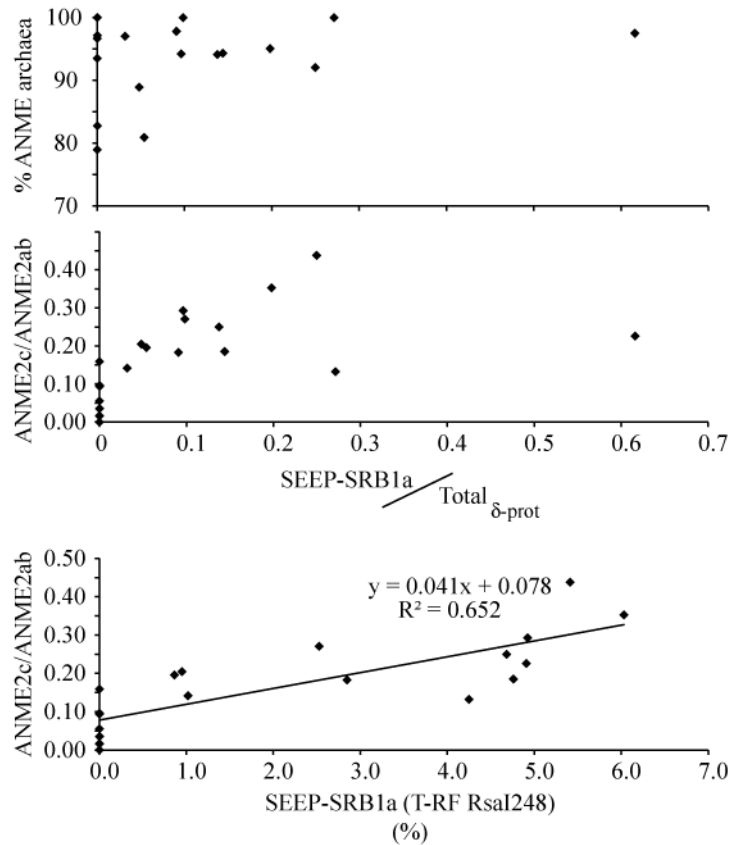


Fig. 8. Correlation of SEEP-SRB1a abundance with trends in ANME archaeal diversity across 20 environmental extracts of bulk sediment and mineral separates. Relative abundance of bacterial and archaeal taxa were determined by T-RFLP using the RsaI restriction enzyme.

ANME 1 phylotypes were absent or less abundant in dense and magnetic partitions across 11 sediment horizons in which the subgroup was identified in bulk, nonmagnetic, or light partitions. This was also the pattern observed in microcosm “control” incubations lacking added pyrite, and is consistent with a possible free-living ecology of ANME 1s. However, across 4 pyrite microcosms, ANME 1 archaea are persistently enriched in the dense fraction (by 3–21% as a proportion of total ANME phylotypes; Table 3). Previous work has suggested that pressure, temperature, and oxygen sensitivity may be important factors selecting between ANME 1 and 2

phylotypes (Kallmeyer and Boetius, 2004; Nauhaus et al., 2005; Knittel et al., 2005). Increased ANME 1 abundance has been observed with greater flow rate (methane flux) in a continuous-flow bioreactor (Girguis et al., 2005). Yanagawa et al. (2011) argue that low or depleted sulfate concentrations in porewater may be associated with increased relative abundance of ANME 1 archaea, an observation consistent with other studies demonstrating the presence of these phylotypes at depths beneath the sulfate-methane interface (e.g., Harrison et al., 2009). These potential factors are assumed to have been consistent between mineral fractions in sediment microcosms. The affinity of ANME 1 OTUs for the dense fraction in pyrite microcosms suggests an ecophysiological difference between AOM archaea independent of temperature, pressure, and porewater concentrations of methane and sulfate. ANME archaea engaged in a methanogenic lifestyle (Orcutt et al., 2005; Orcutt and Meile, 2008; House et al., 2009; Yanagawa et al., 2011) is one possible interpretation of this trend.

Beal et al. (2009) observed increased abundance of ANME 1 signature from PCR amplification of methyl-coenzyme M reductase (*mcr*) in laboratory incubations coupling AOM to manganese reduction. The suppression of putative sulfate-reducing *Deltaproteobacterial* phylotypes and absence of porewater sulfide in pyrite incubations is consistent with introduction of Fe³⁺ phases and other oxidants potentially associated with impure pyrite during microcosm construction. Enrichment of ANME-1 phylotypes correlated with pyrite microcosms may therefore support a preferential role of ANME-1s in AOM coupled to metal reduction. However, the observed distribution of ANME-1s may also be explained only by preferential growth post-microcosm assembly. If turnover of the DNA signal associated with native sediment were limited, cells associated with the pre-sterilized pyrite would be preferentially colonized by cells actively growing cells post-assembly. This second explanation is not consistent with the

apparent turnover of the bacterial community in the microcosms, but cannot be explicitly excluded by the methodology used in this study.

Bacterial mineral affinity and implications for methane seep sulfur cycling

Key phylotypes exhibiting mineral affinity in Eel River Basin sediments have T-RF sizes consistent with sulfate-reducing *Deltaproteobacteria* and putative sulfide-oxidizing *Gammaproteobacteria*. Together with *Epsilonproteobacteria* closely related to the known S-oxidizing genus *Sulfurovum*, putative sulfur cycling OTUs account for 54.4% of the detectable community in density separates by HaeIII. Bulk analyses over the same range of horizons average 36.8% abundance of sulfur cyclers, suggesting that these OTUs are preferentially associated with the particle-adherent microbial community. Involvement in sulfur cycling metabolism is further supported by enrichment culture (CultS; Table 3). Filtered seawater microcosm cultS with added S substrates exhibited enrichment of delta and *Gammaproteobacterial* phylotypes during incubation. *Epsilonproteobacteria* were present in the culture (~ 1%) at a reduced level from the inoculum. Putative S-oxidizing (SOB) and SO₄-reducing (SRB) taxa exhibit clear distinctions between mineral fractions (Fig. 9). Recovered SOB taxa outnumber SRB phylotypes within the dense mineral partition in 9 of 12 studied sediment horizons (average 5.3% enrichment) while SRB are favored in 11 of 13 light fractions (average 13.1%). The range of potential differences appears significantly reduced at lower porewater SO₄, possibly reflecting a relationship between bacterial mineral affinity and porewater geochemistry. Broad correlation in abundance of oxidative and reductive S-cycling phylotypes

(e.g., Hae508, Hae206, Hae208 in Fig. 3) is consistent with a full sulfur cycle driven by methane availability.

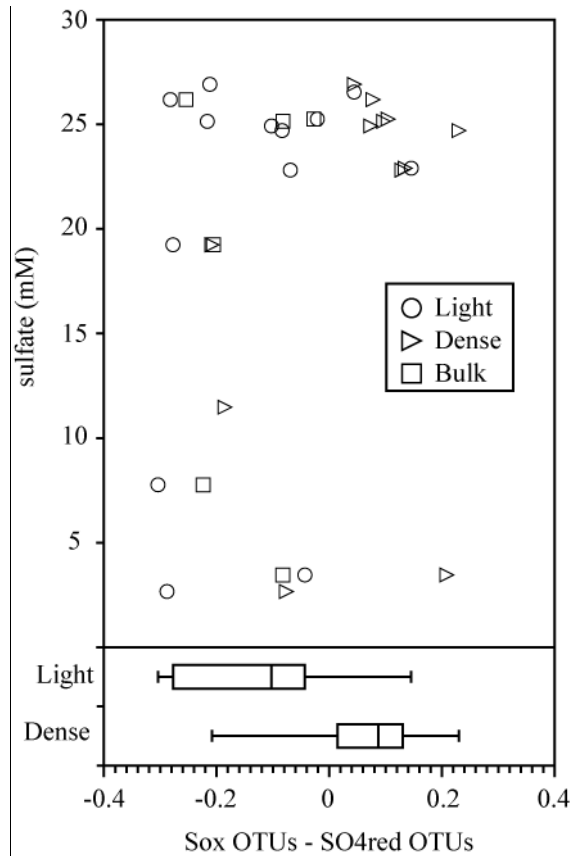


Fig. 9. Relative abundance of oxidative and reductive sulfur-cyclers in Eel River Basin mineral partitions inferred from TRFLP.

Association of putative oxidative S-cycling taxa with the dense mineral partition suggests the possibility of ongoing alteration and redox cycling of sulfide minerals within the sediment column. Specific association of *Gammaproteobacterial* taxa with sulfide minerals is further supported by microcosm FISH cell counts of microcosm mineral separates (Fig. 4), which demonstrated dense fraction enrichment of *Gammaproteobacterial* T-RFs and physical association of hybridized cells with pre-sterilized pyrite. Previous studies have argued that

anaerobic reoxidation may occur immediately following biological reduction of sulfate to hydrogen sulfide in sediments (Bottrell et al., 2000; Schippers and Jorgensen, 2002; Riedinger et al., 2010; Holmkvist et al., 2011) and anoxic water columns (Canfield et al., 2010). Inferred oxidation in these systems is presumed to be driven by reactive Fe^{3+} or Mn^{4+} species thought to persist at depth. The transitory nature of sulfur species not detectable by porewater measurements in these reactions has led to the description “cryptic” sulfur cycling in recent studies (Canfield et al., 2010; Holmkvist et al., 2011). In Eel River Basin dense fractions, mineral affinity of putative SOB taxa persists at depths where sulfate is depleted significantly from seawater concentrations, similarly implying absence of nitrate and oxygen. In addition to potential reoxidation of sulfide minerals coupled to metal reduction, bioturbation may introduce favorable oxidants at depth.

Compared to TRFLP measurement of Eel River Lloyd et al. (2010) observed significantly greater relative abundance of *Deltaproteobacterial* taxa underlying methane seep-associated chemosynthetic mats and relatively lesser abundance of potential SOB taxa (*Epsilon* and *Gammaproteobacteria*) in the Gulf of Mexico using reverse-transcription pcr. While there is considerable diversity in cold seep bacterial communities at the phylum level (Orphan et al., 2001; Teske et al., 2002; Knittel et al., 2003; Harrison et al., 2009), Lloyd et al. and similar studies targeting the metabolically active community in depth profiles (e.g., Martinez et al., 2006) raise the question of whether S-oxidizing taxa exhibiting affinity for the dense partition at depth represent dormant cells buried by ongoing sedimentation. However, several observations support a persistent metabolic relationship between putative S-oxidizing *Gammaproteobacteria* and sulfide particles beneath the sediment-water interface. Authigenic sulfides precipitated within these horizons would likely adopt a microbial signature from the bulk community which

would overprint any signal inherited from shallower sediments. If T-RFs exhibited affinity for the dense partition by exclusion of *Deltaproteobacteria* and *Chloroflexi* linked to the light fraction, we would not expect the dense fraction to select only for *Gammaproteobacteria*. Reoxidation of authigenic sulfide minerals at depths exhibiting sulfate reduction is consistent with observed trends.

Few cultured isolates of the *Chloroflexi* are known despite their common occurrence in marine sediments, and their metabolism is primarily inferred through environmental distribution. Webster et al., (2006) observed that elevated abundance of *Chloroflexi* in marginal marine sediments is associated with deep, organic-rich horizons. Coolen et al. (2002) linked *Chloroflexi* abundance with Mediterranean sapropel horizon, suggesting potential adaptation to high organic matter content. In the Santa Barbara Basin, *Chloroflexi* are negatively associated with the sulfate-methane transition zone (SMTZ) and exhibit peak abundance beneath that zone, supporting heterotrophic metabolism for the group and affinity for organic-rich horizons beneath the SMTZ (Harrison et al., 2009). Association with organic matter may play a role in the light fraction mineral affinity of this group in the Eel River Basin. However, the association should be considered tentative considering the phylogenetic breadth of the *Chloroflexi* and the imprecise nature of TRFLP identities.

Organic matter (OM) in marine environments may also adsorb to or aggregate with minerals with an affinity that varies depending on the composition of both the mineral and organic compound (Keil and Hedges, 1993; Arnarson and Keil, 2000; Satterberg et al., 2003). Mixed-layer smectites and illites in the light fraction may serve to inhibit enzymatic degradation of organic molecules and preserve them to greater depths in the water column and sediment (Zonneveld et al., 2010). Organo-mineral aggregates formed within the water column are likely

to be concentrated preferentially in the light fraction rather than the dense partition enriched in authigenic minerals. Additionally, sediment particles having substantial volume taken up by OM will have bulk density less than 2.8 g/cc unless sulfides are the dominant mineral component, as other mineral phases have densities near or beneath that threshold (Harrison and Orphan, in press). The light fraction is therefore potentially a more significant source of allochthonous OM potentially accessible to heterotrophic metabolism (*Chloroflexi*) or organoclastic sulfate reduction (*Deltaproteobacterial* OTUs exhibiting light fraction mineral affinity). Future research observing community response to a range of carbon substrates or detailed organic geochemistry of methane seep mineral fractions may serve to test this hypothesis. The association of key AOM-independent phylotypes with an OM-rich fraction suggests that non-methane organic carbon sources and potential electron donors may still play an important role in seep ecology.

Although putative *Deltaproteobacteria* with a HaeIII cut site at 270 bp exhibit a positive correlation with *Chloroflexi* consistent with a common factor driving mineral affinity, Hae208 is negatively correlated. Although the phylogenetic identity of Hae208 within the *Deltaproteobacteria* is ambiguous, the T-RF is consistent with AOM-associated syntrophic *Deltaproteobacteria*, which typically exhibit a translucent non-hybridized external shell of extracellular polymeric substances and clay minerals. Most organo-mineral particles exhibit densities less than 2.8 g/cc and are concentrated in the light fraction of bimodal separates. Aggregates lacking mineral shells and unbound to minerals are likely to be discarded during density separation, having densities less than 1.5 g/cc, but would be concentrated in the nonmagnetic fraction during magnetic separation. FISH counts of aggregate abundance in PC29 3–6 cm were consistent with TRFLP results showing 7.5% enrichment of putative-*Deltaproteobacterial* Hae208. However, the T-RF bin is likely only partially composed of

aggregate-forming syntrophs. The ambiguous phylogenetic identification of Hae208 may also prevent clear correlation with *Chloroflexi* OTUs.

Conclusions

Bacterial diversity exhibits multiple discrete patterns of mineral-dependent variability. Association of putative sulfur-oxidizing species with sulfide minerals in the Eel River Basin supports the observation that reoxidation of solid-state sulfides persists at depths where sulfate reduction is the dominant form of microbial respiration. A mineral separation approach may represent an additional means of assessing competing theories of reoxidation, sulfur disproportionation and passive diffusion in future investigations of marine sediment. Microbial alteration of authigenic sulfides at depth and potential impacts on sulfur isotopic records should additionally be taken into account in paleoenvironmental reconstruction. Enrichment of specific bacterial taxa in the “light” < 2.8 g/cc mineral fraction implies a significant role of organic matter distribution in determining spatial heterogeneity of marine microorganisms.

Inconsistency of mineral affinity among major ANME archaeal clades (ANME 2c, ANME 2ab and ANME 1) precludes identifying any single factor driving selective attachment. However, significant differences in attachment behavior between ANME subgroups further supports ecophysiological differences between phylogenetically distinct groups involved in the anaerobic oxidation of methane. These results may serve to inform future work resolving the ecophysiological roles of ANME subgroups.

Mineral attachment in the eutrophic environment of Eel River Basin methane seeps drives variations in the microbial community on a fine spatial scale comparable to those

observed across meter-scale differences and a broad range of geochemical conditions. Given this initial example, future surveys of microbe-mineral interactions in marine sediments should reveal a substantial role in driving diversity. Mineral composition-dependent patterns of microbial diversity represent an important aspect of the marine subsurface and a potential opportunity to gain insight into the ecophysiology of the microbial biosphere's uncultured majority.

Acknowledgements

We thank the crew and shipboard party and chief scientist of R/V Atlantis (October, 2006) for support in sample collection. Josh Steele and Olivia Mason provided invaluable support in review of figures and statistical methods. Thomas Bristow provided assistance with X-ray diffractometry, and Chi Ma provided important support in Scanning Electron Microscopy. Porewater geochemistry was measured with the support of R. Burt Thomas and Nathan Dalleska. This work was supported by a grant from the Gordon and Betty Moore Foundation (to VJO), a Schlanger Ocean Drilling Graduate Fellowship (to BKH), and funding from the NASA Astrobiology Institute (Grant award # 3903-CIT-NASA.A76A) as part of the Penn State Astrobiology Research Center (PSARC). Collection of samples from the Eel River Basin and Lau Basin was supported by funding from the National Science Foundation (MCB-0348492 to VJO).

References

- Alfreider, A., M. Krossbacher, and R. Psenner. 1997. Groundwater samples do not reflect bacterial densities and activity in subsurface systems. *Water Res* 31:832–840.
- Arnarson, T. S., and R. G. Keil. 2000. Mechanisms of pore water organic matter adsorption to montmorillonite. *Mar Chem* 71:309–320.
- Barry, J. P., H. G. Greene, D. L. Orange, C. H. Baxter, B. H. Robison, R. E. Kochevar, J. W. Nybakken, D. L. Reed, and C. M. McHugh. 1996. Biologic and geologic characteristics of cold seeps in Monterey bay, California. *Deep Sea Res I* 43:1739–1755.
- Beal, E. J., C. H. House, and V. J. Orphan. 2009. Manganese- and Iron-Dependent Marine Methane Oxidation. *Science* 325:184–187.

- Boetius, A., K. Ravenschlag, C. J. Schubert, D. Rickert, F. Widdel, A. Gieseke, R. Amann, B. B. Jorgensen, U. Witte, and O. Pfannkuche. 2000. A marine microbial consortium apparently mediating anaerobic oxidation of methane. *Nature* 407:623–626.
- Bottrell, S. H., R. J. Parkes, B. A. Cragg, and R. Raiswell. 2000. Isotopic evidence for anoxic pyrite oxidation and stimulation of bacterial sulphate reduction in marine sediments. *J Geol Soc* 157:711–714.
- Boyd, E. S., D. E. Cummings, and G. G. Geesey. 2007. Mineralogy influences structure and diversity of bacterial communities associated with geological substrata in a pristine aquifer. *Microb Ecol* 54:170–182.
- Canfield, D. E., F. J. Stewart, B. Thamdrup, L. De Brabandere, T. Dalsgaard, E. F. Delong, N. P. Revsbech, and O. Ulloa. 2010. A Cryptic Sulfur Cycle in Oxygen-Minimum-Zone Waters off the Chilean Coast. *Science* 330:1375–1378.
- Cline, J. D. 1969. Spectrophotometric Determination of Hydrogen Sulfide in Natural Waters. *Limnol Oceanogr* 14:454–458.
- Coolen, M. J. L., H. Cypionka, A. M. Sass, H. Sass, and J. Overmann. 2002. Ongoing modification of Mediterranean Pleistocene sapropels mediated by prokaryotes. *Science* 296:2407–2410.
- Dekas, A. E., R. S. Poretsky, and V. J. Orphan. 2009. Deep-Sea Archaea Fix and Share Nitrogen in Methane-Consuming Microbial Consortia. *Science* 326:422–426.
- DeLong, E. F. 1992. Archaea in Coastal Marine Environments. *Proc Natl Acad Sci USA* 89:5685–5689.
- Dufrene, M., and P. Legendre. 1997. Species assemblages and indicator species: The need for a flexible asymmetrical approach. *Ecol Monogr* 67:345–366.
- Edwards, K. J., T. M. McCollom, H. Konishi, and P. R. Buseck. 2003. Seafloor bioalteration of sulfide minerals: Results from in situ incubation studies. *Geochim Cosmochim Acta* 67:2843–2856.
- Girguis, P. R., A. E. Cozen, and E. F. DeLong. 2005. Growth and population dynamics of anaerobic methane-oxidizing archaea and sulfate-reducing bacteria in a continuous-flow bioreactor. *Appl Environ Microbiol* 71:3725–3733.
- Goffredi, S. K., R. Wilpiseski, R. Lee, and V. J. Orphan. 2008. Temporal evolution of methane cycling and phylogenetic diversity of archaea in sediments from a deep-sea whale-fall in Monterey Canyon, California. *ISME J* 2:204–220.
- Harrison, B. K., H. Zhang, W. Berelson, and V. J. Orphan. 2009. Variations in Archaeal and Bacterial Diversity Associated with the Sulfate-Methane Transition Zone in Continental Margin Sediments (Santa Barbara Basin, California). *Appl Environ Microbiol* 75:1487–1499.
- Harrison, B.K., and Orphan, V.J., in press, Method for assessing Mineral Composition-Dependent patterns in Microbial diversity using Magnetic and Density Separation. *Geomicrobiol J*.
- Holmkvist, L., Ferdelman, T.G., and Jørgensen, B.B., 2011, A cryptic sulfur cycle driven by iron in the methane zone of marine sediment (Aarhus Bay, Denmark), *Geochim Cosmochim Acta*, published ahead of print.
- House, C. H., V. J. Orphan, K. A. Turk, B. Thomas, A. Pernthaler, J. M. Vrentas, and S. B. Joye. 2009. Extensive carbon isotopic heterogeneity among methane seep microbiota. *Environ Microbiol* 11:2207–2215.

- Jorgensen, B. B. 1977. Bacterial Sulfate Reduction within Reduced Microniches of Oxidized Marine-Sediments. *Mar Biol* 41:7–17.
- Kallmeyer, J., and A. Boetius. 2004. Effects of temperature and pressure on sulfate reduction and anaerobic oxidation of methane in hydrothermal sediments of Guaymas Basin. *Appl Environ Microbiol* 70:1231–1233.
- Keil, R. G., and J. I. Hedges. 1993. Sorption of Organic-Matter to Mineral Surfaces and the Preservation of Organic-Matter in Coastal Marine-Sediments. *Chem Geol* 107:385–388.
- Knittel, K., and A. Boetius. 2009. Anaerobic Oxidation of Methane: Progress with an Unknown Process. *Annu Rev Microbiol* 63:311–334.
- Knittel, K., T. Losekann, A. Boetius, R. Kort, and R. Amann. 2005. Diversity and distribution of methanotrophic archaea at cold seeps. *Appl Environ Microbiol* 71:467–479.
- Kohn, M. J., L. R. Riciputi, D. Stakes, and D. L. Orange. 1998. Sulfur isotope variability in biogenic pyrite: Reflections of heterogeneous bacterial colonization? *Am Mineral* 83:1454–1468.
- Krukowski, S. T. 1988. Sodium Metatungstate—A New Heavy-Mineral Separation Medium for the Extraction of Conodonts from Insoluble Residues. *J Paleontol* 62:314–316.
- Lane, D. J. 1991. 16S/23S rRNA sequencing, p. 115–175. *In* E. Stackebrandt and M. Goodfellow. (ed.), *Nucleic acid techniques in bacterial systematics*. John Wiley and Sons, New York, NY.
- Levin, L. A. 2005. Ecology of cold seep sediments: Interactions of fauna with flow, chemistry and microbes. *Oceanography and Marine Biology - an Annual Review* 43: 1–46.
- Lloyd, K. G., D. B. Albert, J. F. Biddle, J. P. Chanton, O. Pizarro, and A. Teske. 2010. Spatial Structure and Activity of Sedimentary Microbial Communities Underlying a *Beggiatoa* spp. Mat in a Gulf of Mexico Hydrocarbon Seep. *Plos One* 5: e8738.
- Manz, W., R. Amann, W. Ludwig, M. Wagner, and K. H. Schleifer. 1992. Phylogenetic Oligodeoxynucleotide Probes for the Major Subclasses of Proteobacteria—Problems and Solutions. *Syst Appl Microbiol* 15:593–600.
- Manz, W., M. Eisenbrecher, T. R. Neu., and U. Szewyk. 1998. Abundance and spatial organization of Gram-negative sulfate-reducing bacteria in activated sludge investigated by in situ probing with specific 16S rRNA targeted oligonucleotides. *FEMS Microbiol Ecol* 25:43–61.
- Martinez, R. J., H. J. Mills, S. Story, and P. A. Sobecky. 2006. Prokaryotic diversity and metabolically active microbial populations in sediments from an active mud volcano in the Gulf of Mexico. *Environ Microbiol* 8:1783–1796.
- Mauck, B. S., and J. A. Roberts. 2007. Mineralogic control on abundance and diversity of surface-adherent microbial communities. *Geomicrobiol J* 24:167–177.
- Meyerdierks, A., M. Kube, T. Lombardot, K. Knittel, M. Bauer, F. O. Glockner, R. Reinhardt, and R. Amann. 2005. Insights into the genomes of archaea mediating the anaerobic oxidation of methane. *Environ Microbiol* 7:1937–1951.
- Mielke, P. W., and K. J. Berry. 1982. An Extended Class of Permutation Techniques for Matched Pairs. *Commun Stat Part A* 11:1197–1207.

- Morrow, J. B., R. Stratton, H. H. Yang, B. F. Smets, and D. Grasso. 2005. Macro- and manoscale observations of adhesive behavior for several E-coli strains (O157 : H7 and environmental isolates) on mineral surfaces. *Environ Sci Technol* 39:6395–6404.
- Murray, J. L. S., and P. A. Jumars. 2002. Clonal fitness of attached bacteria predicted by analog modeling. *Bioscience* 52:343–355.
- Nauhaus, K., T. Treude, A. Boetius, and M. Kruger. 2005. Environmental regulation of the anaerobic oxidation of methane: a comparison of ANME-I and ANME-II communities. *Environ Microbiol* 7:98–106.
- Ohfuji, H., and D. Rickard. 2005. Experimental syntheses of framboids—a review. *Earth Sci Rev* 71:147–170.
- Orphan, V. J., K. U. Hinrichs, W. Ussler, 3rd, C. K. Paull, L. T. Taylor, S. P. Sylva, J. M. Hayes, and E. F. Delong. 2001. Comparative analysis of methane-oxidizing archaea and sulfate-reducing bacteria in anoxic marine sediments. *Appl Environ Microbiol* 67:1922–1934.
- Orphan, V. J., W. Ussler, T. H. Naehr, C. H. House, K. U. Hinrichs, and C. K. Paull. 2004. Geological, geochemical, and microbiological heterogeneity of the seafloor around methane vents in the Eel River Basin, offshore California. *Chem Geol* 205:265–289.
- Perenthaler, A., A. E. Dekas, C. T. Brown, S. K. Goffredi, T. Embaye, and V. J. Orphan. 2008. Diverse syntrophic partnerships from-deep-sea methane vents revealed by direct cell capture and metagenomics. *Proc Natl Acad Sci USA* 105:7052–7057.
- Perenthaler, J., F. O. Glöckner, W. Schönhuber, and R. Amann. 2001. Fluorescence in situ hybridization with rRNA-targeted oligonucleotide probes. *In* J. Paul (ed.), *Methods in Microbiology: Marine Microbiology*, vol. 30. Academic Press Ltd, London.
- Ransom, B., R. H. Bennett, R. Baerwald, V. H. Hulbert, and P. J. Burkett. 1999. In situ conditions and interactions between microbes and minerals in fine-grained marine sediments: A TEM microfabric perspective. *Am Mineral* 84:183–192.
- Riedinger, N., B. Brunner, M. J. Formolo, E. Solomon, S. Kasten, M. Strasser, and T. G. Ferdelman. 2010. Oxidative sulfur cycling in the deep biosphere of the Nankai Trough, Japan. *Geology* 38:851–854.
- Roberts, J. A. 2004. Inhibition and enhancement of microbial surface colonization: the role of silicate composition. *Chem Geol* 212:313–327.
- Satterberg, J., T. S. Arnarson, E. J. Lessard, and R. G. Keil. 2003. Sorption of organic matter from four phytoplankton species to montmorillonite, chlorite and kaolinite in seawater. *Mar Chem* 81:11–18.
- Schippers, A., and B. B. Jorgensen. 2002. Biogeochemistry of pyrite and iron sulfide oxidation in marine sediments. *Geochim Cosmochim Acta* 66:85–92.
- Schreiber, L., T. Holler, K. Knittel, A. Meyerdierks, and R. Amann. 2010. Identification of the dominant sulfate-reducing bacterial partner of anaerobic methanotrophs of the ANME-2 clade. *Environ Microbiol* 12:2327–2340.
- Webster, G., R. J. Parkes, B. A. Cragg, C. J. Newberry, A. J. Weightman, and J. C. Fry. 2006. Prokaryotic community composition and biogeochemical processes in deep subseafloor sediments from the Peru Margin. *FEMS Microbiol Ecol* 58:65–85.

- Yanagawa, K., M. Sunamura, M. A. Lever, Y. Morono, A. Hiruta, O. Ishizaki, R. Matsumoto, T. Urabe, and F. Inagaki. 2011. Niche Separation of Methanotrophic Archaea (ANME-1 and-2) in Methane-Seep Sediments of the Eastern Japan Sea Offshore Joetsu. *Geomicrobiol J* 28:118–129.
- Zonneveld, K. A. F., G. J. M. Versteegh, S. Kasten, T. I. Eglinton, K. C. Emeis, C. Huguet, B. P. Koch, G. J. de Lange, J. W. de Leeuw, J. J. Middelburg, G. Mollenhauer, F. G. Prahl, J. Rethemeyer, and S. G. Wakeham. 2010. Selective preservation of organic matter in marine environments; processes and impact on the sedimentary record. *Biogeosci* 7:483–511.

Appendix I. Error analysis in Terminal Restriction Fragment Length Polymorphism

Summary

—Precision of fragment length estimates are within 0.7 bp for 4th- and 5th-degree polynomial size models (95% confidence intervals). Precision may vary with fragment length, but < 1 bp values are consistent throughout the region of interest. For 3rd-degree polynomial models, 95% confidence intervals are 1.236 bp and < 1.5 bp values are consistent.

—Estimates of run-to-run reproducibility of relative abundance measures are within 0.6% using peak height and 1.35% using peak area.

—Peak area relative abundance measures are highly sensitive to changes in peak shape which may cause erroneous estimates of width, leading to false signals derived from machine operation. ~ 1 bp phylogenetic differences in co-eluted fragments may not be resolved as individual peaks, and may instead be reflected in peak width.

—A small (1%–2%) trend of secularly decreasing relative abundance may be observed for peak area measurements (i.e., long fragments are artificially less abundant).

—The use of both peak height and peak area to characterize differences in T-RF peak intensity is encouraged. Significant differences in characterizing an individual sample between the two methods could indicate analytical artifacts which could be resolved by inspecting the original data.

Introduction

Since the original introduction of Terminal Restriction Fragment Length Polymorphism (T-RFLP) investigating microbial communities (Liu et al., 1997) the method has seen increasing use in the characterization of environmental samples and numerous studies attempting to quantify methodological error. These efforts fall in several distinct categories:

- 1) Resolving signal-to-noise ratio (Osborn et al., 2000; Lueders and Friedrich, 2003; Abdo et al., 2006; Osborne et al., 2006). Authors have attempted to refine the use of statistical methods to resolve “true” peaks that are not subject to removal on replication of the method. The typical practice in the Orphan lab has been to apply a 1% relative abundance threshold (Lueders and Friedrich, 2003).
- 2) Characterizing PCR amplification bias and sample loading error in the relative abundance (amplicon frequency) of terminal restriction fragments (Osborne et al., 2000; Lueders and Friedrich, 2003).
- 3) Instrument precision (Liu et al., 1997; Osborne et al., 2000) and accuracy of fragment length measurement (Marsh, 2005).
- 4) Proper alignment of disparate TRFLP electropherograms for statistical analyses (Abdo et al., 2006).

Schutte et al. (2008) offer a thorough review of extant literature.

Measures of peak height and peak area have both been used in the literature to assess the relative abundance of specific phylotypes in T-RFLP profiles, and no clear consensus exists in favor of either method for general use (Lueders and Friedrich, 2003; see discussion between Grant and Ogilvie (2003) and Blackwood et al. (2003)). Choosing the proper method for

assessing relative phylotype abundance on a case-by-case basis is recommended. This report assesses the Orphan Lab's in-house reproducibility and accuracy (with respect to relative fluorescence) of T-RFLP based on repeated analysis of a DNA size standard. Instrument precision and the accuracy of relative fluorescence measures are likely to vary with different labs, standard, and sequencer setup. However, biases of using capillary electrophoresis and automated peak search algorithms will approach a minimum error of which this serves as a decent approximation.

Methods

Fragment analyses were carried out on aliquots of the GenomeLab 600 bp size standard labeled with WellRed dye D1 (Beckman Coulter, Fullerton, CA) by capillary electrophoresis using a Beckman CEQ 8800 system (Beckman Coulter). Analyses presented in this study are derived from 37 discrete measurements of the DNA standard on 7 machine runs between Dec. 2008 and April 2010 using separately ordered batches of size standard. Peak search, height, and area were determined using Beckman CEQ system software for 3rd- and 4th-degree polynomial size models for DNA standard curves. 5th-degree polynomial standard curves were derived from manual peak search and regression calculations in Gnumeric (<http://projects.gnome.org/gnumeric/>). Peak length precision for 3rd-, 4th-, and 5th-degree polynomial size models were assessed by comparing standard peak size to the length estimate from model output using 27, 10, and 28 samples, respectively (multiple size models were generated independently for individual electropherograms in select cases). Individual measurements of difference between estimated size and standard size numbered 881, 328, and 914 data points, respectively.

From the 37 original electropherograms, 29 were selected for analysis of peak height and area reproducibility, excluding machine runs by the following criteria: 1) total peak area of the size standards was < 100000 units (fluorescence vs. peak width in bp); 2) $\text{TotalHeight/TotalArea} < 0.5$ or > 1.5 ; 3) the standard deviation of the relative height or area of peaks within a single run was $>2\sigma$ from the average standard deviation of the original 35 (i.e. abnormal change in peak height and area between the beginning and end of an individual electropherogram). Select runs were trimmed to 580 bp (the length of the shortest), leaving 30 standard peaks between 60 bp and 580, and peak height and area normalized to the total height and area within the run. Subsequently, run-to-run error of a 10-peak fragment pattern was assessed using the 120, 160, 180, 190, 200, 220, 280, 300, 320, and 340 standard peaks.

Results and Analysis

Precision of fragment length measurement

Migration of a DNA standard series by capillary electrophoresis is significantly nonlinear. However, a polynomial regression line fit to a standard curve may strongly mimic migration (Fig. 1), allowing for precise measurement of DNA fragment size within the range of added standard peaks. For a 5th-degree polynomial fit to standard peaks, the difference between known length of standard peaks model estimate of standard length is consistently less than 1 nucleotide (Fig. 2), although precision of the size model varied over the course of a run depending upon the size model used. Over 914 data points, 2σ of the difference between standard and estimate was 0.685, exhibiting a very high degree of confidence that size estimates are within 1 bp of true fragment length. For 4th- and 3rd-degree polynomial fits (Fig. 3), 2σ is 0.634 ($n = 328$) and 1.236

(n = 881), respectively. These values are consistent with the ± 1 bp estimate typically reported in the literature (Schutte et al., 2008).

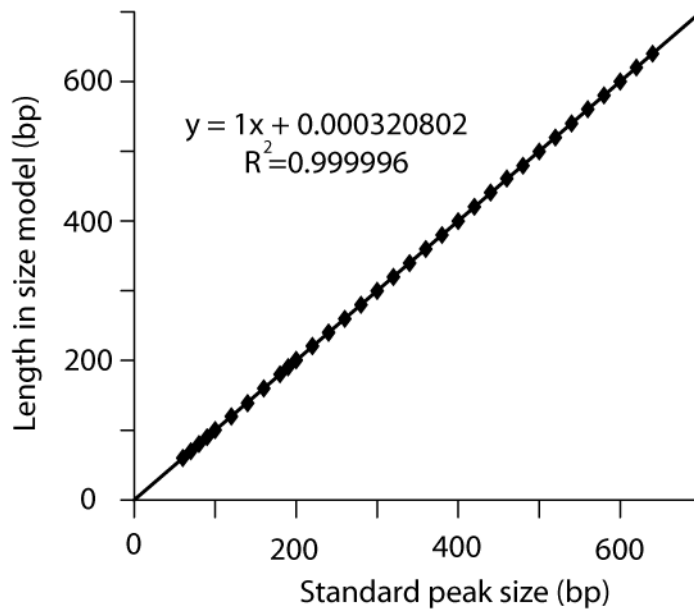


Fig. 1. Precision of 5th-degree polynomial size model vs. manually identified standard peaks for 28 discrete sample runs on the Beckman CEQ 8800.

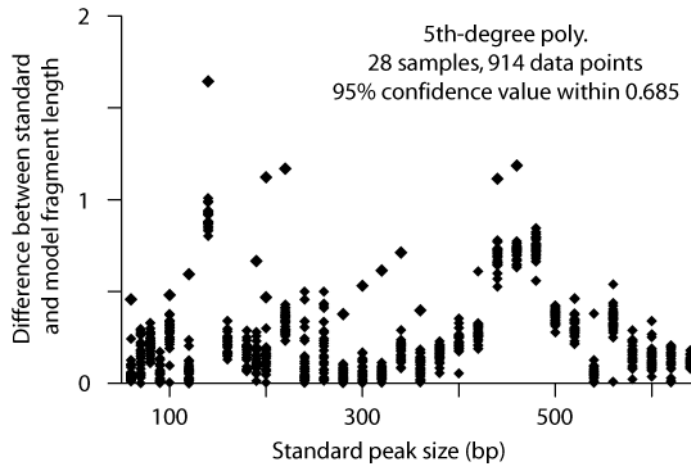


Fig. 2. Absolute value of difference between 5th-degree polynomial size model and known fragment lengths of the 600 bp size standard. Increases in error at 140 bp and 440–460 bp are likely due in part to the regression algorithm.

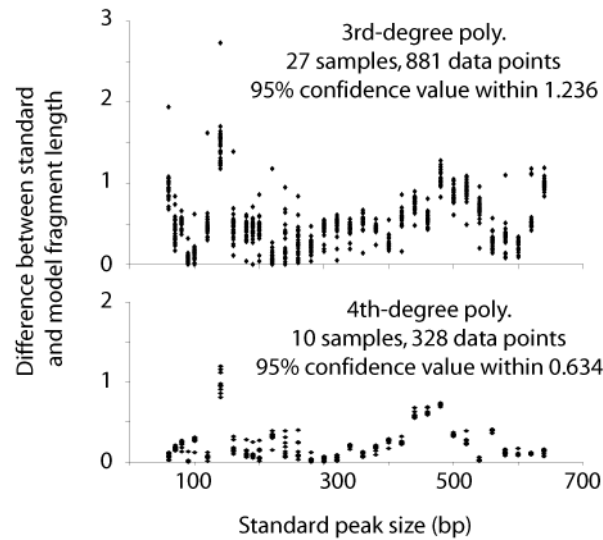


Fig. 3. Absolute value of difference between 3rd- and 4th-degree polynomial size models and known fragment lengths of the 600 bp size standard.

The 3rd-degree model is the default parameter for the Beckman CEQ. ~ 1 bp error in precision of fragment length measurement should not generate significant error in comparing electropherograms (i.e., contrasting community signatures between different extracts) if a sufficiently large bin size is used to group peaks (≥ 2 bp). However, this model is not sufficient to resolve 1 bp differences when identifying phylotypes based on *in silico* cut site predictions, and for this purpose a 4th-degree (at least) polynomial size model is preferred.

All size models exhibit irregular error depending upon fragment length. This is, in part, due to the poor fit of a polynomial function to DNA fragment migration. The increased error of the 60 and 640 bp peaks in the 3rd-degree fit when compared to 4th- and 5th-degree fits illustrates the biases of the regression model. However, the lack of precision of specific peaks (e.g., 140 bp) which is consistent between the three models may also be due to the limitations of peak searching (even when peaks are identified manually). Poor peak identification may be due to broader and irregularly-sized peaks which are consistently encountered at specific

fragment lengths (e.g., 140, 240, 260). This trend is apparent when characterizing peak width measurements output by the Beckman CEQ system (Fig. 4). For several peaks, width measurements fall into 2–3 distinct populations. Characteristic peak shapes distinguishing these populations for fragment 240 are shown in Fig. 5. These differences are not attributable to separate aliquots of standard (as each appear within discrete instrument runs). However, the observation that the increased error is specific to a select few peaks suggests that the formulation of the standard plays a role in which peaks are likely to exhibit such irregular behavior.

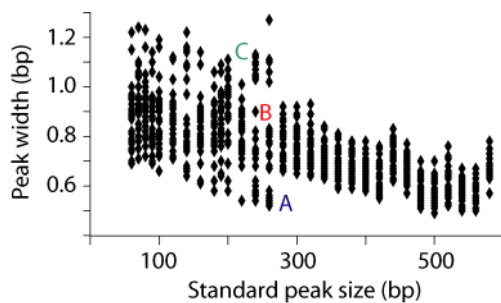


Fig. 4. Fragment length vs. peak width for 29 representative analyses of the GenomeLab 600 bp size standard. Peak types A, B, and C are characterized in Fig. 5.

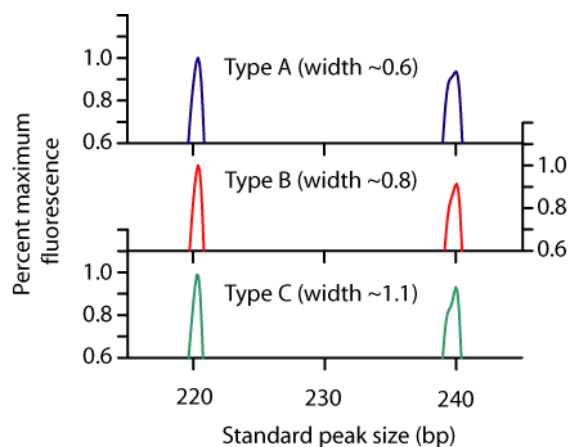


Fig. 5. Peak shapes of types A, B, and C defined by peak width as shown in Fig. 4. The 220 bp fragment exhibits little run-to-run variability, while the 240 bp fragment regularly exhibits a shoulder/double peak.

Reproducibility of relative abundance measures

2σ error for relative abundance of individual standard peaks is broadly similar when using peak area or peak height (Fig. 6). However, difficulty in resolving irregular peak shapes as discussed above leads to poor reproducibility associated with several specific peaks (e.g., 140, 240, and 260 bp). As these irregularities appear to be influenced by formulation of the standard,

it would not be appropriate to estimate reproducibility of environmental samples on such variability. For the 30-peak profile, 2σ error margins averaged 0.46% for peak height and 0.52% for peak area (excluding the values for 140, 240, and 260; area error is 0.65 when included while height remains the same). A more representative selection of 10 peaks (120, 160, 180, 190, 200, 220, 280, 300, 320, and 340) was chosen within the main region of interest for identifying microbial phylotypes. A ten-fragment pattern is more representative of the fragment diversity in environmental samples (although bacterial diversity in particular may be significantly greater). For this analysis, 2σ error was 0.60% for height and 1.35% for area. Methodological error of this type is therefore significantly less than that associated with re-extraction and amplification of pre-homogenized samples (Harrison and Orphan, in press). However, the impact of instrument variability is significantly greater in low-diversity datasets (e.g., archaeal communities) and it may be important to conduct repeat analyses of low-diversity samples to improve confidence in measures of relative abundance.

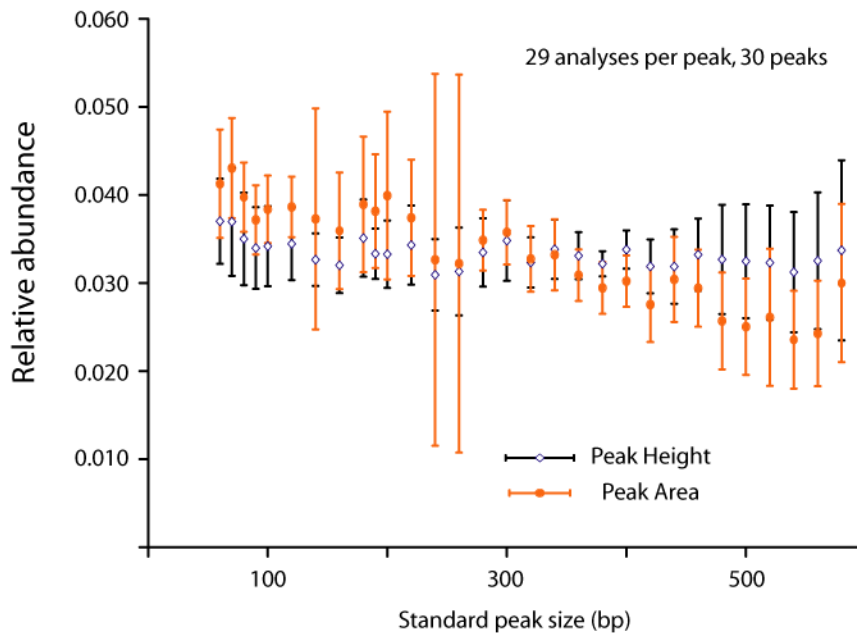


Fig. 6. Reproducibility of relative height and area over 29 analyses of the 600 bp size standard.

It is not clear how much of the secular decrease in relative abundance using peak area (negative slope of the average values in Fig. 6) is due to the formulation of the standard and how much may instead be attributed to the method. Capillary electrophoresis is known to exhibit bias of increased fluorescent signal for low-bp fragments (Osborn et al., 2000; Marsh, 2005; Schutte et al., 2008). In either case, the trend does not contribute a systematic error to T-RFLP analysis if the same metric is consistently used for analysis of each electropherogram. If additional information is available regarding relative abundance (e.g., clone libraries, qpcr) then such information may be used to decide between peak height and area on a case-by-case basis.

Peak area is subject to error derived from peak shape irregularities (as with 140, 240, and 260) which may be influenced by machine operation and sample preparation. However, these results also demonstrate that peak search software may not resolve discrete fragments with ~ 1 bp resolution. In environmental samples containing closely-related phylotypes of interest, relying on peak height may lead to exclusion of a portion of the community of interest. It is important to establish whether such factors could bias analysis of environmental samples either by comparison of T-RFLP analyses with data from other methods or use of peak height and area metrics in parallel.

Pitfalls

—D1 dye signal is more resistant to degradation (see Beckman-Coulter literature), and analysis of other dyes may lead to error in excess of that evaluated here, particularly if samples are handled improperly (excess heat or light).

—Differences in dye labeling may lead to differences in fragment migration by capillary electrophoresis, which may cause low accuracy of fragment length measurement despite high precision (Marsh, 2005; Schutte et al., 2008). This factor should be considered when evaluating fragment identification based on predicted cut sites of known sequences.

References

- Abdo, Z., U. M. E. Schuette, S. J. Bent, C. J. Williams, L. J. Forney, and P. Joyce. 2006. Statistical methods for characterizing diversity of microbial communities by analysis of terminal restriction fragment length polymorphisms of 16S rRNA genes. *Env Microbiol* 8:929–938.
- Blackwood, C. B., T. Marsh, S. H. Kim, and E. A. Paul. 2003. Terminal restriction fragment length polymorphism data analysis for quantitative comparison of microbial communities. *Appl Env Microbiol* 69:926–932.
- Grant, A., and L. A. Ogilvie. 2003. Terminal restriction fragment length polymorphism data analysis. *Appl Env Microbiol* 69:6342–6342.
- Liu, W. T., T. L. Marsh, H. Cheng, and L. J. Forney. 1997. Characterization of microbial diversity by determining terminal restriction fragment length polymorphisms of genes encoding 16S rRNA. *Appl Env Microbiol* 63:4516–4522.
- Lueders, T., and M. W. Friedrich. 2003. Evaluation of PCR amplification bias by terminal restriction fragment length polymorphism analysis of small-subunit rRNA and mcrA genes by using defined template mixtures of methanogenic pure cultures and soil DNA extracts. *Appl Env Microbiol* 69:320–326.
- Marsh, T. L. 2005. Culture-independent microbial community analysis with terminal restriction fragment length polymorphism. *Env Microbiol* 397-308–329.
- Osborn, A. M., E. R. B. Moore, and K. N. Timmis. 2000. An evaluation of terminal-restriction fragment length polymorphism (T-RFLP) analysis for the study of microbial community structure and dynamics. *Env Microbiol* 2:39–50.
- Osborne, C. A., G. N. Rees, Y. Bernstein, and P. H. Janssen. 2006. New threshold and confidence estimates for terminal restriction fragment length polymorphism analysis of complex bacterial communities. *Appl Env Microbiol* 72:1270–1278.
- Schutte, U. M. E., Z. Abdo, S. J. Bent, C. Shyu, C. J. Williams, J. D. Pierson, and L. J. Forney. 2008. Advances in the use of terminal restriction fragment length polymorphism (T-RFLP) analysis of 16S rRNA genes to characterize microbial communities. *Appl Microbiol Biotech* 80:365–380.

Appendix II. Supplemental methods—Variations in archaeal and bacterial diversity associated with the sulfate-methane transition zone in continental margin sediments (Santa Barbara Basin, CA)

Correspondence analysis

The dataset of marine environmental clone libraries used for correspondence analysis ((3); Table S1) is modified from Webster et al. (19). Data was collected from a variety of marine sediment studies available in the literature (1, 2, 4–10, 12–19), as well as Santa Barbara Basin samples. Environmental assignments for specific clone libraries were based primarily upon geochemical data published alongside the clone library. Where such information was unavailable, core descriptions were used to infer environmental setting.

UniFrac

Where a full sequence was unavailable for UniFrac analysis (11), a substitute phylotype > 92% similarity from Santa Barbara Basin clone libraries or from Genbank would be chosen to represent the partial sequence. In a given library, OTUs for which a full sequence could not be identified represented < 10% of the total clones. UniFrac clustering patterns were not significantly altered by changing the similarity threshold in proxy sequence selection.

References

1. Bowman, J. P., and R. D. McCuaig. 2003. Biodiversity, Community Structural Shifts, and Biogeography of Prokaryotes within Antarctic Continental Shelf Sediment. *Appl. Environ. Microbiol.* 69:2463–2483.

2. Heijs, S. K., A. M. Laverman, L. J. Forney, P. R. Hardoim, and J. D. van Elsas. 2008. Comparison of deep-sea sediment microbial communities in the Eastern Mediterranean. *FEMS Microbiol. Ecol.* 64:362–377.
3. Hill, M. O. 1974. Correspondence analysis: a neglected multivariate method. *Appl. Stat.* 23:340–354.
4. Inagaki, F., T. Nunoura, S. Nakagawa, A. Teske, M. Lever, A. Lauer, M. Suzuki, K. Takai, M. Delwiche, F. S. Colwell, K. H. Nealson, K. Horikoshi, S. D'Hondt, and B. B. Jorgensen. 2006. Biogeographical distribution and diversity of microbes in methane hydrate-bearing deep marine sediments on the Pacific Ocean Margin. *Proc. Nat. Acad. Sci. U.S.A.* 103:2815–2820.
5. Inagaki, F., M. Suzuki, K. Takai, H. Oida, T. Sakamoto, K. Aoki, K. H. Nealson, and K. Horikoshi. 2003. Microbial communities associated with geological horizons in coastal subseafloor sediments from the sea of okhotsk. *Appl. Environ. Microbiol.* 69:7224–7235.
6. Jiang, H. 2007. Microbial diversity in the deep marine sediments from the Qiongdongnan Basin in South China Sea. *Geomicrobiol. J.* 24:505–517.
7. Kormas, K. A., D. C. Smith, V. Edgcomb, and A. Teske. 2003. Molecular analysis of deep subsurface microbial communities in Nankai Trough sediments (ODP Leg 190, Site 1176). *FEMS Microbiol. Ecol.* 45:115–125.
8. Lanoil, B. D., R. Sassen, M. T. La Duc, S. T. Sweet, and K. H. Nealson. 2001. Bacteria and Archaea Physically Associated with Gulf of Mexico Gas Hydrates. *Appl. Environ. Microbiol.* 67:5143–5153.
9. Li, L., C. Kato, and K. Horikoshi. 1999. Microbial Diversity in Sediments Collected from the Deepest Cold-Seep Area, the Japan Trench. *Mar. Biotechnol.* 1:391–400.
10. Lloyd, K. G., L. Lapham, and A. Teske. 2006. An anaerobic methane-oxidizing community of ANME-1b archaea in hypersaline Gulf of Mexico sediments. *Appl. Environ. Microbiol.* 72:7218–7230.
11. Lozupone, C., and R. Knight. 2005. UniFrac: a new phylogenetic method for comparing microbial communities. *Appl. Environ. Microbiol.* 71:8228–8235.
12. Martinez, R. J., H. J. Mills, S. Story, and P. A. Sobecky. 2006. Prokaryotic diversity and metabolically active microbial populations in sediments from an active mud volcano in the Gulf of Mexico. *Environ. Microbiol.* 8:1783–1796.
13. Mills, H. J., R. J. Martinez, S. Story, and P. A. Sobecky. 2005. Characterization of Microbial Community Structure in Gulf of Mexico Gas Hydrates: Comparative Analysis of DNA-and RNA-Derived Clone Libraries. *Appl. Environ. Microbiol.* 71:3235–3247.
14. Mu, C., Z. Bao, G. Chen, J. Hu, L. Hao, Z. Qi, and G. Li. 2005. Bacterial diversity in the sediments collected from the Shikoku Basin. *Acta. Oceanol. Sin.* 24:114–121.
15. Newberry, C. J., G. Webster, B. A. Cragg, R. J. Parkes, A. J. Weightman, and J. C. Fry. 2004. Diversity of prokaryotes and methanogenesis in deep subsurface sediments from the Nankai Trough, Ocean Drilling Program Leg 190. *Environ. Microbiol.* 6:274–287.
16. Reed, A. J., R. A. Lutz, and C. Vetriani. 2006. Vertical distribution and diversity of bacteria and archaea in sulfide and methane-rich cold seep sediments located at the base of the Florida Escarpment. *Extremophiles* 10:199–211.

17. Reed, D. W., Y. Fujita, M. E. Delwiche, D. B. Blackwelder, P. P. Sheridan, T. Uchida, and F. S. Colwell. 2002. Microbial communities from methane hydrate-bearing deep marine sediments in a forearc basin. *Appl. Environ. Microbiol.* 68:3759–3770.
18. Teske, A., K. U. Hinrichs, V. Edgcomb, A. de Vera Gomez, D. Kysela, S. P. Sylva, M. L. Sogin, and H. W. Jannasch. 2002. Microbial diversity of hydrothermal sediments in the Guaymas Basin: evidence for anaerobic methanotrophic communities. *Appl. Environ. Microbiol.* 68:1994–2007.
19. Webster, G., R. J. Parkes, B. A. Cragg, C. J. Newberry, A. J. Weightman, and J. C. Fry. 2006. Prokaryotic community composition and biogeochemical processes in deep seafloor sediments from the Peru Margin. *FEMS Microbiol. Ecol.* 58:65–85.

Supplemental Figures

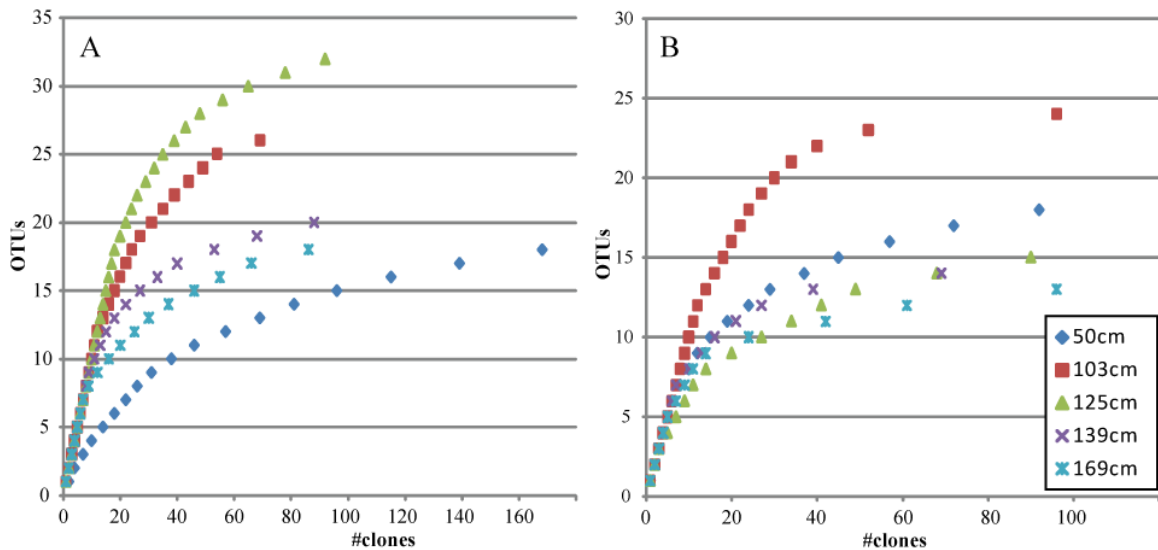


Fig. S1. A) Bacterial rarefaction curves for 16S rRNA clone libraries derived from unique RFLP patterns and sequence comparison. B) Archaeal rarefaction curves for 16S rRNA clone libraries.

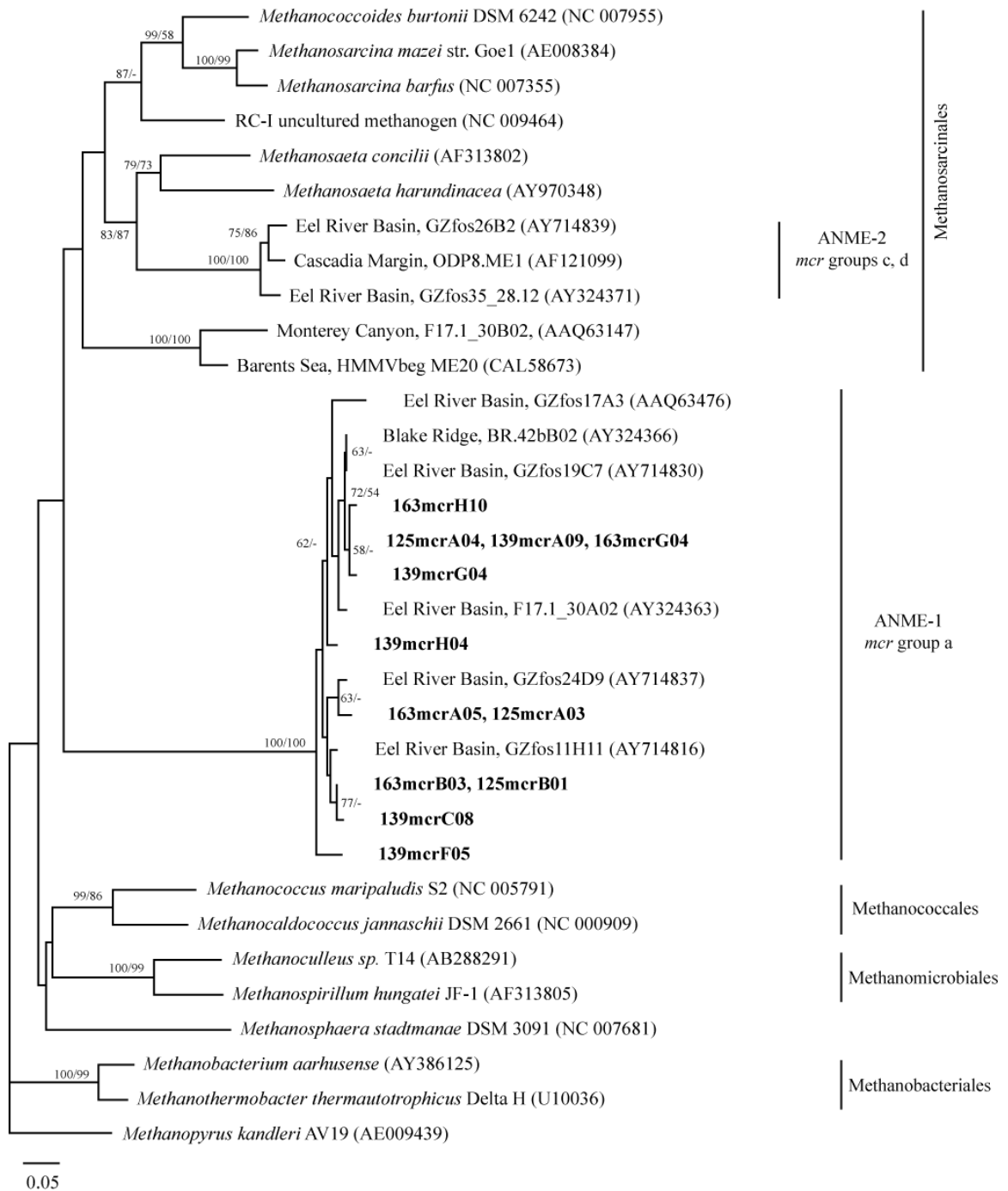


Fig. S2. Neighbor-joining distance tree based on translated partial methyl coenzyme M reductase (mcrA) amino acid sequences from the Santa Barbara Basin (in bold). Bootstrap values are labeled by distance/parsimony. Values <50 are not marked. Group names follow Hallam et al. (2003).

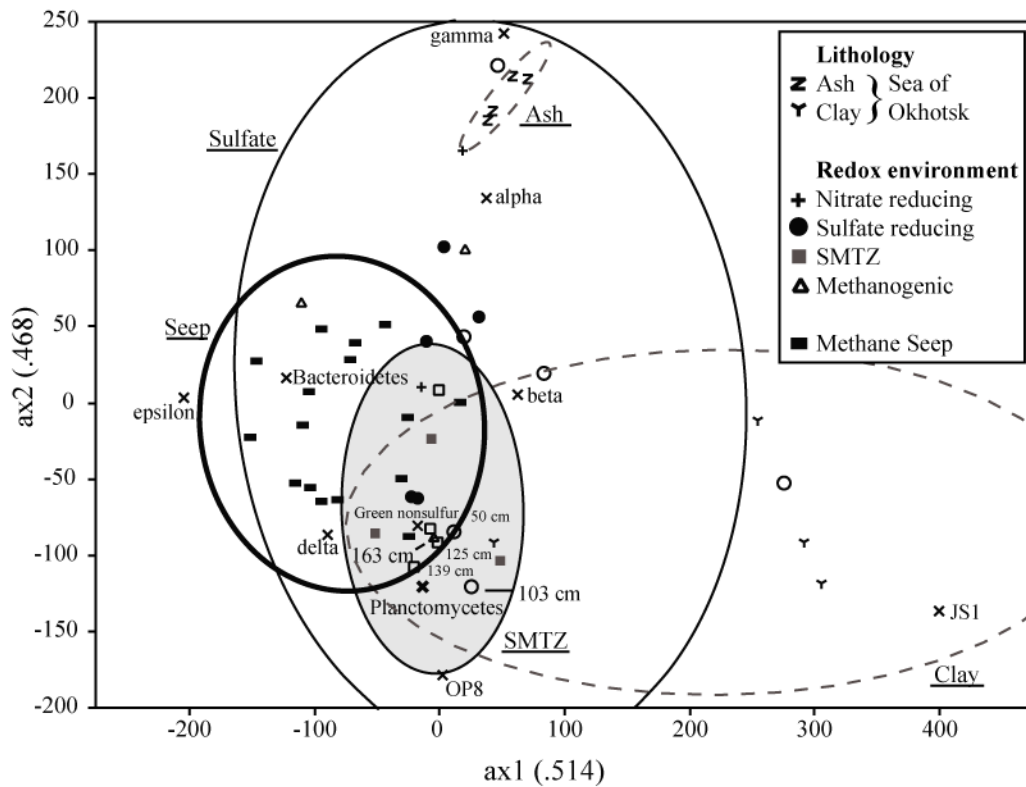


Fig. S3. Correspondence analysis (Hill, 1974) of marine sedimentary bacterial communities assigned to specific redox zones. SMI-related communities are similar in abundance of broad phylogenetic groups, exhibiting enrichment particularly in the deltaproteobacteria and, to a lesser extent, Planctomycetes. Alpha, Beta, Gamma, Delta and Epsilon correspond to their respective divisions among the proteobacteria.

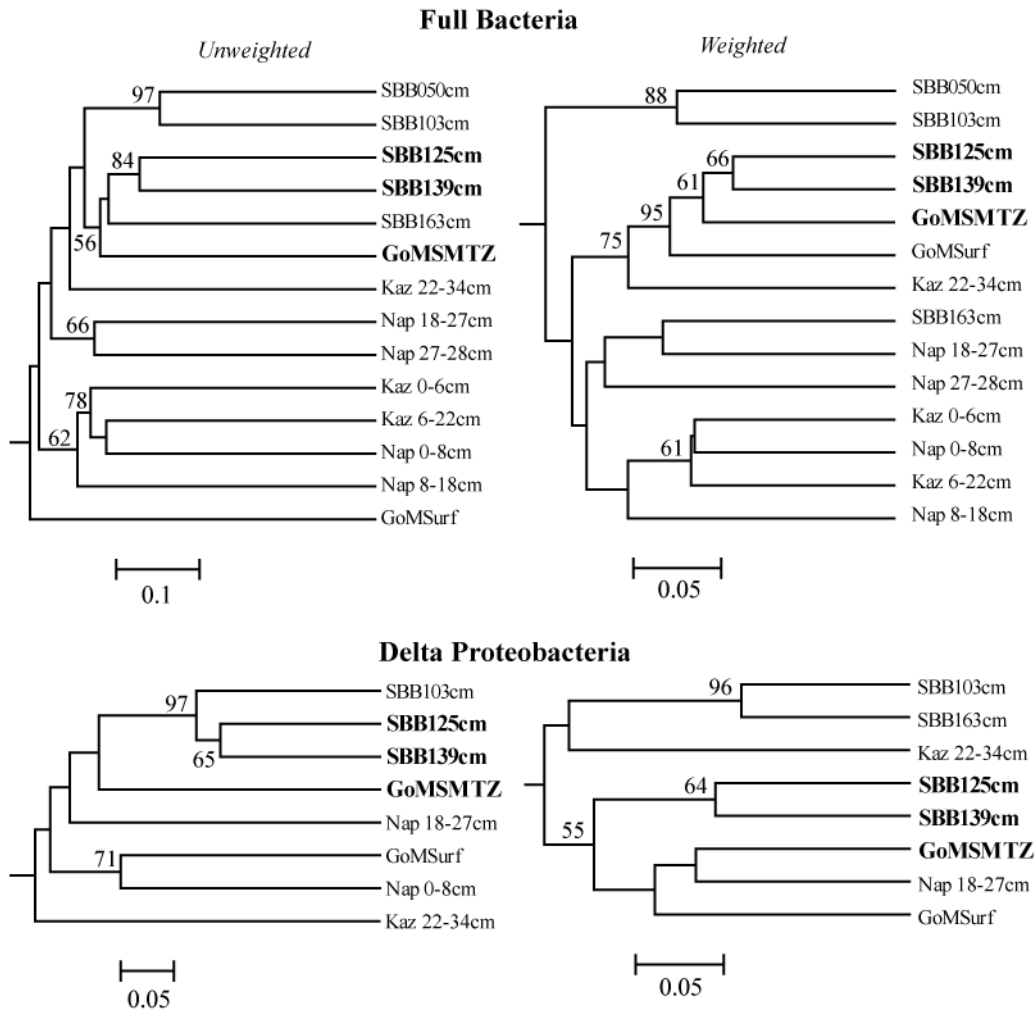


Fig. S4. UniFrac clustering of environmental clone libraries of marine sediments. SMTZ horizons are in bold. Unlabeled jackknife values are <50. Horizons were considered for the unweighted analysis for the delta proteobacteria where three unique phlotypes were recovered. Weighted analysis included only horizons with >4% deltaproteobacteria in the selected clone library. GoMSurf: Gulf of Mexico surface sediment, GoMSMTZ: Gulf of Mexico SMTZ (Lloyd et al., 2006); Kaz: Kazan Mud Volcano, Mediterranean Sea; Nap: Napoli Mud Volcano, Mediterranean Sea (Heijs et al., 2008).

Table S1. Bacterial Diversity of Marine Sediments

author	locality	library	Proteobacteria										GNS	γ	α	β	δ	ε	Bact	Planc	J51	OP8	Other	# clone	Env*	Tag
			γ	α	β	δ	ε	Bact	Planc	J51	OP8	Other														
Webster 06	ODP 1229 (Peru)	6.7 mbsf	51	36	0	2	0	0	0	0	0	0	0	0	0	0	0	0	2	2	7	58	soil	W06_6		
		30.2 mbsf	76	1	0	0	0	0	0	0	0	0	0	0	0	0	0	0	2	4	17	86	SMTZ	W06_30		
		42.03 mbsf	57	24	2	2	2	2	2	2	2	2	2	2	2	2	2	2	0	2	4	61	SMTZ	W06_42		
Newberry 04	Nankai Trough	86.67 mbsf	34	47	3	2	1	0	1	0	1	0	0	0	0	0	0	0	0	1	11	92	SMTZ	W06_86		
		4.15 mbsf	0	14	0	11	0	0	0	0	0	4	53	0	0	0	0	0	0	0	18	40	soil	N04		
		1 mbsf	22	0	22	0	0	0	0	0	0	0	0	50	6	0	0	0	0	0	0	18	0	K03_1		
Kormas 03	Nankai Trough	51 mbsf	25	25	0	12	0	0	0	0	0	0	25	0	0	0	0	0	0	0	0	8	0	K03_51		
		98 mbsf	40	60	0	0	0	0	0	0	0	0	0	0	0	0	0	0	0	0	0	5	0	K03_98		
		194 mbsf	0	23	0	7	3	53	0	0	0	0	0	0	0	0	0	0	0	0	13	30	meth	K03_194		
Reed 02	Nankai Forearc	165.5 mbsf	13	19	0	3	3	0	13	0	13	0	16	0	0	0	0	0	0	0	32	37	meth	R02_165		
		248.4 mbsf	4	0	0	0	18	0	0	0	0	0	22	0	0	0	0	0	0	0	56	50	meth	R02_248		
		297.6 mbsf	18	0	0	3	0	0	0	0	0	9	0	0	0	0	0	0	0	0	70	34	meth	R02_297		
Inagaki 03	Okhotsk pelagic clay	7.5 mbsf	60	0	0	0	17	0	0	0	0	17	0	0	0	0	0	0	0	0	6	64	clay	I03_7		
		22.2 mbsf	13	0	13	0	0	0	0	0	0	0	0	70	0	0	0	0	0	0	4	62	clay	I03_22		
		45.3 mbsf	6	27	4	0	0	0	0	0	0	0	55	0	0	0	0	0	0	0	6	48	clay	I03_45		
Okhotsk volcanic ash	Okhotsk volcanic ash	57.8 mbsf	13	0	3	0	5	0	0	0	0	73	0	0	0	0	0	0	0	0	6	75	clay	I03_57		
		18.3 mbsf	4	60	27	0	4	0	0	0	0	0	0	0	0	0	0	0	0	0	0	52	ash	I03_18		
		24.8 mbsf	7	60	20	0	0	0	0	0	0	0	0	0	0	0	0	0	0	0	13	61	ash	I03_24		
Mu 05	Shikoku Basin	30.9 mbsf	0	77	6	0	0	0	0	0	0	5	0	0	0	0	0	0	0	0	10	59	ash	I03_30		
		45.7 mbsf	3	87	6	0	0	0	0	0	0	0	3	0	0	0	0	0	0	0	150	ash	I03_45			
		surface	15	30	15	7	11	0	0	0	0	15	0	0	0	0	0	0	0	0	7	27	meth	M05		
Inagaki 02	Japan Trench cold seep	surface	0	28	6	0	34	10	0	11	0	2	0	0	0	0	0	0	0	0	9	93	Seep	I99		
		<0.16 mbsf	0	7	3	4	36	42	0	0	0	0	2	1	0	0	0	0	0	0	5	137	Seep	I02		
		surface core a	15	0	0	13	32	0	0	3	0	3	0	6	0	0	0	0	0	0	31	68	Seep	TeskeA		
this study	Santa Barbara Basin	surface core c	6	22	0	0	13	28	9	1	3	1	13	0	0	0	0	0	0	0	1	68	Seep	TeskeC		
		50cm	14	4	2	9	0	0	27	1	1	17	25	164	0	0	0	0	0	0	25	164	soil	S88050cm		
		103cm	6	3	1	0	6	0	0	20	6	28	30	66	0	0	0	0	0	0	30	66	soil	S88103cm		
Lloyd 06	Gulf of Mexico	125cm	9	0	3	0	48	0	0	0	8	11	4	0	0	0	0	0	0	0	17	92	SMTZ	S88125cm		
		139cm	2	0	0	0	40	0	0	0	30	6	5	0	0	0	0	0	0	0	17	92	SMTZ	S88139cm		
		169cm	41	0	0	0	35	4	0	2	7	5	1	0	0	0	0	0	0	0	31	89	meth	S88169cm		
Heijs 08	Kazan Mud Volcano	0-3cm	0	4	0	0	0	0	0	0	4	0	4	0	0	0	0	0	0	0	4	23	meth	GoMSurf		
		15-18cm	5	0	0	0	41	1	0	3	19	3	28	74	0	0	0	0	0	0	28	74	SMTZ	GoMSMTZ		
		0-6cm	10	8	0	0	0	0	0	13	0	0	0	0	0	0	0	0	0	0	69	48	SMTZ	Kaz 0-6cm		
Bowman 03	Antarctic Sediment	6-22cm	38	7	4	0	2	0	0	0	2	0	0	0	0	0	0	0	0	0	47	45	SMTZ	Kaz 6-22cm		
		22-34cm	38	0	0	0	38	0	0	0	4	0	0	0	0	0	0	0	0	0	20	45	meth	Kaz 22-34cm		
		0-0.4cm	1	55	5	1	5	5	0	4	0	4	0	0	0	0	0	0	0	0	24	255	nitr	MertzTop		
Heijs 08	Urania brine pool	1.5-2.5cm	4	45	4	1	18	2	0	7	0	2	18	0	0	0	0	0	0	0	2	313	sulf	MertzMid		
		20-21cm	6	24	4	0	18	1	0	11	0	2	33	268	0	0	0	0	0	0	2	33	sulf	MertzBot		
		0-10cm	27	4	23	2	10	4	0	2	0	0	0	0	0	0	0	0	0	0	27	48	nitr	Ura1		
Jiang 07	South China Sea	10-20cm	9	0	42	20	2	0	0	0	5	0	0	0	0	0	0	0	0	0	23	66	nitr	Ura2		
		0-8cm	19	3	4	0	7	1	0	24	0	0	0	0	0	0	0	0	0	0	40	67	sulf	Nap 0-8cm		
		8-18cm	49	6	2	0	8	0	0	16	0	0	0	0	0	0	0	0	0	0	20	51	sulf	Nap 8-18cm		
Martinez 06	Gulf of Mexico	18-27cm	40	0	0	3	11	0	0	0	17	0	0	0	0	0	0	0	0	0	29	63	SMTZ	Nap 18-27cm		
		27-28cm	25	0	19	19	4	0	0	4	0	0	0	0	0	0	0	0	0	0	35	57	SMTZ	Nap 27-28cm		
		0-14cm	24	15	0	0	17	2	0	7	0	0	0	0	0	0	0	0	0	0	30	54	Seep	Ams1		
Reed 06	Florida Escarpment	14-31cm	17	6	1	4	23	0	0	10	0	0	0	0	0	0	0	0	0	0	39	71	Seep	Ams2		
		4.8m	0	82	13	0	2	0	0	0	0	0	0	0	0	0	0	0	0	0	3	95	sulf	J07		
		0-2cm	2	6	9	0	2	62	9	2	0	0	0	0	0	0	0	0	0	0	9	47	Seep	M06_0		
Lanoll 01	GoM Hydrate	6-8cm	2	4	29	0	7	42	4	0	0	0	0	0	0	0	0	0	0	0	11	45	Seep	M06_6		
		10-12cm	5	14	0	0	0	30	28	16	0	0	0	0	0	0	0	0	0	0	7	43	Seep	M06_10		
		top	4	0	0	0	21	53	14	4	0	0	0	0	0	0	0	0	0	0	4	42	Seep	R06_top		
Mills 05	GoM Hydrates	middle	9	24	0	0	31	18	12	0	0	0	0	0	0	0	0	0	0	0	6	39	Seep	R06_mid		
		bottom	25	0	0	0	49	6	14	0	0	0	0	0	0	0	0	0	0	0	6	39	Seep	R06_bot		
		GoMHyd	0	30	6	9	5	0	1	0	0	0	0	0	0	0	0	0	0	0	50	127	Seep	L01_Hyd		
this study	GoM Hydrates	SeefHyd	15	0	0	0	26	12	0	0	0	0	0	0	0	0	0	0	0	0	47	34	Seep	M05_SH		
		InHyd	17	0	0	0	20	17	0	0	0	0	0	0	0	0	0	0	0	0	46	46	Seep	M05_IH		

Shaded regions indicate clone libraries selected for correspondence analysis. Environmental assignments are derived from coupled geochemical data or from core descriptions. In some cases, the assignment may be ambiguous, and these examples should be considered a rough estimate of their respective environments.

Table S2. Correspondence Analysis Results

Tag	Env*	Correspondence Analysis			
		Ax1 (.514)	Ax2 (.468)	Ax3 (.403)	Ax4 (.272)
Ams1	Seep	-25	-10	-53	-45
Ams2	Seep	-30	-50	-59	-3
GoMSMTZ	SMTZ	49	-104	48	-42
I02	Seep	-109	-15	109	23
I03_18	ash	39	185	-34	25
I03_22	clay	292	-92	118	31
I03_24	ash	43	191	-39	6
I03_30	ash	71	212	-16	-57
I03_45	clay	59	214	-25	-61
I03_45	ash	255	-12	98	-21
I03_57	clay	306	-119	136	-6
I03_7	clay	44	-92	-31	-33
J07	sulf	47	221	-29	-37
K03_194	meth	-110	65	127	50
Kaz2	meth	-6	-24	-93	-10
Kaz3	SMTZ	-51	-86	-47	-46
L99	Seep	-43	51	52	-31
M05_IH	Seep	-103	-56	49	-13
M05_SH	Seep	-94	-65	35	-28
M06_0	Seep	-146	27	163	62
M06_10	Seep	-104	7	103	-26
M06_6	Seep	-94	48	100	118
MertzBot	sulf	-10	40	-46	-26
MertzMid	sulf	4	102	-31	-40
MertzTop	nitr	19	165	-18	-32
N04	sulf	276	-53	99	34
Nap1	sulf	-22	-62	-103	11
Nap2	SMTZ	-17	-63	-105	-21
Nap3	SMTZ	-24	-88	-106	-5
Nap4	sulf	17	0	-85	190
R02_165	meth	84	19	52	-29
R06_bot	Seep	-81	-64	28	-48
R06_mid	Seep	-71	28	60	-43
R06_top	Seep	-151	-23	150	13
SBB050cm	sulf	12	-85	-147	58
SBB103cm	sulf	26	-121	-127	4
SBB125cm	SMTZ	-1	-92	2	-30
SBB139cm	SMTZ	-20	-108	-52	-25
SBB163cm	meth	-4	-89	-62	-31
TeskeA	Seep	-115	-53	60	14
TeskeC	Seep	-67	39	91	-19
Una1	nitr	-14	10	-47	86
Ura2	nitr	32	56	-72	271
W06_30	SMTZ	-7	-83	-111	-27
W06_42	SMTZ	0	8	-83	-28
W06_6	sulf	20	43	-75	-42
W06_86	SMTZ	21	100	-61	-42

Values by axes titles correspond to the axis eigenvalue

Appendix III. Supplemental figures—Eel River Basin community analyses by terminal restriction fragment length polymorphism

This section contains data matrices used in assessing relative abundance of terminal restriction fragments and corresponding operational taxonomic units for Chapter 2 and Chapter 3. All Eel River Basin environmental sediment horizon TRFLP analyses conducted in this study are summarized in Table 1 (paramag = magnetic; diamag = nonmagnetic). Abundance of T-RF bins in environmental samples (Tables 2–4) are presented as the relative proportion of detectable community (row sum = 1). Abundance of microcosm microbial communities (Tables 5, 6) are presented as percent relative abundance (row sum = 100).

TABLE 1. Summary of Eel River Basin environmental sample analyses

sample	Dive	Core	Core Type	Depth	Bacteria			Archaea		
					bulk >2.8g/cc	<2.8g/cc	paramag diamag	bulk >2.8g/cc	<2.8g/cc	paramag diamag
2561	AD4252	PC4	clam	12-15cm	X	X	X	X	X	X
2573	AD4252	PC16	low-flux	12-15cm	X	X	X	X	X	X
2685	AD4256	PC17	clam	12-15cm	X	X	X	X	X	X
2686	AD4256	PC29	mat	0-3cm	X	X	X	X	X	X
2687	AD4256	PC29	mat	3-6cm	X	X	X	X	X	X
2688	AD4256	PC29	mat	6-9cm	X	X	X	X	X	X
2689	AD4256	PC29	mat	9-12cm	X	X	X	X	X	X
2690	AD4256	PC29	mat	12-15cm	X	X	X	X	X	X
2691	AD4256	PC29	mat	15-18cm	X	X	X	X	X	X
2692	AD4256	PC29	mat	18-21cm	X	X	X	X	X	X
2693	AD4256	PC23	clam	0-3cm	X	X	X	X	X	X
2694	AD4256	PC23	clam	3-6cm	X	X	X	X	X	X
2695	AD4256	PC23	clam	6-9cm	X	X	X	X	X	X
2696	AD4256	PC23	clam	9-12cm	X	X	X	X	X	X
2697	AD4256	PC23	clam	12-15cm	X	X	X	X	X	X
2698	AD4256	PC23	clam	15-18cm	X	X	X	X	X	X
2700	AD4256	PC20	low-flux	0-3cm	X	X	X	X	X	X
2701	AD4256	PC20	low-flux	3-6cm	X	X	X	X	X	X
2702	AD4256	PC20	low-flux	6-9cm	X	X	X	X	X	X
2704	AD4256	PC20	low-flux	12-15cm	X	X	X	X	X	X
2776	AD4258	PC17	clam	3-6cm	X	X	X	X	X	X
2777	AD4258	PC17	clam	6-9cm	X	X	X	X	X	X
2778	AD4258	PC17	clam	9-12cm	X	X	X	X	X	X

TABLE 2. Relative abundance of ERB T-RFs by HaeIII

sample	Fraction	Hae083	Hae106	Hae111	Hae116	Hae119	Hae123	Hae126	Hae128	Hae131	Hae133	Hae138	Hae144	Hae147	Hae149
B2686u	<2.8 g/cc	0.00	0.00	0.00	0.00	0.00	0.00	0.00	0.00	0.00	0.00	0.00	0.00	0.00	0.00
B2687u	<2.8 g/cc	0.00	0.00	0.00	0.00	0.00	0.00	0.01	0.00	0.00	0.00	0.00	0.00	0.00	0.00
B2688u	<2.8 g/cc	0.00	0.00	0.00	0.00	0.00	0.00	0.01	0.00	0.00	0.00	0.00	0.00	0.00	0.00
B2693u	<2.8 g/cc	0.00	0.00	0.00	0.00	0.00	0.00	0.00	0.00	0.00	0.00	0.00	0.00	0.00	0.00
B2694u	<2.8 g/cc	0.00	0.00	0.00	0.00	0.00	0.00	0.00	0.00	0.00	0.00	0.00	0.00	0.00	0.00
B2695u	<2.8 g/cc	0.00	0.00	0.00	0.00	0.00	0.00	0.00	0.00	0.00	0.00	0.00	0.00	0.00	0.00
B2698u	<2.8 g/cc	0.01	0.00	0.00	0.00	0.00	0.00	0.00	0.00	0.00	0.00	0.00	0.00	0.00	0.00
B2700u	<2.8 g/cc	0.00	0.00	0.00	0.00	0.00	0.00	0.00	0.00	0.00	0.00	0.00	0.00	0.00	0.00
B2701u	<2.8 g/cc	0.00	0.00	0.00	0.00	0.00	0.00	0.00	0.00	0.00	0.00	0.00	0.00	0.00	0.00
B2702u	<2.8 g/cc	0.00	0.00	0.00	0.00	0.00	0.00	0.00	0.00	0.00	0.00	0.01	0.00	0.00	0.00
B2704u	<2.8 g/cc	0.00	0.00	0.00	0.00	0.00	0.00	0.00	0.00	0.00	0.00	0.02	0.00	0.00	0.00
B2685o	>2.8 g/cc	0.00	0.00	0.00	0.00	0.00	0.00	0.00	0.00	0.00	0.00	0.00	0.00	0.00	0.00
B2686o	>2.8 g/cc	0.00	0.00	0.00	0.00	0.00	0.00	0.00	0.00	0.00	0.00	0.00	0.00	0.00	0.00
B2687o	>2.8 g/cc	0.00	0.00	0.00	0.00	0.00	0.00	0.01	0.00	0.00	0.00	0.00	0.00	0.00	0.00
B2688o	>2.8 g/cc	0.00	0.00	0.00	0.00	0.00	0.00	0.00	0.00	0.00	0.00	0.00	0.00	0.00	0.00
B2693o	>2.8 g/cc	0.00	0.00	0.00	0.01	0.00	0.00	0.00	0.00	0.00	0.00	0.00	0.00	0.01	0.00
B2694o	>2.8 g/cc	0.00	0.00	0.00	0.02	0.00	0.00	0.00	0.00	0.00	0.00	0.00	0.00	0.00	0.00
B2695o	>2.8 g/cc	0.00	0.00	0.00	0.00	0.00	0.00	0.00	0.00	0.01	0.00	0.00	0.00	0.00	0.00
B2698o	>2.8 g/cc	0.00	0.00	0.00	0.00	0.00	0.00	0.00	0.00	0.00	0.00	0.00	0.00	0.00	0.00
B2700o	>2.8 g/cc	0.00	0.00	0.00	0.00	0.00	0.00	0.00	0.00	0.00	0.00	0.00	0.00	0.00	0.00
B2701o	>2.8 g/cc	0.00	0.00	0.00	0.00	0.00	0.00	0.00	0.00	0.00	0.00	0.00	0.00	0.00	0.00
B2704o	>2.8 g/cc	0.00	0.00	0.00	0.00	0.00	0.01	0.00	0.00	0.00	0.00	0.00	0.00	0.00	0.00
B2687b	bulk	0.00	0.00	0.00	0.00	0.00	0.00	0.00	0.01	0.00	0.00	0.00	0.00	0.00	0.00
B2688b	bulk	0.00	0.00	0.00	0.00	0.00	0.00	0.00	0.00	0.00	0.00	0.00	0.00	0.00	0.00
B2693b	bulk	0.00	0.00	0.00	0.00	0.00	0.00	0.00	0.01	0.00	0.00	0.00	0.00	0.00	0.00
B2694b	bulk	0.00	0.00	0.00	0.01	0.01	0.00	0.00	0.01	0.00	0.00	0.00	0.01	0.01	0.01

Hae152	Hae162	Hae167	Hae171	Hae173	Hae175	Hae177	Hae179	Hae182	Hae184	Hae187	Hae189	Hae190	Hae193	Hae195	Hae198
0.00	0.00	0.00	0.00	0.00	0.00	0.00	0.00	0.00	0.00	0.00	0.00	0.02	0.01	0.00	0.00
0.00	0.00	0.00	0.00	0.00	0.00	0.00	0.00	0.00	0.00	0.00	0.00	0.00	0.00	0.00	0.00
0.00	0.00	0.00	0.00	0.00	0.00	0.00	0.00	0.00	0.00	0.00	0.00	0.00	0.00	0.00	0.00
0.00	0.00	0.00	0.00	0.00	0.00	0.00	0.00	0.00	0.00	0.00	0.00	0.02	0.02	0.00	0.00
0.00	0.00	0.00	0.00	0.00	0.00	0.00	0.00	0.00	0.00	0.00	0.00	0.01	0.01	0.00	0.00
0.00	0.00	0.00	0.00	0.00	0.00	0.00	0.00	0.00	0.00	0.00	0.01	0.00	0.00	0.01	0.00
0.00	0.00	0.00	0.00	0.00	0.00	0.00	0.00	0.00	0.00	0.00	0.01	0.00	0.00	0.00	0.00
0.00	0.00	0.00	0.00	0.00	0.00	0.00	0.00	0.00	0.00	0.00	0.01	0.01	0.02	0.01	0.00
0.00	0.00	0.00	0.00	0.00	0.00	0.00	0.00	0.00	0.00	0.00	0.01	0.01	0.01	0.00	0.00
0.00	0.00	0.00	0.00	0.00	0.00	0.00	0.00	0.00	0.00	0.00	0.00	0.00	0.01	0.00	0.00
0.00	0.00	0.00	0.00	0.00	0.00	0.00	0.00	0.00	0.00	0.00	0.00	0.00	0.00	0.00	0.00
0.00	0.00	0.00	0.00	0.00	0.00	0.00	0.00	0.00	0.00	0.00	0.00	0.02	0.02	0.00	0.00
0.00	0.00	0.00	0.00	0.00	0.00	0.00	0.00	0.02	0.00	0.00	0.01	0.01	0.01	0.00	0.01
0.00	0.00	0.00	0.00	0.00	0.00	0.00	0.04	0.00	0.00	0.00	0.00	0.00	0.00	0.07	0.01
0.01	0.00	0.00	0.00	0.00	0.00	0.00	0.00	0.00	0.00	0.00	0.00	0.03	0.00	0.00	0.00
0.00	0.00	0.00	0.00	0.00	0.00	0.00	0.00	0.00	0.00	0.00	0.00	0.01	0.00	0.00	0.00
0.00	0.01	0.00	0.00	0.00	0.00	0.00	0.00	0.02	0.02	0.00	0.01	0.04	0.04	0.01	0.00
0.00	0.00	0.00	0.00	0.00	0.00	0.00	0.00	0.00	0.00	0.00	0.00	0.00	0.01	0.00	0.00
0.00	0.00	0.00	0.00	0.00	0.00	0.00	0.00	0.01	0.02	0.01	0.00	0.01	0.03	0.00	0.01
0.00	0.00	0.00	0.00	0.00	0.00	0.00	0.00	0.00	0.02	0.01	0.00	0.02	0.02	0.00	0.01
0.00	0.00	0.01	0.00	0.00	0.00	0.00	0.00	0.00	0.01	0.00	0.00	0.01	0.02	0.00	0.00
0.00	0.00	0.00	0.00	0.00	0.01	0.01	0.00	0.01	0.01	0.00	0.01	0.01	0.01	0.00	0.01
0.00	0.00	0.00	0.00	0.01	0.00	0.03	0.01	0.00	0.01	0.00	0.00	0.02	0.02	0.00	0.01
0.00	0.00	0.00	0.01	0.00	0.00	0.00	0.01	0.01	0.01	0.00	0.00	0.00	0.02	0.00	0.01
0.00	0.00	0.00	0.00	0.00	0.00	0.00	0.01	0.01	0.00	0.00	0.00	0.00	0.04	0.00	0.01
0.00	0.00	0.00	0.00	0.00	0.00	0.00	0.00	0.00	0.00	0.00	0.00	0.01	0.01	0.00	0.00

Hae201	Hae203	Hae206	Hae208	Hae211	Hae214	Hae216	Hae218	Hae220	Hae222	Hae225	Hae227	Hae229	Hae230	Hae234	Hae235
0.01	0.08	0.08	0.05	0.00	0.00	0.00	0.00	0.01	0.02	0.03	0.00	0.03	0.01	0.01	0.03
0.02	0.14	0.13	0.19	0.01	0.00	0.00	0.00	0.01	0.02	0.01	0.00	0.02	0.00	0.02	0.00
0.03	0.07	0.14	0.19	0.01	0.00	0.00	0.00	0.02	0.04	0.02	0.01	0.01	0.01	0.01	0.01
0.04	0.09	0.12	0.05	0.00	0.00	0.00	0.01	0.01	0.02	0.04	0.01	0.02	0.01	0.01	0.01
0.02	0.12	0.18	0.10	0.02	0.00	0.00	0.00	0.02	0.01	0.03	0.01	0.01	0.00	0.00	0.00
0.02	0.05	0.14	0.19	0.01	0.00	0.01	0.00	0.01	0.02	0.02	0.01	0.01	0.01	0.01	0.00
0.03	0.06	0.12	0.20	0.01	0.00	0.00	0.00	0.01	0.04	0.04	0.01	0.01	0.00	0.00	0.00
0.03	0.11	0.15	0.04	0.00	0.00	0.00	0.01	0.01	0.02	0.05	0.01	0.02	0.00	0.01	0.01
0.02	0.13	0.19	0.03	0.00	0.00	0.00	0.01	0.01	0.02	0.03	0.00	0.02	0.00	0.00	0.01
0.00	0.00	0.00	0.15	0.00	0.00	0.00	0.00	0.01	0.07	0.13	0.01	0.01	0.00	0.00	0.00
0.04	0.00	0.05	0.03	0.00	0.00	0.00	0.00	0.02	0.22	0.22	0.02	0.00	0.00	0.00	0.01
0.01	0.07	0.37	0.04	0.00	0.00	0.00	0.00	0.00	0.01	0.05	0.00	0.00	0.00	0.00	0.00
0.01	0.07	0.13	0.01	0.00	0.00	0.00	0.00	0.00	0.02	0.03	0.00	0.09	0.00	0.02	0.06
0.02	0.02	0.09	0.12	0.01	0.00	0.02	0.03	0.02	0.00	0.02	0.00	0.02	0.03	0.00	0.00
0.03	0.05	0.20	0.17	0.00	0.00	0.00	0.00	0.00	0.00	0.00	0.00	0.00	0.04	0.00	0.01
0.00	0.11	0.00	0.00	0.00	0.00	0.00	0.00	0.03	0.04	0.04	0.00	0.07	0.00	0.00	0.00
0.00	0.13	0.00	0.00	0.00	0.00	0.00	0.03	0.00	0.00	0.05	0.00	0.03	0.00	0.00	0.02
0.01	0.02	0.19	0.04	0.00	0.00	0.00	0.01	0.00	0.01	0.03	0.00	0.00	0.00	0.00	0.00
0.02	0.09	0.13	0.19	0.00	0.00	0.00	0.00	0.02	0.00	0.01	0.00	0.02	0.00	0.00	0.00
0.03	0.04	0.13	0.04	0.01	0.00	0.00	0.01	0.01	0.01	0.03	0.01	0.01	0.01	0.01	0.01
0.03	0.04	0.10	0.05	0.01	0.00	0.00	0.00	0.01	0.02	0.01	0.00	0.00	0.01	0.00	0.01
0.01	0.01	0.04	0.01	0.00	0.00	0.00	0.00	0.01	0.10	0.07	0.00	0.00	0.00	0.00	0.00
0.05	0.04	0.13	0.17	0.01	0.00	0.00	0.01	0.02	0.04	0.02	0.01	0.01	0.01	0.04	0.00
0.02	0.04	0.19	0.07	0.01	0.01	0.01	0.01	0.02	0.06	0.00	0.02	0.02	0.00	0.03	0.00
0.00	0.25	0.00	0.00	0.02	0.01	0.00	0.00	0.02	0.00	0.05	0.00	0.02	0.00	0.01	0.02
0.02	0.13	0.08	0.11	0.00	0.00	0.00	0.01	0.02	0.01	0.03	0.01	0.01	0.00	0.01	0.02

Hae237	Hae239	Hae241	Hae244	Hae247	Hae251	Hae253	Hae255	Hae257	Hae259	Hae263	Hae266	Hae268	Hae270	Hae272	Hae274
0.02	0.01	0.01	0.01	0.02	0.00	0.00	0.02	0.01	0.01	0.00	0.00	0.00	0.03	0.01	0.00
0.03	0.00	0.01	0.01	0.02	0.00	0.00	0.04	0.01	0.01	0.00	0.00	0.01	0.03	0.02	0.00
0.04	0.01	0.01	0.01	0.03	0.00	0.00	0.02	0.00	0.01	0.00	0.00	0.01	0.03	0.02	0.01
0.04	0.01	0.01	0.01	0.02	0.00	0.01	0.04	0.02	0.01	0.00	0.00	0.01	0.02	0.02	0.01
0.00	0.00	0.00	0.00	0.02	0.00	0.00	0.02	0.00	0.02	0.00	0.00	0.00	0.02	0.02	0.04
0.04	0.03	0.00	0.01	0.02	0.00	0.00	0.01	0.01	0.00	0.00	0.00	0.01	0.03	0.02	0.01
0.03	0.01	0.00	0.00	0.02	0.00	0.00	0.01	0.00	0.00	0.00	0.00	0.01	0.05	0.05	0.02
0.05	0.01	0.01	0.00	0.01	0.00	0.00	0.05	0.04	0.01	0.00	0.00	0.01	0.03	0.02	0.00
0.03	0.01	0.01	0.00	0.01	0.00	0.00	0.04	0.02	0.01	0.00	0.00	0.00	0.04	0.00	0.00
0.00	0.00	0.01	0.01	0.01	0.00	0.00	0.03	0.02	0.02	0.00	0.02	0.00	0.02	0.12	0.04
0.01	0.06	0.01	0.00	0.00	0.00	0.00	0.00	0.00	0.01	0.00	0.01	0.00	0.02	0.17	0.01
0.02	0.00	0.00	0.00	0.02	0.00	0.00	0.00	0.00	0.01	0.00	0.00	0.00	0.00	0.02	0.03
0.05	0.01	0.01	0.00	0.01	0.00	0.00	0.03	0.01	0.01	0.00	0.00	0.00	0.03	0.01	0.00
0.00	0.01	0.00	0.00	0.00	0.00	0.01	0.03	0.00	0.00	0.00	0.00	0.00	0.01	0.00	0.00
0.04	0.00	0.00	0.02	0.03	0.00	0.02	0.01	0.00	0.01	0.00	0.00	0.00	0.00	0.00	0.01
0.08	0.00	0.00	0.03	0.03	0.02	0.00	0.04	0.00	0.06	0.00	0.00	0.00	0.06	0.00	0.00
0.05	0.01	0.00	0.02	0.03	0.00	0.00	0.02	0.08	0.03	0.00	0.01	0.02	0.04	0.03	0.02
0.00	0.00	0.01	0.00	0.01	0.00	0.00	0.04	0.02	0.08	0.03	0.00	0.02	0.00	0.01	0.03
0.00	0.03	0.00	0.00	0.01	0.00	0.00	0.05	0.00	0.07	0.01	0.00	0.00	0.02	0.00	0.01
0.00	0.04	0.01	0.01	0.01	0.00	0.00	0.06	0.02	0.11	0.01	0.01	0.00	0.01	0.01	0.00
0.02	0.02	0.00	0.01	0.02	0.00	0.01	0.05	0.04	0.11	0.02	0.00	0.00	0.01	0.00	0.00
0.02	0.30	0.03	0.00	0.00	0.00	0.00	0.01	0.01	0.16	0.03	0.03	0.00	0.00	0.06	0.00
0.04	0.00	0.01	0.00	0.02	0.00	0.00	0.03	0.02	0.00	0.00	0.00	0.00	0.01	0.03	0.02
0.03	0.00	0.01	0.00	0.02	0.00	0.00	0.03	0.02	0.00	0.01	0.00	0.00	0.00	0.03	0.00
0.02	0.02	0.01	0.01	0.02	0.00	0.00	0.04	0.00	0.04	0.00	0.00	0.00	0.02	0.03	0.01
0.02	0.00	0.01	0.01	0.01	0.00	0.00	0.04	0.05	0.04	0.00	0.00	0.00	0.00	0.03	0.00

Hae411	Hae413	Hae423	Hae426	Hae435	Hae438	Hae455	Hae462	Hae469	Hae471	Hae499	Hae504	Hae506	Hae508	Hae522	Hae525
0.02	0.02	0.00	0.00	0.00	0.00	0.00	0.00	0.00	0.00	0.00	0.01	0.03	0.34	0.00	0.00
0.01	0.02	0.00	0.00	0.00	0.00	0.00	0.00	0.00	0.00	0.00	0.00	0.00	0.16	0.00	0.00
0.01	0.01	0.00	0.00	0.00	0.00	0.00	0.00	0.00	0.00	0.00	0.00	0.00	0.14	0.00	0.00
0.01	0.02	0.00	0.00	0.00	0.00	0.00	0.00	0.00	0.00	0.00	0.00	0.00	0.18	0.00	0.00
0.01	0.00	0.01	0.00	0.00	0.00	0.00	0.00	0.00	0.00	0.00	0.02	0.00	0.21	0.00	0.00
0.00	0.01	0.00	0.00	0.00	0.00	0.00	0.00	0.00	0.00	0.00	0.00	0.00	0.21	0.00	0.00
0.00	0.01	0.00	0.00	0.00	0.00	0.00	0.00	0.00	0.00	0.00	0.00	0.00	0.14	0.00	0.00
0.00	0.02	0.00	0.00	0.00	0.00	0.00	0.00	0.00	0.00	0.00	0.01	0.02	0.11	0.00	0.00
0.00	0.02	0.00	0.00	0.00	0.00	0.00	0.00	0.00	0.00	0.00	0.02	0.00	0.22	0.00	0.00
0.00	0.01	0.00	0.00	0.00	0.01	0.00	0.00	0.00	0.00	0.00	0.01	0.00	0.17	0.00	0.00
0.00	0.00	0.00	0.00	0.00	0.00	0.00	0.00	0.00	0.00	0.00	0.00	0.00	0.03	0.00	0.00
0.00	0.00	0.00	0.00	0.00	0.00	0.00	0.00	0.00	0.00	0.00	0.00	0.00	0.30	0.00	0.00
0.02	0.01	0.00	0.00	0.00	0.00	0.00	0.00	0.00	0.00	0.00	0.00	0.00	0.33	0.00	0.00
0.00	0.00	0.00	0.00	0.00	0.00	0.00	0.00	0.01	0.00	0.00	0.00	0.00	0.29	0.00	0.00
0.00	0.00	0.00	0.00	0.00	0.00	0.00	0.00	0.00	0.00	0.00	0.00	0.08	0.19	0.00	0.00
0.00	0.04	0.00	0.00	0.00	0.00	0.00	0.00	0.00	0.00	0.00	0.00	0.01	0.16	0.00	0.01
0.02	0.01	0.00	0.00	0.00	0.00	0.00	0.00	0.00	0.00	0.00	0.01	0.00	0.14	0.00	0.01
0.00	0.00	0.00	0.00	0.00	0.00	0.00	0.00	0.00	0.00	0.00	0.02	0.03	0.18	0.00	0.00
0.00	0.01	0.00	0.00	0.00	0.00	0.00	0.00	0.00	0.00	0.00	0.00	0.00	0.24	0.00	0.00
0.00	0.01	0.00	0.00	0.00	0.00	0.00	0.00	0.00	0.00	0.00	0.00	0.01	0.09	0.00	0.00
0.00	0.00	0.00	0.00	0.00	0.00	0.00	0.00	0.00	0.00	0.01	0.03	0.00	0.21	0.00	0.00
0.00	0.00	0.00	0.00	0.00	0.00	0.00	0.00	0.00	0.00	0.00	0.00	0.00	0.00	0.00	0.00
0.00	0.01	0.00	0.00	0.00	0.00	0.00	0.00	0.00	0.00	0.00	0.01	0.01	0.05	0.00	0.00
0.00	0.01	0.00	0.00	0.00	0.00	0.00	0.00	0.00	0.00	0.00	0.01	0.00	0.05	0.00	0.00
0.01	0.03	0.00	0.00	0.00	0.01	0.00	0.00	0.00	0.00	0.00	0.01	0.01	0.08	0.00	0.00
0.00	0.01	0.00	0.00	0.00	0.01	0.00	0.00	0.00	0.00	0.00	0.03	0.00	0.07	0.00	0.00

TABLE 3. Relative abundance of FRB T-RFs by RsaI

sample	Fraction	Rsa081	Rsa086	Rsa091	Rsa104	Rsa107	Rsa113	Rsa120	Rsa125	Rsa140	Rsa146	Rsa149	Rsa169	Rsa173	Rsa175	Rsa187	Rsa190	Rsa193	Rsa197	Rsa199	Rsa221	Rsa226	Rsa242	Rsa244	Rsa246	Rsa248	Rsa253
B2686b	bulk	0.05	0.00	0.00	0.00	0.00	0.00	0.00	0.00	0.00	0.00	0.00	0.00	0.07	0.10	0.00	0.00	0.00	0.00	0.00	0.00	0.03	0.11	0.02	0.03	0.00	
B2687b	bulk	0.00	0.00	0.00	0.00	0.00	0.00	0.02	0.00	0.00	0.00	0.00	0.00	0.00	0.00	0.00	0.00	0.00	0.00	0.00	0.00	0.00	0.08	0.00	0.03	0.00	
B2688b	bulk	0.00	0.00	0.00	0.00	0.00	0.00	0.01	0.00	0.00	0.00	0.00	0.00	0.00	0.00	0.00	0.00	0.00	0.00	0.00	0.00	0.00	0.05	0.00	0.06	0.02	
B2690b	bulk	0.00	0.00	0.00	0.00	0.00	0.00	0.01	0.00	0.00	0.00	0.00	0.00	0.00	0.00	0.00	0.00	0.00	0.00	0.00	0.00	0.00	0.12	0.09	0.00	0.00	
B2691b	bulk	0.00	0.00	0.00	0.00	0.10	0.13	0.00	0.00	0.00	0.00	0.00	0.00	0.00	0.00	0.00	0.00	0.00	0.00	0.00	0.00	0.00	0.05	0.00	0.00	0.00	
B2692b	bulk	0.00	0.00	0.00	0.00	0.00	0.00	0.00	0.00	0.00	0.00	0.00	0.00	0.00	0.00	0.00	0.00	0.00	0.00	0.00	0.00	0.00	0.03	0.00	0.00	0.00	
B2693b	bulk	0.00	0.00	0.00	0.00	0.00	0.00	0.00	0.00	0.00	0.00	0.00	0.00	0.02	0.00	0.00	0.00	0.00	0.00	0.01	0.01	0.00	0.03	0.00	0.00	0.00	
B2694b	bulk	0.00	0.00	0.00	0.00	0.00	0.00	0.00	0.00	0.00	0.00	0.00	0.00	0.00	0.00	0.00	0.00	0.00	0.00	0.00	0.00	0.00	0.03	0.00	0.05	0.00	
B2695b	bulk	0.00	0.00	0.02	0.00	0.12	0.14	0.00	0.00	0.01	0.00	0.00	0.00	0.00	0.01	0.00	0.01	0.00	0.00	0.00	0.00	0.00	0.04	0.03	0.02	0.00	
B2698b	bulk	0.02	0.00	0.00	0.00	0.02	0.04	0.01	0.00	0.00	0.00	0.00	0.00	0.00	0.00	0.00	0.00	0.00	0.00	0.00	0.00	0.02	0.16	0.08	0.06	0.00	
B2704b	bulk	0.00	0.00	0.00	0.01	0.00	0.00	0.00	0.00	0.02	0.01	0.01	0.01	0.01	0.01	0.01	0.03	0.03	0.01	0.01	0.00	0.01	0.03	0.00	0.00	0.00	
B2685m	mug	0.00	0.00	0.00	0.00	0.00	0.00	0.01	0.00	0.00	0.00	0.00	0.00	0.01	0.01	0.01	0.00	0.00	0.00	0.00	0.00	0.04	0.17	0.00	0.00	0.00	
B2688m	mug	0.01	0.00	0.00	0.00	0.01	0.02	0.01	0.01	0.00	0.00	0.00	0.00	0.01	0.01	0.00	0.00	0.00	0.00	0.00	0.00	0.02	0.11	0.02	0.06	0.00	
B2698m	mug	0.00	0.00	0.00	0.00	0.00	0.00	0.00	0.00	0.00	0.00	0.00	0.00	0.00	0.00	0.00	0.00	0.00	0.00	0.00	0.00	0.00	0.00	0.04	0.06	0.00	
B2700m	mug	0.03	0.00	0.00	0.00	0.00	0.03	0.00	0.00	0.00	0.00	0.00	0.00	0.00	0.00	0.01	0.01	0.00	0.00	0.01	0.00	0.04	0.06	0.00	0.01	0.00	
B2778m	mug	0.00	0.00	0.00	0.00	0.01	0.06	0.01	0.00	0.00	0.00	0.00	0.00	0.00	0.00	0.01	0.00	0.00	0.00	0.00	0.00	0.02	0.00	0.00	0.00	0.00	
B2685n	nomneg	0.00	0.00	0.00	0.00	0.00	0.00	0.00	0.00	0.00	0.00	0.00	0.00	0.00	0.01	0.00	0.00	0.00	0.00	0.00	0.00	0.01	0.10	0.00	0.00	0.00	
B2688n	nomneg	0.00	0.00	0.00	0.00	0.00	0.00	0.00	0.00	0.00	0.00	0.00	0.00	0.00	0.01	0.00	0.00	0.00	0.00	0.00	0.00	0.02	0.10	0.01	0.03	0.00	
B2698n	nomneg	0.01	0.00	0.00	0.00	0.00	0.00	0.00	0.00	0.00	0.00	0.00	0.00	0.00	0.00	0.00	0.00	0.00	0.00	0.00	0.00	0.01	0.06	0.03	0.02	0.00	
B2700n	nomneg	0.00	0.00	0.00	0.00	0.12	0.18	0.00	0.00	0.00	0.00	0.00	0.00	0.00	0.00	0.01	0.00	0.00	0.00	0.00	0.00	0.00	0.01	0.00	0.00	0.00	
B2776n	nomneg	0.01	0.00	0.00	0.00	0.00	0.00	0.01	0.00	0.00	0.00	0.00	0.00	0.00	0.01	0.01	0.00	0.00	0.00	0.00	0.00	0.01	0.05	0.00	0.03	0.00	
B2777n	nomneg	0.00	0.00	0.00	0.00	0.00	0.00	0.01	0.00	0.00	0.00	0.00	0.00	0.00	0.02	0.00	0.00	0.00	0.00	0.00	0.00	0.01	0.09	0.01	0.00	0.00	
B2778n	nomneg	0.00	0.00	0.00	0.00	0.00	0.01	0.00	0.00	0.00	0.00	0.00	0.00	0.00	0.01	0.00	0.00	0.00	0.00	0.00	0.00	0.00	0.02	0.01	0.00	0.00	
B2686o	>2.8 g/cc	0.00	0.00	0.00	0.00	0.00	0.10	0.00	0.00	0.00	0.00	0.00	0.00	0.00	0.00	0.00	0.00	0.00	0.00	0.00	0.00	0.00	0.09	0.00	0.00	0.00	
B2687o	>2.8 g/cc	0.00	0.00	0.00	0.00	0.00	0.11	0.00	0.00	0.00	0.00	0.00	0.00	0.00	0.00	0.00	0.00	0.00	0.00	0.00	0.00	0.16	0.00	0.00	0.00	0.00	
B2688o	>2.8 g/cc	0.00	0.00	0.00	0.00	0.00	0.05	0.00	0.00	0.00	0.00	0.00	0.00	0.00	0.00	0.00	0.00	0.00	0.00	0.00	0.00	0.20	0.00	0.00	0.00	0.00	
B2690o	>2.8 g/cc	0.00	0.00	0.00	0.00	0.00	0.03	0.00	0.00	0.00	0.00	0.00	0.00	0.00	0.00	0.00	0.00	0.00	0.00	0.00	0.00	0.01	0.00	0.00	0.00	0.00	
B2694o	>2.8 g/cc	0.00	0.00	0.00	0.00	0.00	0.00	0.01	0.00	0.00	0.00	0.00	0.00	0.01	0.02	0.00	0.00	0.00	0.00	0.01	0.00	0.02	0.10	0.03	0.01	0.02	
B2695o	>2.8 g/cc	0.02	0.02	0.01	0.02	0.04	0.09	0.01	0.00	0.01	0.00	0.00	0.00	0.00	0.00	0.00	0.00	0.00	0.00	0.00	0.01	0.02	0.05	0.03	0.04	0.00	
B2697o	>2.8 g/cc	0.00	0.00	0.00	0.00	0.00	0.00	0.00	0.00	0.00	0.00	0.00	0.00	0.00	0.00	0.00	0.00	0.00	0.00	0.00	0.00	0.19	0.00	0.00	0.00	0.00	
B2698o	>2.8 g/cc	0.00	0.00	0.00	0.00	0.01	0.02	0.00	0.00	0.00	0.00	0.00	0.00	0.00	0.00	0.00	0.00	0.00	0.00	0.00	0.00	0.04	0.13	0.00	0.00	0.00	
B2700o	>2.8 g/cc	0.00	0.00	0.00	0.00	0.00	0.05	0.00	0.00	0.00	0.00	0.00	0.00	0.00	0.01	0.00	0.00	0.00	0.00	0.00	0.00	0.03	0.07	0.00	0.01	0.00	
B2701o	>2.8 g/cc	0.00	0.00	0.00	0.00	0.01	0.06	0.01	0.00	0.00	0.00	0.00	0.00	0.00	0.01	0.00	0.01	0.00	0.00	0.00	0.00	0.02	0.09	0.00	0.00	0.00	
B2704o	>2.8 g/cc	0.00	0.00	0.00	0.00	0.01	0.06	0.00	0.00	0.00	0.00	0.00	0.00	0.00	0.00	0.00	0.00	0.00	0.00	0.00	0.00	0.02	0.03	0.01	0.00	0.00	
B2686u	<2.8 g/cc	0.00	0.00	0.01	0.22	0.00	0.07	0.00	0.00	0.00	0.00	0.00	0.00	0.00	0.00	0.00	0.00	0.00	0.00	0.00	0.01	0.04	0.00	0.00	0.00	0.00	
B2687u	<2.8 g/cc	0.00	0.00	0.00	0.00	0.04	0.00	0.00	0.00	0.00	0.00	0.00	0.00	0.00	0.00	0.00	0.00	0.00	0.00	0.00	0.05	0.25	0.00	0.00	0.05	0.01	
B2688u	<2.8 g/cc	0.00	0.00	0.00	0.00	0.00	0.05	0.00	0.00	0.00	0.00	0.00	0.00	0.00	0.00	0.00	0.00	0.00	0.00	0.00	0.03	0.14	0.00	0.00	0.05	0.01	
B2690u	<2.8 g/cc	0.00	0.00	0.00	0.00	0.00	0.01	0.00	0.00	0.00	0.00	0.00	0.00	0.00	0.00	0.00	0.00	0.00	0.00	0.00	0.00	0.04	0.14	0.10	0.01	0.00	
B2692u	<2.8 g/cc	0.01	0.00	0.00	0.00	0.00	0.01	0.00	0.01	0.00	0.00	0.00	0.00	0.00	0.00	0.00	0.00	0.00	0.00	0.00	0.00	0.05	0.00	0.00	0.00	0.00	
B2694u	<2.8 g/cc	0.00	0.00	0.00	0.00	0.00	0.00	0.00	0.00	0.00	0.00	0.00	0.00	0.01	0.00	0.00	0.00	0.00	0.00	0.00	0.03	0.15	0.02	0.04	0.00	0.00	
B2695u	<2.8 g/cc	0.00	0.01	0.00	0.00	0.00	0.00	0.00	0.00	0.00	0.00	0.00	0.00	0.00	0.00	0.00	0.00	0.00	0.00	0.00	0.00	0.09	0.00	0.00	0.00	0.00	
B2698u	<2.8 g/cc	0.00	0.00	0.00	0.00	0.00	0.00	0.00	0.00	0.00	0.00	0.00	0.00	0.00	0.00	0.00	0.00	0.00	0.00	0.00	0.03	0.09	0.06	0.03	0.00	0.00	
B2700u	<2.8 g/cc	0.01	0.00	0.00	0.00	0.00	0.00	0.01	0.00	0.00	0.00	0.00	0.00	0.00	0.00	0.00	0.00	0.00	0.00	0.01	0.00	0.02	0.13	0.01	0.00	0.00	
B2701u	<2.8 g/cc	0.00	0.00	0.00	0.00	0.00	0.00	0.00	0.00	0.00	0.00	0.00	0.00	0.01	0.01	0.00	0.00	0.00	0.00	0.00	0.00	0.05	0.16	0.02	0.01	0.00	
B2702u	<2.8 g/cc	0.01	0.00	0.00	0.00	0.00	0.00	0.01	0.00	0.00	0.00	0.00	0.00	0.00	0.01	0.00	0.00	0.00	0.00	0.00	0.02	0.13	0.08	0.03	0.00	0.00	
B2704u	<2.8 g/cc	0.00	0.00	0.00	0.00	0.00	0.00	0.00	0.00	0.00	0.00	0.00	0.00	0.00	0.00	0.00	0.00	0.00	0.00	0.00	0.00	0.01	0.06	0.00	0.00	0.00	

TABLE 4. Relative abundance of archaeal ERB T-RFs by RsaI

sample	Fraction	Rsa165	Rsa172	Rsa244	Rsa246	Rsa248	Rsa267	Rsa278	Rsa285	Rsa388
A2685u	<2.8 g/cc	0.00	0.00	0.82	0.13	0.00	0.00	0.00	0.00	0.05
A2686u	<2.8 g/cc	0.00	0.00	0.84	0.13	0.00	0.01	0.00	0.00	0.02
A2687u	<2.8 g/cc	0.00	0.00	0.73	0.21	0.00	0.02	0.00	0.00	0.04
A2688u	<2.8 g/cc	0.00	0.00	0.75	0.19	0.04	0.02	0.00	0.00	0.00
A2690u	<2.8 g/cc	0.16	0.01	0.23	0.44	0.09	0.04	0.03	0.00	0.00
A2691u	<2.8 g/cc	0.00	0.00	0.32	0.41	0.05	0.04	0.17	0.00	0.00
A2692u	<2.8 g/cc	0.07	0.01	0.42	0.35	0.00	0.02	0.12	0.00	0.00
A2693u	<2.8 g/cc	0.00	0.00	0.81	0.05	0.00	0.00	0.00	0.00	0.14
A2694u	<2.8 g/cc	0.00	0.00	0.80	0.15	0.00	0.00	0.00	0.00	0.06
A2695u	<2.8 g/cc	0.00	0.00	0.81	0.01	0.00	0.00	0.00	0.00	0.17
A2698u	<2.8 g/cc	0.00	0.00	0.79	0.21	0.00	0.00	0.00	0.00	0.00
A2700u	<2.8 g/cc	0.34	0.00	0.42	0.04	0.00	0.00	0.12	0.00	0.07
A2701u	<2.8 g/cc	0.00	0.00	0.85	0.12	0.00	0.03	0.00	0.00	0.00
A2702u	<2.8 g/cc	0.00	0.00	0.83	0.15	0.00	0.00	0.00	0.00	0.02
A2704u1	<2.8 g/cc	0.03	0.00	0.24	0.46	0.06	0.03	0.13	0.04	0.00
A2704u3	<2.8 g/cc	0.03	0.00	0.27	0.42	0.04	0.10	0.13	0.00	0.02
A2685o	>2.8 g/cc	0.00	0.00	0.89	0.07	0.00	0.00	0.00	0.00	0.04
A2686o	>2.8 g/cc	0.00	0.00	1.00	0.00	0.00	0.00	0.00	0.00	0.00
A2687o	>2.8 g/cc	0.00	0.00	0.90	0.03	0.00	0.00	0.00	0.00	0.06
A2688o	>2.8 g/cc	0.00	0.00	0.92	0.05	0.00	0.00	0.00	0.00	0.03
A2690o	>2.8 g/cc	0.00	0.00	0.63	0.28	0.00	0.04	0.00	0.00	0.05
A2692o	>2.8 g/cc	0.00	0.00	0.71	0.12	0.08	0.00	0.00	0.00	0.09
A2693o	>2.8 g/cc	0.00	0.00	0.77	0.05	0.00	0.00	0.00	0.00	0.18
A2694o	>2.8 g/cc	0.06	0.12	0.65	0.13	0.00	0.04	0.00	0.00	0.00
A2695o	>2.8 g/cc	0.00	0.00	0.88	0.12	0.00	0.00	0.00	0.00	0.00
A2698o	>2.8 g/cc	0.00	0.00	0.98	0.02	0.00	0.00	0.00	0.00	0.00
A2700o	>2.8 g/cc	0.00	0.00	0.68	0.13	0.00	0.00	0.00	0.00	0.19
A2701o	>2.8 g/cc	0.00	0.00	0.72	0.07	0.03	0.00	0.00	0.00	0.18
A2702o	>2.8 g/cc	0.00	0.00	0.56	0.44	0.00	0.00	0.00	0.00	0.00
A2704o1	>2.8 g/cc	0.00	0.00	0.09	0.65	0.26	0.00	0.00	0.00	0.00
A2704o3	>2.8 g/cc	0.00	0.00	0.28	0.56	0.11	0.05	0.00	0.00	0.00
A2685b	bulk	0.00	0.00	0.74	0.22	0.00	0.00	0.00	0.00	0.05
A2686b	bulk	0.00	0.00	0.74	0.22	0.00	0.00	0.00	0.00	0.05
A2687b	bulk	0.00	0.00	0.64	0.28	0.00	0.04	0.00	0.00	0.04
A2688b	bulk	0.00	0.00	0.70	0.25	0.00	0.00	0.00	0.00	0.05
A2689b	bulk	0.00	0.00	0.46	0.31	0.04	0.05	0.15	0.00	0.00
A2694b	bulk	0.03	0.00	0.80	0.18	0.00	0.00	0.00	0.00	0.00
A2700b	bulk	0.00	0.00	0.91	0.00	0.00	0.00	0.09	0.00	0.00
A2704b	bulk	0.09	0.03	0.21	0.43	0.00	0.02	0.22	0.00	0.00
A2685m	mag	0.00	0.00	0.93	0.00	0.00	0.00	0.00	0.00	0.07
A2688m	mag	0.00	0.00	0.83	0.17	0.00	0.00	0.00	0.00	0.00
A2691m	mag	0.00	0.00	0.41	0.42	0.15	0.00	0.03	0.00	0.00
A2698m	mag	0.00	0.00	0.57	0.41	0.00	0.01	0.00	0.00	0.00
A2776m	mag	0.00	0.00	0.08	0.14	0.07	0.04	0.42	0.26	0.00

A2777m	mag	0.04	0.00	0.00	0.05	0.00	0.00	0.58	0.33	0.00
A2778m	mag	0.00	0.00	0.00	0.04	0.00	0.00	0.23	0.73	0.00
A2685n	nonmag	0.00	0.00	0.64	0.27	0.00	0.02	0.06	0.00	0.00
A2688n	nonmag	0.00	0.04	0.53	0.24	0.00	0.00	0.19	0.00	0.00
A2691n	nonmag	0.00	0.00	0.16	0.38	0.09	0.05	0.33	0.00	0.00
A2698n	nonmag	0.00	0.00	0.61	0.33	0.00	0.00	0.05	0.00	0.00
A2776n	nonmag	0.00	0.00	0.00	0.22	0.07	0.06	0.65	0.00	0.00
A2777n	nonmag	0.02	0.00	0.00	0.01	0.00	0.04	0.61	0.32	0.00
A2778n	nonmag	0.00	0.00	0.00	0.00	0.00	0.00	0.25	0.75	0.00

TABLE 5. Relative abundance of microcosm Bacterial T-RFs by HaeIII

Sample	Fraction	Hae125	Hae127	Hae148	Hae150	Hae171	Hae174	Hae189	Hae192	Hae198	Hae200	Hae202	Hae204	Hae205	Hae207	Hae210	Hae213
cult04b	<2.8 g/cc	0.0	0.0	0.0	0.0	0.0	0.0	0.0	0.0	0.0	14.7	4.7	4.7	5.5	9.2	0.0	0.0
cult04u	<2.8 g/cc	0.0	0.0	0.0	0.0	0.0	0.0	0.0	0.0	0.0	16.5	0.0	0.0	0.0	0.0	1.4	0.0
cult05u	<2.8 g/cc	2.1	1.9	3.1	0.0	0.0	0.0	0.0	0.0	0.0	10.8	0.0	0.0	11.9	0.0	0.0	0.0
cult07u	<2.8 g/cc	0.0	0.0	0.0	0.0	0.0	0.0	0.0	0.0	0.0	3.9	0.0	0.0	0.0	0.0	0.0	15.7
cult08u	<2.8 g/cc	0.0	0.0	0.0	15.9	0.0	0.0	0.0	0.0	0.0	2.4	0.0	0.0	0.0	0.0	0.0	0.0
cult09u	<2.8 g/cc	0.0	0.0	0.0	0.0	0.0	0.0	0.0	0.0	0.0	0.0	0.0	1.7	0.0	0.0	0.0	6.6
cult10u	<2.8 g/cc	0.0	0.0	0.0	0.0	0.0	0.0	0.0	0.0	0.0	0.0	0.0	0.0	0.0	0.0	0.0	0.0
cult11u	<2.8 g/cc	0.0	0.0	0.0	0.0	0.0	5.8	9.4	71.7	0.0	0.0	0.0	0.0	0.0	0.0	0.0	0.0
cult02o	>2.8 g/cc	0.0	0.0	0.0	0.0	0.0	0.0	0.0	0.0	0.0	0.0	0.0	0.0	0.0	0.0	0.0	4.2
cult04o	>2.8 g/cc	0.0	0.0	0.0	0.0	0.0	0.0	0.0	0.0	1.7	10.2	3.9	9.5	5.0	7.2	0.0	0.0
cult05o	>2.8 g/cc	0.5	0.0	0.0	0.0	0.7	0.0	0.9	0.8	0.7	10.7	0.0	7.0	10.3	1.1	0.6	1.1
cult07o	>2.8 g/cc	0.0	0.0	0.0	0.0	0.0	0.0	0.0	0.0	0.0	0.0	0.0	0.0	0.0	0.0	0.0	14.6
cult08o	>2.8 g/cc	0.0	0.0	0.0	7.0	0.0	0.0	0.0	0.0	0.0	0.0	0.0	0.0	0.0	0.0	0.0	0.0
cult09o	>2.8 g/cc	1.6	2.0	0.0	0.0	0.0	0.0	0.0	2.2	12.6	0.0	5.5	0.0	0.0	0.0	0.0	3.5
cult10o	>2.8 g/cc	0.0	0.0	0.0	0.0	0.0	0.0	0.0	0.0	0.0	0.0	0.0	0.0	0.0	0.0	0.0	0.0
cult11o	>2.8 g/cc	0.0	0.0	0.0	0.0	0.0	0.0	0.0	0.0	0.0	0.0	0.0	0.0	0.0	0.0	0.0	7.6
cult02b	bulk	0.0	0.0	0.0	0.0	0.0	0.0	0.0	0.0	0.0	3.1	0.0	0.0	3.2	0.0	0.0	0.0
cult05b	bulk	0.0	0.9	2.3	0.0	1.6	1.2	2.0	1.5	1.1	8.5	0.0	2.1	7.0	2.7	1.5	0.0
cult08b	bulk	0.0	0.0	0.0	0.0	0.0	0.0	0.0	0.0	0.0	0.0	0.0	0.0	0.0	0.0	0.0	0.0
cult09b	bulk	0.0	0.0	1.5	0.0	0.0	0.0	0.0	0.0	0.0	4.8	1.4	3.4	2.6	1.3	0.0	5.9
cult10b	bulk	0.0	0.0	0.0	0.0	0.0	0.0	0.0	0.0	0.0	4.7	0.0	0.0	0.0	1.2	0.0	0.0
cult11b	bulk	0.0	0.0	0.0	0.0	0.0	0.0	0.0	0.0	0.0	0.0	0.0	0.0	0.0	0.0	0.0	0.0
inoculum	bulk	0.0	0.0	0.0	0.0	0.0	0.0	0.0	0.0	3.2	13.1	0.0	3.2	6.6	11.9	2.0	0.0

Hae214	Hae216	Hae219	Hae221	Hae222	Hae223	Hae226	Hae227	Hae229	Hae230	Hae232	Hae233	Hae235	Hae236	Hae239	Hae240	Hae243	Hae246
0.0	0.0	0.0	0.0	0.0	4.4	0.0	0.0	0.0	0.0	0.0	0.0	0.0	3.1	4.1	18.9	0.0	0.0
0.0	0.0	2.2	1.5	3.9	4.6	4.2	1.4	1.2	1.5	3.7	1.4	2.8	6.2	11.0	1.8	0.0	3.4
2.9	0.0	6.0	0.0	0.0	10.6	0.0	0.0	0.0	0.0	8.8	0.0	0.0	5.9	9.4	0.0	0.0	3.1
22.2	0.0	0.0	0.0	0.0	3.5	0.0	8.8	0.0	0.0	8.2	0.0	0.0	1.4	4.7	6.8	0.0	0.0
0.0	0.0	0.0	0.0	0.0	0.0	0.0	0.0	0.0	0.0	0.0	0.0	0.0	0.0	0.0	0.0	0.0	0.0
0.0	3.4	0.0	0.0	2.7	0.0	2.6	0.0	18.5	27.8	5.6	0.0	0.0	1.9	4.0	0.0	0.0	0.0
0.0	2.1	0.0	0.0	0.0	0.0	0.0	5.5	5.4	40.8	0.0	0.0	0.0	1.8	1.6	0.0	0.0	0.0
0.0	0.0	0.0	0.0	0.0	0.0	0.0	0.0	0.0	0.0	0.0	0.0	0.0	0.0	0.0	0.0	0.0	0.0
9.6	0.0	0.0	0.0	0.0	0.0	0.0	0.0	0.0	7.9	19.2	0.0	0.0	0.0	0.0	0.0	0.0	0.0
0.0	0.0	1.9	0.0	0.0	5.3	2.3	0.0	0.0	0.0	0.0	1.8	0.0	7.2	3.0	10.0	0.0	1.8
0.8	0.8	5.7	0.0	3.3	4.4	1.9	2.1	2.3	0.0	7.5	0.0	3.2	4.9	7.7	0.0	0.5	2.9
31.7	0.0	0.0	0.0	0.0	0.0	3.9	6.5	2.5	4.5	6.2	0.0	0.0	0.0	4.9	6.3	0.0	0.0
0.0	0.0	0.0	0.0	0.0	0.0	0.0	0.0	0.0	0.0	0.0	0.0	0.0	0.0	0.0	0.0	0.0	0.0
0.0	1.7	0.0	0.0	0.0	5.4	6.1	0.0	14.3	14.3	0.0	0.0	5.3	0.0	0.0	0.0	0.0	2.5
0.0	5.1	0.0	0.0	0.0	0.0	0.0	0.0	12.5	54.9	0.0	0.0	0.0	3.7	0.0	0.0	0.0	0.0
0.0	0.0	0.0	0.0	0.0	0.0	0.0	0.0	2.6	12.2	52.4	4.0	4.8	0.0	0.0	0.0	0.0	0.0
18.5	0.0	0.0	0.0	0.0	0.0	2.0	0.0	0.0	0.0	13.8	0.0	1.9	0.0	0.0	4.3	0.0	0.0
2.1	0.0	3.5	1.9	0.0	5.5	4.0	0.6	0.0	1.5	4.9	0.0	4.3	3.1	11.9	2.4	0.9	1.9
0.0	0.0	0.0	0.0	0.0	0.0	0.0	0.0	0.0	0.0	0.0	0.0	0.0	0.0	0.0	0.0	0.0	0.0
0.0	1.2	2.5	1.6	2.9	2.8	4.8	5.2	9.5	11.6	7.8	1.6	1.8	2.6	5.9	1.0	0.0	1.2
0.0	0.0	0.0	0.0	0.0	0.0	3.1	0.0	13.6	0.0	54.2	0.0	0.0	4.2	0.0	0.0	0.0	0.0
0.0	0.0	0.0	0.0	0.0	0.0	0.0	0.0	0.0	7.1	76.5	0.0	5.5	0.0	0.0	0.0	0.0	0.0
0.0	0.0	0.0	0.0	0.0	0.0	3.3	0.0	0.0	0.0	0.0	0.0	0.0	3.1	4.1	5.3	0.0	1.5

Hae251	Hae255	Hae258	Hae259	Hae264	Hae266	Hae272	Hae274	Hae275	Hae278	Hae281	Hae290	Hae293	Hae298	Hae301	Hae304	Hae307	Hae315
0.0	2.5	0.0	0.0	0.0	0.0	6.4	0.0	0.0	0.0	0.0	0.0	0.0	0.0	0.0	0.0	0.0	0.0
0.0	1.9	0.0	0.0	0.0	2.3	7.1	0.0	0.0	0.0	0.0	0.0	0.0	0.0	0.0	0.0	0.0	0.0
0.0	2.6	0.0	0.0	2.1	2.2	4.1	0.0	0.0	0.0	1.4	1.6	0.0	0.0	0.0	0.0	0.0	1.3
0.0	4.1	0.0	1.6	0.0	0.0	0.0	0.0	1.7	4.2	1.9	0.0	0.0	0.0	0.0	1.6	0.0	2.6
22.6	0.0	0.0	0.0	0.0	0.0	0.0	0.0	0.0	0.0	0.0	3.4	58.1	0.0	0.0	0.0	0.0	0.0
0.0	0.0	0.0	0.0	0.0	0.0	0.0	0.0	0.0	5.5	0.0	0.0	0.0	2.2	0.0	0.0	0.0	9.6
0.0	0.0	0.0	0.0	2.4	0.0	0.0	0.0	0.0	0.0	0.0	1.2	15.3	0.0	0.0	3.6	8.4	2.8
0.0	0.0	0.0	0.0	0.0	13.1	0.0	0.0	0.0	0.0	0.0	0.0	0.0	0.0	0.0	0.0	0.0	0.0
0.0	0.0	0.0	0.0	0.0	0.0	0.0	0.0	0.0	0.0	0.0	0.0	0.0	16.9	2.7	6.0	11.0	4.6
0.0	0.0	1.9	2.1	0.0	0.0	2.5	0.0	0.0	0.0	0.0	0.0	0.0	0.0	0.0	0.0	0.0	0.0
0.0	1.8	2.7	0.0	0.9	0.6	2.3	0.8	0.0	0.0	0.0	1.3	0.0	1.0	0.0	0.0	0.0	0.0
0.0	4.3	3.6	0.0	0.0	0.0	0.0	0.0	0.0	4.7	0.0	0.0	0.0	0.0	0.0	0.0	0.0	0.0
38.4	0.0	0.0	0.0	0.0	0.0	0.0	0.0	0.0	0.0	0.0	5.5	49.1	0.0	0.0	0.0	0.0	0.0
0.0	0.0	8.2	0.0	0.0	0.0	0.0	0.0	0.0	1.5	0.0	0.0	0.0	1.5	0.0	0.0	0.0	5.3
0.0	0.0	0.0	0.0	0.0	0.0	0.0	0.0	0.0	0.0	0.0	0.0	13.1	0.0	0.0	0.0	4.7	0.0
0.0	0.0	0.0	0.0	0.0	0.0	0.0	0.0	0.0	0.0	0.0	0.0	0.0	0.0	0.0	0.0	16.4	0.0
0.0	2.3	0.0	0.0	0.0	0.0	1.9	0.0	0.0	0.0	0.0	0.0	0.0	19.2	6.5	6.5	5.4	1.8
0.0	1.9	4.4	0.0	0.0	0.0	2.1	0.0	0.0	0.0	0.5	0.0	0.0	0.0	0.0	0.0	0.0	0.0
27.6	0.0	0.0	0.0	0.0	0.0	0.0	0.0	0.0	0.0	0.0	13.4	59.0	0.0	0.0	0.0	0.0	0.0
0.0	1.2	0.0	0.0	0.0	0.0	0.0	0.0	0.0	1.8	0.0	0.0	0.0	1.3	0.0	0.7	0.0	2.9
0.0	0.0	0.0	0.0	0.0	0.0	0.0	0.0	0.0	0.0	0.0	0.0	7.2	2.4	0.0	0.0	3.2	0.0
0.0	0.0	0.0	0.0	0.0	0.0	0.0	0.0	0.0	0.0	0.0	0.0	0.0	0.0	0.0	0.0	10.9	0.0
0.0	4.8	3.2	0.0	0.0	0.0	2.4	1.9	0.0	0.0	1.9	0.0	0.0	5.9	0.0	0.0	0.0	0.0

	Hae316	Hae317	Hae323	Hae331	Hae407	Hae504	Hae506	Hae508	Hae524	Hae545
1.8	2.5	0.0	0.0	0.0	0.0	0.0	0.0	15.9	1.4	0.0
0.0	1.2	0.0	0.0	0.0	0.0	0.7	5.0	12.2	1.0	0.0
0.0	1.2	0.0	0.0	0.0	0.0	0.0	0.0	5.8	0.0	1.2
4.0	0.0	3.0	0.0	0.0	0.0	0.0	0.0	0.0	0.0	0.0
0.0	0.0	0.0	0.0	0.0	0.0	0.0	0.0	0.0	0.0	0.0
3.3	0.0	0.0	0.0	0.0	0.0	0.0	0.0	2.4	0.0	0.0
7.6	0.0	0.0	0.0	0.0	0.0	0.0	0.0	1.4	0.0	0.0
0.0	0.0	0.0	0.0	0.0	0.0	0.0	0.0	0.0	0.0	0.0
16.1	0.0	1.9	0.0	0.0	0.0	0.0	0.0	0.0	0.0	0.0
0.0	0.0	0.0	0.0	0.0	0.0	0.0	3.5	19.3	0.0	0.0
0.0	1.0	0.0	0.7	0.0	0.0	0.0	0.0	4.2	0.0	0.0
6.4	0.0	0.0	0.0	0.0	0.0	0.0	0.0	0.0	0.0	0.0
0.0	0.0	0.0	0.0	0.0	0.0	0.0	0.0	0.0	0.0	0.0
0.0	0.0	2.9	0.0	0.0	0.0	0.0	0.0	1.8	2.0	0.0
6.0	0.0	0.0	0.0	0.0	0.0	0.0	0.0	0.0	0.0	0.0
0.0	0.0	0.0	0.0	0.0	0.0	0.0	0.0	0.0	0.0	0.0
7.7	0.0	0.0	0.0	0.0	0.0	0.0	0.0	1.7	0.0	0.0
1.1	0.4	0.0	0.7	0.9	0.8	0.8	0.0	4.9	0.8	0.6
0.0	0.0	0.0	0.0	0.0	0.0	0.0	0.0	0.0	0.0	0.0
4.8	0.0	0.0	0.0	0.0	0.0	0.0	0.0	2.1	0.6	0.0
4.2	0.0	0.0	0.0	0.0	0.0	0.0	0.0	1.9	0.0	0.0
0.0	0.0	0.0	0.0	0.0	0.0	0.0	0.0	0.0	0.0	0.0
1.0	1.3	0.0	0.0	0.0	2.9	2.9	0.0	16.5	0.8	0.0

TABLE 6. Relative abundance of microcosm Archaeal T-RFs by HaeIII

Sample	Fraction	Hae115	Hae129	Hae132	Hae133	Hae219	Hae221	Hae230	Hae231	Hae236	Hae237	Hae246	Hae254	Hae293	Hae314	Hae318	Hae320
Acult02u	<2.8 g/cc	0.0	0.0	0.0	0.0	16.9	0.0	37.7	0.0	12.3	0.0	0.0	0.0	3.1	3.6	21.9	0.0
Acult04u	<2.8 g/cc	0.0	0.0	0.0	0.0	16.4	0.0	36.4	0.0	7.3	0.0	0.0	0.0	0.0	0.0	39.9	0.0
Acult05u	<2.8 g/cc	0.0	0.0	0.0	0.0	27.5	0.0	38.7	0.0	5.3	0.0	0.0	0.0	3.8	0.0	24.6	0.0
Acult07u	<2.8 g/cc	4.0	8.6	0.0	0.0	11.2	0.0	32.8	0.0	11.1	0.0	0.0	2.1	0.0	0.0	17.5	0.0
Acult09u	<2.8 g/cc	4.5	6.2	4.7	2.5	9.6	0.0	23.5	0.0	8.0	0.0	2.2	4.2	0.0	2.0	16.6	1.6
Acult10u	<2.8 g/cc	0.0	0.0	0.0	0.0	11.7	0.0	28.9	0.0	13.3	0.0	0.0	0.0	11.5	5.1	16.6	0.0
Acult02o	>2.8 g/cc	0.0	0.0	0.0	0.0	8.3	0.0	43.2	0.0	10.7	0.0	0.0	0.0	7.6	0.0	24.1	0.0
Acult04o	>2.8 g/cc	0.0	0.0	0.0	0.0	15.7	0.0	27.5	0.0	9.7	0.0	0.0	0.0	0.0	0.0	41.9	5.3
Acult05o	>2.8 g/cc	0.0	0.0	0.0	0.0	29.0	0.0	24.6	0.0	3.4	0.0	0.0	0.0	4.1	0.0	36.6	0.0
Acult07o	>2.8 g/cc	0.0	0.0	0.0	0.0	9.1	0.0	46.0	0.0	6.6	0.0	0.0	7.2	6.2	0.0	14.7	0.0
Acult09o	>2.8 g/cc	4.3	9.2	5.3	3.5	8.7	0.0	26.3	0.0	6.6	0.0	3.2	4.2	3.4	0.0	12.5	1.7
Acult10o	>2.8 g/cc	0.0	0.0	0.0	0.0	6.9	0.0	49.1	0.0	13.5	0.0	0.0	0.0	14.6	0.0	9.5	0.0
Acult02b	bulk	0.0	0.0	0.0	0.0	14.7	0.0	45.0	0.0	9.2	0.0	0.0	0.0	5.6	0.0	15.8	0.0
Acult10b	bulk	0.0	0.0	0.0	0.0	10.8	0.0	71.2	0.0	0.0	0.0	0.0	0.0	0.0	0.0	12.6	0.0
inoculum	bulk	0.0	0.0	0.0	0.0	13.8	0.0	42.9	0.0	4.6	0.0	0.0	0.0	10.8	0.0	25.7	0.0

Hae334	Hae436	Hae456	Hae530	Hae559
0.0	0.0	0.0	4.5	0.0
0.0	0.0	0.0	0.0	0.0
0.0	0.0	0.0	0.0	0.0
10.4	0.0	2.3	0.0	0.0
9.3	0.0	3.8	0.0	1.4
0.0	4.4	0.0	8.5	0.0
0.0	2.9	0.0	3.2	0.0
0.0	0.0	0.0	0.0	0.0
0.0	0.0	0.0	0.0	2.3
6.3	0.0	0.0	3.8	0.0
7.8	0.0	3.2	0.0	0.0
0.0	0.0	0.0	6.5	0.0
0.0	2.4	0.0	7.3	0.0
0.0	0.0	0.0	5.3	0.0
0.0	0.0	0.0	2.3	0.0